



THE UNIVERSITY OF
WAIKATO
Te Whare Wānanga o Waikato

Research Commons

<http://researchcommons.waikato.ac.nz/>

Research Commons at the University of Waikato

Copyright Statement:

The digital copy of this thesis is protected by the Copyright Act 1994 (New Zealand).

The thesis may be consulted by you, provided you comply with the provisions of the Act and the following conditions of use:

- Any use you make of these documents or images must be for research or private study purposes only, and you may not make them available to any other person.
- Authors control the copyright of their thesis. You will recognise the author's right to be identified as the author of the thesis, and due acknowledgement will be made to the author where appropriate.
- You will obtain the author's permission before publishing any material from the thesis.

**Temporal dynamics of microbial
communities in geothermal hotsprings of the
Taupō Volcanic Zone**

A thesis
submitted in partial fulfilment
of the requirements for the degree
of
Master of Science (Research)
at
The University of Waikato
by
CAITLIN LOUISE LOWE



THE UNIVERSITY OF
WAIKATO
Te Whare Wānanga o Waikato

2017

Abstract

Few studies of microbial biogeography address temporal variability in physicochemical conditions and communities in geothermal environments. Here we examine the temporal variability of 43 chemical analytes, temperature and pH in association with microbial community composition of 69 water samples collected bimonthly from 12 hotsprings of the Taupo Volcanic Zone between December 2015 and October 2016. Communities and physicochemical parameters were characterized using a combination of next generation Ion Torrent sequencing (16S rRNA), UV-spectrometry, ICP-MS, FIA and gas chromatography. Using correlation association tests, significant physicochemical changes ($P < 0.05$) were correlated with temporal variations in microbial community composition in six of the target hotsprings. Of these six hotsprings, temperature and pH were the most influential variables associated with community changes and commonly covaried with the *Aquificae*, *Deinococcus-Thermus* and *Proteobacteria* at four sites. Downstream effects of rainfall using rainfall and geothermal bore water datasets could be linked with physicochemical and microbial community changes during the winter months at two of these sites. This study contributes to our understanding of geothermal microbial dynamics in stable and variable geothermal environments, and highlights that geothermal hotsprings are not isolated from their surrounding environment.

Acknowledgements

I would first like to thank my supervisors Professor Craig Cary and Associate Professor Ian McDonald for the opportunity to complete this research at Waikato University. For without their direction, guidance and support this project would not have existed. I would also like to thank the amazing team at GNS Science Taupō who managed the sampling and chemical side of this research. From this team, I would especially like to thank Dr. Matthew Stott who was always available to answer questions, give advice and kept myself and the team safe in the field. The coolest Irish lass, Jean Power who was the central rock of this project, managing sampling trips, organising everything impeccably, staying late nights with me in the laboratory, constantly answering my emails and still managing to push her way through her own PhD. Hanna Peach, who was an immense help both in the field and laboratory, and Karen Houghton and Carlo Carere for their friendly nature and direction while in Taupō.

I would also like to thank my awesome lab family and flatmates for getting me through this testing but rewarding year of my life. Georgia, who was the first to help when there was a problem and kept me company when spending late nights in the lab. Shelly, Maria, Rachelle, Maud and Josh who were always supportive, great listeners and excellent distractions when talking about everything unrelated to our own work. Jay Viswam, who was a great problem solver and gave solid direction for the many queries I had. And who was always there for a casual Friday beverage, touch or cricket game and an inappropriate or lame dad joke. My flatmates Jean, Rory and Laurence who were always great entertainment value and who kept me relatively sane throughout this year. In particular, a special thanks to Rory, who was very helpful with the computer processing and analytical side of my project.

Finally, I would like to thank my Mum and Dad for feeding and looking after me when on sampling trips in Taupō and for giving unconditional support and love throughout this whole project. And Josh, my rock, for his constant love and support during this learning experience.

Table of Contents

Abstract	iii
Acknowledgements	iv
List of Figures	vii
List of Tables.....	x
1 Chapter One	12
Introduction	12
1.1 Introduction to the geothermal environment.....	12
1.2 Extremophiles	12
1.2.1 Archaea in geothermal environments.....	14
1.2.2 Bacteria in geothermal environments.....	18
1.3 Microbial biogeography.....	20
1.4 Hotspring microbial communities changing over time.....	21
1.5 Factors influencing geothermal microbial growth.....	24
1.5.1 Temperature	25
1.5.2 pH.....	26
1.5.3 Water	27
1.5.4 Elements, minerals and nutrient availability	27
1.5.5 Redox potential	28
1.6 Taupō Volcanic Zone.....	29
1.6.1 Setting and formation.....	29
1.6.2 TVZ temporal microbial studies	30
1.7 Research aims	32
2 Chapter Two:	34
Temporal dynamics of microbial communities in geothermal hotspots of the Taupō Volcanic Zone	34
2.1 Introduction.....	34
2.2 Materials and methods	36

2.2.1	Site selection and description	36
2.2.2	Field sampling and processing	38
2.2.3	Post-sampling laboratory processing	40
2.2.4	Geochemical analyses	40
2.2.5	Extraction and quantification of microbial DNA	41
2.2.6	Ion Torrent preparation	42
2.2.7	Next Generation Sequencing	43
2.2.8	Data analyses	44
2.2.9	Meteoric data analyses	44
2.3	Results	45
2.3.1	Hotspring selection and sampling	45
2.3.2	Observed patterns in spring temperature and pH	50
2.3.3	Relating spring community variation to physicochemical conditions	51
2.3.4	Determining primary and secondary physicochemical drivers	69
2.3.5	Meteoric and field observations	71
2.4	Discussion	74
3	Chapter Three	85
	Conclusions and future directions	85
3.1	Conclusions	85
3.2	Future directions	85
	References	87
4	Appendices	97
4.1	Supplementary material for Chapter Two	97
4.2	Supplementary: Full site physicochemical dataset	116

List of Figures

Figure 1.1: Phylogenetic tree with “TACK” and “DPANN” super-phyla and Euryarchaeota	17
Figure 1.2: Phylogenetic tree showing eukaryotes branching within Lokiarchaeota	17
Figure 1.3: Observed colour variations found in microbial mats at Whakarewarewa Village, Rotorua.	19
Figure 1.4: Taupō Volcanic Zone	30
Figure 2.1 Taupō Volcanic Zone.....	38
Figure 2.2: Sampling procedure using specialized water column sampler and personal protective equipment at Ohaaki geothermal field.....	39
Figure 2.3: Labelled and recapped Sterivex column filters (Millipore) used in CTAB extraction protocol.....	42
Figure 2.4: Location of geothermal springs within the Rotorua geothermal system.....	47
Figure 2.5: Location of geothermal springs within Waiotapu, Ohaaki and Atiamuri geothermal systems	48
Figure 2.6: Temperature vs. pH scatterplot of target hotsprings across temporal samples	51
Figure 2.7: Whkr1 phylum-level community composition (%) based upon the relative abundances of 16S rRNA gene sequence reads	54
Figure 2.8: Total sulfur, sodium and potassium trend observed at Whkr1	55
Figure 2.9: Whkr3 phylum-level community composition (%) based upon the relative abundances of 16S rRNA gene sequence reads	56
Figure 2.10: pH trend observed at Whkr3.....	57
Figure 2.11: TeP phylum-level community composition (%) based upon the relative abundances of 16S rRNA gene sequence reads	57
Figure 2.12: Waiotapu springs phylum-level community composition (%) based upon the relative abundances of 16S rRNA gene sequence reads	59
Figure 2.13: Methane trend observed at Waiol and bicarbonate and temperature trends observed at Waiol2	60
Figure 2.14: Kui3 phylum-level community composition (%) based upon the relative abundances of 16S rRNA gene sequence reads	61

Figure 2.15: Sulfate (ppm) trend observed across temporal samples at Kui3	62
Figure 2.16: Whgpa phylum-level community composition (%) based upon the relative abundances of 16S rRNA gene sequence reads	63
Figure 2.17: Methane (μm) and pH trends observed across temporal samples at Whgpa	63
Figure 2.18: Kui1 phylum-level community composition (%) based upon the relative abundances of 16S rRNA gene sequence reads	64
Figure 2.19: Whkr2 phylum-level community composition (%) based upon the relative abundances of 16S rRNA gene sequence reads	65
Figure 2.20: Temperature ($^{\circ}\text{C}$) trend observed across temporal samples at Whkr2	66
Figure 2.21: Whkr4 phylum-level community composition (%) based upon the relative abundances of 16S rRNA gene sequence reads	67
Figure 2.22: Temperature ($^{\circ}\text{C}$) trend observed across temporal samples at Whkr4	68
Figure 2.23: Ohaaki phylum-level community composition (%) based upon the relative abundances of 16S rRNA gene sequence reads	68
Figure 2.24: Location of geothermal bores in association with target geothermal sites in Rotorua (A) Position of geothermal bores M25 and M26 in proximity to Te Puia and Whakarewarewa hot springs (B) and M27 and M28 with Kuirau Park hot springs (C).....	72
Figure 2.25: Daily rainfall in Rotorua and geothermal bore water level	73
Figure 2.26: Aquificae and Crenarchaeota community composition in association with pH at Whkr3	75
Figure 2.27: Trend observed in community composition in association with pH and methane at Whgpa	76
Figure 2.28: Trend observed in community composition in association with temperature at Whkr4	77
Figure 2.29: Trend observed in community composition in association with temperature at Whkr2	78
Figure 2.30: Trend observed in community composition in association with sulfate and temperature at Kui3	80
Figure 2.31: Trend observed in community composition in association with total sulfur at Whkr1	81
Supplementary Figures 4.1: Target hotspring sketches and sample location	98

Supplementary Figures 4.2: Target hotspring photographs 100

List of Tables

Table 2.1: Target hotsprings within pH Groups.....	46
Table 2.2: Overview of spring locations and descriptions.....	49
Table 2.3: Summary table of Pearson’s correlation coefficient association test between dominant phyla and environmental variables at target springs	53
Table 2.4: Whkr1 community percentage of 16S rRNA gene sequence reads grouping to genera.....	55
Table 2.5: Whkr3 community percentage of 16S rRNA gene sequence reads grouping to Aquificae.....	56
Table 2.6: TeP community percentage of 16S rRNA gene sequence reads grouping to genera.....	58
Table 2.7: Wai01 and Wai02 community percentage of sequences grouping to Aquificae	59
Table 2.8: Kui3 community percentage of 16S rRNA gene sequence reads grouping to Aquificae and Proteobacteria.....	61
Table 2.9: Whgpa community percentage of 16S rRNA gene sequence reads grouping to genera.....	63
Table 2.10: Kui1 community percentage of 16S rRNA gene sequence reads grouping to Aquificae.....	64
Table 2.11: Whkr2 community percentage of 16S rRNA gene sequence reads grouping to Aquificae.....	66
Table 2.12: Whkr4 community percentage of 16S rRNA gene sequence reads grouping to genera.....	67
Table 2.13: Ohaaki community percentage of 16S rRNA gene sequence reads grouping to Aquificae and Deinococcus-Thermus.....	69
Table 2.14: Summary table of target hotspring temporal dynamics	70
Supplementary Table 4.1: Sample number log of target pools	97
Supplementary Table 4.2: Hotspring temperature and pH measurements.....	101
Supplementary Table 4.3: Whkr3 community composition percentages of sequences grouping to genera	102
Supplementary Table 4.4: Wai01 community composition percentages of sequences grouping to genera	103

Supplementary Table 4.5: Waio2 community composition percentages of sequences grouping to genera	104
Supplementary Table 4.6: Kui3 community composition percentages of sequences grouping to genera	105
Supplementary Table 4.7: Whgpa community composition percentages of sequences grouping to genera	107
Supplementary Table 4.8: Kui1 community composition percentages of sequences grouping to genera	109
Supplementary Table 4.9: Whkr2 community composition percentages of sequences grouping to genera	111
Supplementary Table 4.10: Whkr4 community composition percentages of sequences grouping to genera	113
Supplementary Table 4.11: Ohaaki community composition percentages of sequences grouping to genera	115

Chapter One

Introduction

1.1 Introduction to the geothermal environment

Geothermal areas are distributed across the globe but are mainly confined to zones of high tectonic activity which involve the movement of the Earth's tectonic plates in a divergent, convergent, or transforming nature. These boundaries form between plates where the Earth's crust is thin and are associated with earthquakes, volcanism, oceanic trenches, mountain building and the development of geothermal features, including mud pools, hot springs, and geysers (Hreggvidsson et al., 2012; Panosyan & Birkeland, 2014). Geothermal hot springs are defined as bodies of water characterized by steep temperature gradients, the presence of steam, extreme pH variations, and a high degree of mineralization (Boothroyd, 2009; Hreggvidsson et al., 2012). Geothermal waters are derived from rainwater, groundwater or snow melt which percolates through faults and fractures in basement rock, forming large water bodies known as aquifers, deep under the Earth's crust (New Zealand Institute of Chemistry, 2008; Hreggvidsson et al., 2012). This water becomes pressurized and heated to temperatures greater than 250 °C by intrusive magma bodies. A proportion of this water can reach the Earth's surface to naturally form hot springs, with some remaining in the aquifer which can be exploited for geothermal power (New Zealand Institute of Chemistry, 2008).

1.2 Extremophiles

Thomas D. Brock pioneered the study of microorganisms in geothermal waters. He was one of the first to analyse and describe the presence of bacterial and archaeal species in Yellowstone National Park (YNP), USA (Brock, 1978; Sand, 2003). These initial discoveries opened up the world of microbial life forms in a previously unexplored environment which was thought to be limited due to the environment's extreme physicochemical conditions (Sand, 2003). From a human perspective, the term "extreme" is used to describe an environment which does not support our own existence. By removing the anthropocentric sense, it can be described as a set of conditions under which certain organisms may thrive, and

others not (Brock, 1978; Bell & Callaghan, 2012). Many such environments are present on Earth, including deep sea hydrothermal vents, hot deserts, polar regions and geothermal hotspots. These environments present unique and harsh physiological extremes in physical and geochemical factors including pH, temperature, pressure, water availability, and salt and oxygen limitations (Purcell et al., 2007; Bell & Callaghan, 2012; Cayol et al., 2015). “Extremophiles” are organisms that can withstand extremes in environmental conditions which are inhospitable to other life-forms (Purcell et al., 2007; Rampelotto, 2013). They belong to three major groups; Eukaryotes, Archaea and Bacteria, and are classified based on the parameters of temperature (psychrophiles or thermophiles), pH (acidophiles or alkaliphiles), salinity (halophiles) and pressure (barophiles) (Rothschild & Mancinelli, 2001; Stan-Lotter, 2012; Rampelotto, 2013). Most extremophiles are from the domains Archaea and Bacteria which are both prokaryotes. Prokaryotes are unicellular microscopic organisms, that unlike the third kingdom, Eukaryotes, have no nucleus and other membrane bound organelles (Matheron & Caumette, 2015). Extremophiles can be classified based on the optimal temperature and pH ranges which support their metabolic lifestyle. Thermophiles are microorganisms which grow optimally at temperatures between 50 °C and 70 °C, and hyperthermophiles thrive from 75 °C to over 120 °C (Castenholz, 1969; Stan-Lotter, 2012). Acidophilic species can be moderate, strict or extreme with their optimal growth conditions within the range of pH 5.5 to <pH 3, while alkaliphilic species have an optimal growth range from pH 7 to pH 12 (Normand et al., 2015). Microorganisms can be further classified based on their metabolic lifestyle and oxygen dependency which ranges from a strict aerobe to strict anaerobe (Sand, 2003).

Research on extremophiles from geothermal environments has many biological and economic benefits. Geothermal exploration provides an insight into the Earth’s ecosystem over the past ~3.8 million years due to the similarities present in physicochemical conditions (high levels of gases, temperatures and extreme pH variations) (Cowan et al., 2012; Cayol et al., 2015). This research has been pivotal in helping us understand and expand our known tree of life. Extremophile research can also provide insight into basic molecular knowledge of microorganisms, importantly, the enzymes from geothermal microbes which today have formed a multibillion-dollar industry with their application to detergents, pharmaceuticals,

agriculture and biotechnology (Rothschild & Mancinelli, 2001). Most importantly, extremophiles can be used to understand ecological processes and a variety of metabolisms present in different extreme environments.

1.2.1 Archaea in geothermal environments

Archaea are one of the main groups of organisms known to thrive in extreme environments with their enhanced ability to adapt to extreme conditions (Rampelotto, 2013). Historically, this domain was thought to include predominantly extremophiles within strict high-temperature, acidic or anoxic environments, however today Archaea display a more ubiquitous distribution (DeLong & Pace, 2001; Kan et al., 2011). Archaea are found within soils, lake and marine water and sediments, as well as geothermal environments, and are the only prokaryotes to thrive above 100 °C (extreme thermophiles) (DeLong & Pace, 2001; Kan et al., 2011; Coman et al., 2013; Cayol et al., 2015). Even with the advances in high-throughput sequencing technology, the diversity of Archaea is still relatively understudied (Kan et al., 2011). One of the main areas where geothermal archaeal diversity is studied is YNP, USA, which comprises over 10,000 geysers, pools and vents. Large scale analysis of archaeal diversity in Yellowstone revealed *Thaumarchaeota* as the dominant phylum (Kan et al., 2011). *Thaumarchaeota* are one of the most abundant Archaea on Earth, which were initially classified as ‘mesophilic *Crenarchaeota*’ before the emergence of comparative genomics (Pester et al., 2011). This phylum (*Thaumarchaeota*) has been discovered in many diverse environments, including freshwater lakes and hot springs, as well as in association with animals (Caumette et al., 2015). All known archaeal ammonium oxidisers are included in this phylum, and these play a key role in global nitrification (Pester et al., 2011; Cowan et al., 2012). This phylum diverged before the split of two other major hyperthermophilic archaeal phyla, *Crenarchaeota* and *Euryarchaeota* (Pester et al., 2011). *Crenarchaeota* are a dominant archaeal phylum found in geothermal hot springs at temperatures above 50 °C and low to neutral pH (Purcell et al., 2007; Cole et al., 2013; Wang et al., 2013; Sharp, Brady, et al., 2014). *Crenarchaeota* includes anaerobes, facultative anaerobes and aerobic thermophiles, and are split into three orders; *Sulfolobales*, *Desulfurococcales*, and *Thermoproteales* (Caumette et al., 2015). *Sulfolobales* are extreme thermophilic

acidophiles which thrive at low pH (1-5) and high temperature (65-90 °C). *Desulfurococcales* are neutrophilic or acidophilic thermophiles which thrive at 85 °C to 106 °C. Their main habitats include deep sea hydrothermal vents (black smokers) as well as hot terrestrial systems such as hot springs and mud pools (Caumette et al., 2015). *Thermoproteales* include both thermophiles and hyperthermophiles which grow optimally between 75 °C and 100 °C, and pH 3.7 to 7.0 (Caumette et al., 2015). *Euryarchaeota* are more diverse than *Crenarchaeota* and have been discovered in all types of environments including marine, desert and terrestrial ecosystems (Caumette et al., 2015). Within *Euryarchaeota* are a major group of Archaea known as the methanogens. Methanogens are strict anaerobes which produce methane (CH₄) via energy metabolism as a carbon source for methanotrophic organisms present within the ecosystem (Coman et al., 2013; Caumette et al., 2015). Methanogens are split into two categories; class I and class II. Class I includes *Methanobacteriales*, *Methanococcales*, and *Methanopyrales*, while class II includes *Methanocellales*, *Methanomicrobiales*, and *Methanosarcinales* (Caumette et al., 2015).

Phylogenetic ribosomal RNA analysis of samples taken from Obsidian Pool, YNP led to the discovery of a new phylum, *Korarchaeota* (Barns et al., 1996; Auchtung et al., 2006). This deep-branching phylum was proposed to have diverged before the split of *Crenarchaeota* and *Euryarchaeota* (Reigstad et al., 2010; Auchtung et al., 2011). *Korarchaeota* 16S rRNA sequences have been isolated from hydrothermal environments globally, such as Iceland, Russia and Japan, and cluster phylogenetically based on location and environmental variables. This suggests a high degree of endemism within this phylum (Reigstad et al., 2010; Auchtung et al., 2011). The first isolated genome from this phylum was '*Candidatus Korarchaeum cryptofilum*' sequenced in 2008. This species relies on simple peptide fermentation for carbon and energy, suggesting a lifestyle as a symbiotic organism or efficient scavenger (Elkins et al., 2008; Reigstad et al., 2010). Further in 2011, the genomic analysis of '*Candidatus (Ca.) Caldiarchaeum subterraneum*' (a species discovered in a geothermal stream in Japan) placed this species into another deep-branching phylum proposed to be named *Aigarchaeota* (Brochier-Armanet et al., 2011). This led to the formation of a proposed acronym 'TACK', which includes *Thaumarchaeota*, *Aigarchaeota*, *Crenarchaeota* and *Korarchaeota* (Guy & Ettema, 2011; Castelle et al., 2015; Petitjean et al., 2015). A further acronym 'DPANN' was

also developed, including all ultra-small Archaea: *Diapherotrites*, *Parvarchaeota*, *Aenigmarchaeota*, *Nanoarchaeota*, and *Nanohaloarchaea* phyla (Figure 1.1) (Castelle et al., 2015; Petitjean et al., 2015). Of these phyla, *Nanoarchaeota* have been linked to geothermal sites. The representative species, '*Nanoarchaeum equitans*' was discovered in a hydrothermal vent in 2002 off the coast of Iceland (Huber et al., 2002). The microbial cells are ~400 nm in diameter and grow anaerobically between 70-98 °C attached to the surface of crenarchaeal *Ignicoccus* species as an obligate symbiont (Huber et al., 2002; Brochier et al., 2005; Castelle et al., 2015). Strains have been found in Obsidian Pool at Yellowstone, and sub-polar mid ocean ridges (Clingenpeel et al., 2013; Munson-McGee et al., 2015). Recently, Wurch et al. (2016) isolated and characterized *Nanoarchaeum equitans* cells from an acidic hot spring in YNP.

In 2015, *Lokiarchaeota* was established from mid-ocean sediment samples collected in 2010 near the hydrothermal vent known as Loki's Castle, in the Arctic Ocean (Spang et al., 2015). This phylum forms a monophyletic clade with eukaryotes, and has increased the complexity of the currently inferred archaeal ancestor of eukaryotes (due to the presence of components crucial for the eukaryotic lifestyle earlier than previously thought) (Spang et al., 2015). Discoveries over the past decade of *Korarchaeota*, *Aigarchaeota*, and *Lokiarchaeota* have given a new insight into the true root of the Archaeal tree due to their deep-branching nature within Archaea and Eukaryotes (Figure 1.2) (Petitjean et al., 2015).

In summary, Archaea are a diverse and expanding domain. Recent discoveries have highlighted their increasing abundance in a range of extreme environments, and led to the reclassification of numerous species, and the formation of the new super-phyla, 'TACK' and 'DPANN'. These discoveries have improved our understanding of the known tree of life and emphasized the large majority of archaeal species that are yet to be discovered.

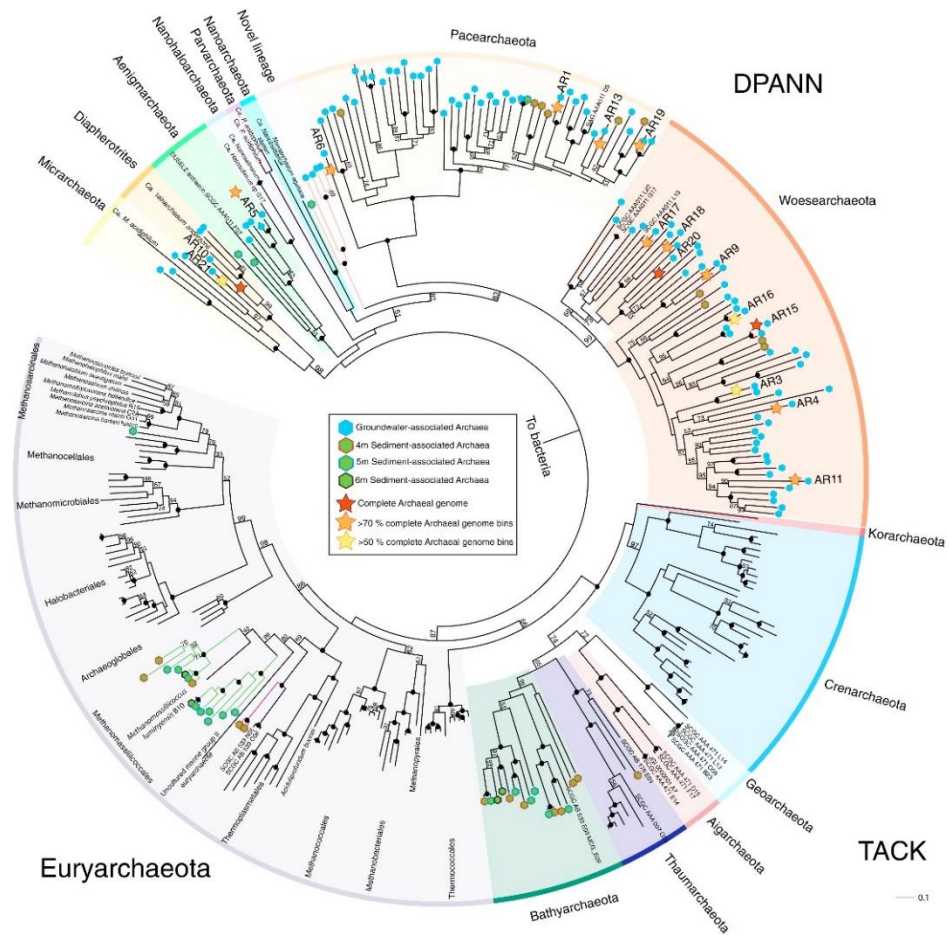


Figure 1.1: Phylogenetic tree with “TACK” and “DPANN” super-phyla and Euryarchaeota

Tree placing 153 subsurface sampled Archaea based on 15-ribosomal-protein concatenated alignment. Sourced from Castelle et al, 2015.

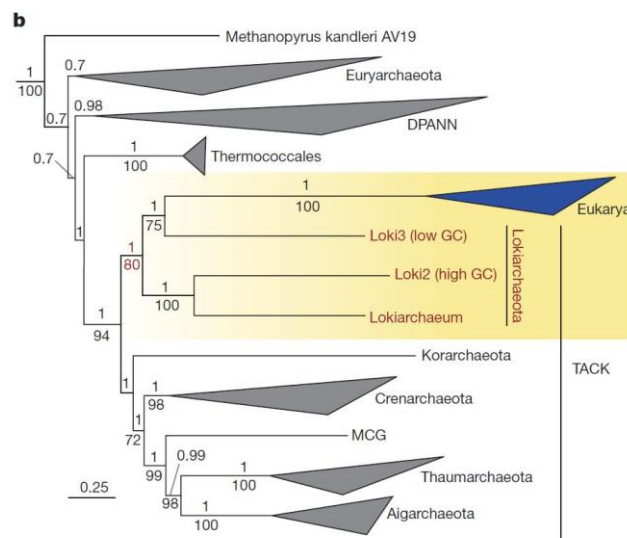


Figure 1.2: Phylogenetic tree showing eukaryotes branching within Lokiarchaeota

Tree based on Bayesian phylogeny. Sourced from Spang et al, 2015.

1.2.2 Bacteria in geothermal environments

The discovery of *Thermus aquaticus* (Phylum *Deinococcus-Thermus*) by Thomas Brock in the Lower Geyser Basin of YNP in 1969, was one of the first key discoveries of Bacteria within geothermal hotsprings. This discovery was the beginning of the revolution of DNA amplification with polymerase chain reaction (PCR) using a heat stable enzyme from *T. aquaticus* named ‘Taq’ polymerase (Brock, 1997). The phylum *Deinococcus-Thermus* contains heterotrophic organisms which consume the organic matter produced by cyanobacteria and primary producers within ecosystems. Members of this phylum are common at geothermal sites at temperatures over 50 °C and at neutral pH. Also present in these environments are other chemolithotrophic phyla, including *Aquificae* which are ubiquitous in hyperthermophilic communities (Purcell et al., 2007; Cole et al., 2013; Mackenzie et al., 2013; Wang et al., 2013; Sharp, Brady, et al., 2014).

Within geothermal environments, Bacteria commonly form microbial mats. These mats consist of stratified layers of microorganisms, dominated by thermophilic cyanobacteria which are a fundamental component of Earth’s ecosystems due to their role in photosynthesis (Boothroyd, 2009; Coman et al., 2013; Normand et al., 2015). These mats tend to develop within neutral or alkaline hotsprings, with three separate layers: the uppermost layer of cyanobacteria, anoxic phototrophs below and a third layer of anaerobic heterotrophs (Coman et al., 2013). Colour changes can be observed in the microbial mats across a geothermal landscape, which can indicate a change in temperature range facilitating the growth of a different dominant species, or a change in the chemistry of the system (Figure 1.3) (Hreggvidsson et al., 2012). Geothermal microbial mats are common focus sites of spatial geothermal studies (Childs et al., 2008; Sharp, Brady, et al., 2014), which are more frequently explored than temporal studies. This will be discussed in more detail in section 1.3.



Figure 1.3: Observed colour variations found in microbial mats at Whakareware wa Village, Rotorua.

Alpha, beta and gamma classes of the phylum *Proteobacteria* are also frequently present in these geothermal waters (Lau et al., 2009; Pagaling et al., 2012; Coman et al., 2013; Panosyan & Birkeland, 2014). Some representative species include *Paracoccus bogoriensis* (alpha) and *Tepidicella xavieri* (beta) retrieved from a 55 °C hot spring at pH 8 in Romania, and the genus *Lysobacter* (gamma) within an Armenian hot spring (~44 °C, pH 7.0-7.2) (Coman et al., 2013; Panosyan & Birkeland, 2014). Other phyla including *Acidobacteria*, *Bacteroidetes* and *Firmicutes* have been isolated from 55-65 °C, slightly alkaline springs across Tibet, Patagonia and Romania (Lau et al., 2009; Coman et al., 2013; Mackenzie et al., 2013). *Acidobacteria* and *Firmicutes* are major phyla of Gram-positive bacteria, while *Bacteroidetes* is composed of three classes of Gram-negative bacteria (Caumette et al., 2015). Interestingly, these heterotrophic groups are not specifically associated with geothermal environments. However, as our knowledge of these groups increases, it is becoming more apparent that their presence is more common across a range of environments. These organisms, like *Thermus*, consume organic matter derived from cyanobacteria and other non-sulfur bacteria within these ecosystems (Mackenzie et al., 2013).

Another group of geothermal microorganisms are aerobic methanotrophs which use methane as their sole source of carbon and energy (Coman et al., 2013; Sharp, Smirnova, et al., 2014). Methanotrophs are members of the *Gammaproteobacteria* and *Alphaproteobacteria*, and were recently described in acidic (pH 1.8 - 5.0), moderate temperature (22.5-81.6 °C) geothermal pools in New

Zealand as part of the *Verrucomicrobia* phylum (Sharp, Smirnova, et al., 2014). These strains were collectively grouped into a new genus, *Methylacidiphilum*, which grows at pH 1, and are therefore the most acidophilic methanotrophs currently known (Sharp, Smirnova, et al., 2014).

In summary, Bacteria dominate geothermal environments at temperatures below 100 °C. Their discovery in geothermal sites has grown exponentially since the 1960's, with phyla such as *Aquificae* and *Deinococcus-Thermus* commonly isolated from most thermophilic geothermal communities. Microbial mat communities are an ideal environment for spatial geothermal studies. Gradients in abiotic factors, such as temperature, can be linked to changes in dominant microbial phyla visualized by colour differentiation.

1.3 Microbial biogeography

Biogeography describes the distribution of organisms through ecological time and space. This proven concept suggests that macro-organisms, such as plants and animals, which are subject to dispersal limitation, will form isolated populations across the globe based on variable environmental factors. An opposing theory has been proposed for microorganisms, due to their advanced ability to disperse, produce spores, and rapidly adapt to their new environment, that these organisms rarely form geographically isolated populations, and that conceivably “everything is found everywhere” (Fenchel, 2003; Papke et al., 2003). Many studies, however, on microbial communities and associated abiotic and biotic factors have highlighted the importance of local environmental conditions and their influence on microbial communities. The large majority of these studies have focused on non-geothermal sites. These studies range from microbial communities associated with temperate soils, river and ocean gradients as well as horticultural applications, and all highlight the presence of geographically distinct populations, based on several influential environmental factors (Fortunato et al., 2012; Pasternak et al., 2013; Bokulich et al., 2014).

In geothermal environments, the limited number of studies also suggest that thermophilic microbial communities are subject to local environmental conditions and historical dispersal limitation events, which can cause the formation of geographically isolated populations, regionally and globally (Whitaker et al., 2003;

Takacs-Vesbach et al., 2008; Bahl et al., 2011; Sharp, Brady, et al., 2014). These studies suggest that geothermal microbial communities have greater species richness and biodiversity than previously thought, which suggests that local populations affected by dispersal barriers may face rapid extinction if efforts are not directed at conserving them (Bahl et al., 2011). This concept, in relation to the abiotic and biotic factors expanded upon in section 1.5, demonstrates the importance of understanding local microbial communities within geothermal regions, as temporal alterations to these factors could lead to dramatic shifts in community structure and composition.

1.4 Hotspring microbial communities changing over time

Geothermal springs are scattered throughout the globe, in both terrestrial and marine settings. The most common and extensively studied springs are in Japan, Iceland, New Zealand, United States, Russia, Italy and North Africa (Sayeh et al., 2010; Stan-Lotter, 2012). They provide an ideal environment to study geochemical conditions spatially and temporally, as well as their variable ability to constrain microbial communities (Alsop et al., 2014).

An initial study used a DNA fingerprinting method to evaluate seasonal distribution of microbial mat populations within an effluent channel of Octopus Spring, YNP, USA (Ferris & Ward, 1997). Populations were seasonally sampled at sites along a thermal gradient, with results revealing that populations collected at the same, or temperature-equivalent sites, only exhibited slight changes in fingerprints over the annual study period. Seasonal variations in phototrophic microbial mat populations and geochemistry were therefore not present in this study, although light reduction did play a role in the ability of a green non-sulfur bacterium to inhabit the extremely high temperature sites (Ferris & Ward, 1997). A similar study expanded the long-term investigation to include removal of ultraviolet radiation (UVR) in two alkaline lakes at YNP. This study indicated that, within a temperature range of 40-47 °C, community structure was stable during summer, either with or without UVR (Norris et al., 2002). Although the communities were relatively constant throughout variations in UVR levels, competence values for photosynthesis for UVR-restricted photosynthetic cyanobacteria at the surface were lower than those communities maintained under UVR. This decrease in

photosynthetic ability was hypothesized to reflect changes in gene expression of the dominant species, not species composition variations (Norris et al., 2002).

Following these initial findings, Lacap et al. (2007) published the first long-term seasonal dynamics study on thermophilic cyanobacteria-based microbial mat communities within tropical geothermal springs, on the island of Luzon in the Philippines. In direct contrast to previous studies where results suggested no significant seasonal variations in temperate hotspring microbial communities (Ferris & Ward, 1997; Norris et al., 2002), this study described a pronounced seasonal effect based on species richness, standing biomass, and abundance of microbial communities in these tropical hotsprings over the 21-month study period (Lacap et al., 2007). *Synechococcus* phylotypes in lower-temperature pools, and *Fischerella* and *Oscillatoria*-like phylotypes in warmer pools, were identified as the main cyanobacterial genera accounting for seasonal dynamics. Over the dry season (Jan-Apr), an increase in species richness was observed, in contrast to the wet season (Jul-Oct) when species richness decreased (Lacap et al., 2007). The authors noted that although seasonal variations altered the richness of certain phylotypes, the overall taxonomic composition of the mats did not change significantly. Temperature was the primary driver for variations in site diversity, and due to the lack of variation observed in previous temperate sites (Ferris & Ward, 1997; Norris et al., 2002) these tropical environments were clearly functioning under a different set of ecological variables (Lacap et al., 2007).

A further study on seasonal shifts within three geothermal hotsprings in Patagonia (Cahuelmo Hotspring, Porcelana Geyser, and Porcelana Hotspring) using DNA fingerprinting analysis, revealed temperature as the main, but not the singular driving factor of bacterial community composition and structure (Mackenzie et al., 2013). Samples within Porcelana Hotspring showed 40% similarity between winter (June) and summer (December) 2009 although temperature varied by 7°C, whereas no variation was observed in Cahuelmo Hotspring and Porcelana Geyser communities (Mackenzie et al., 2013).

A multi-year study by Siering et al. (2013) at Boiling Springs Lake, USA, monitored the environmental conditions and integrated them with microbial water samples collected in July 2004 and 2009. Boiling Springs Lake is located in Lassen Volcanic National Park, California, and has an average temperature of 52 °C, a pH of 2.0, and distinct geochemical conditions to other major geothermal systems

found globally (Siering et al., 2013). A seven-year study using T-RFLP analysis indicated low community variation, despite a seasonal temperature cycle. Greater environmental variability was noted during the winter months, compared to the summer months. Although microbial samples were not collected annually, the data suggest the absence of a temporal effect of environmental factors on the microbial community of Boiling Spring Lake (Siering et al., 2013).

A study by Briggs et al. (2014) revealed atmospheric precipitation as a key driver of seasonal microbial community variations in hotspots of Tengchong, China. The source water of these hotspots was solely meteorically driven which resulted in rapid variations in the volume of surface water input, based on seasonality, and subsequent rainfall. From January to June (2011), significant changes in microbial community structure were observed due to atmospheric precipitation into the hotspots, which led to an increase in the abundance of non-thermophilic microbes derived from the surrounding environment (Briggs et al., 2014).

A final geochemical study at Obsidian Pool (YNP) from 2000 to 2010 used 16S rRNA analysis to monitor community dynamics of Bacteria and Archaea in parallel (Havig et al., 2011). A decrease in bacterial abundance was observed and correlated with a decrease in pH, however archaeal abundance did not change significantly between 2005 and 2010. This indicated an increase in bacterial species richness which suggested an increase in energy availability at lower pH (Havig et al., 2011). Temperature and pH had the most impact on the microbial community, and strong links were observed between environmental parameters and the functional diversity of the microbial community (Havig et al., 2011).

To summarize, the findings from these temporal studies highlight the difficulty in forming a consensus about microbial community dynamics at geothermal sites. Some studies identified temperature and/or pH as the main drivers of temporal changes in microbial communities (Lacap et al., 2007; Havig et al., 2011; Mackenzie et al., 2013), while others demonstrated stable microbial communities in the presence of changing environmental variables (Ferris & Ward, 1997; Norris et al., 2002; Siering et al., 2013). Combined, these findings highlight the need for more research into temporal variations of microbial communities in association with abiotic factors.

1.5 Factors influencing geothermal microbial growth

To investigate changing microbial communities over time, the local physicochemical environment needs to be analysed as changing abiotic factors can shape and constrain the taxonomic and metabolic composition of ecosystems (Alsop et al., 2014). Microbial communities inhabiting terrestrial and marine environments are influenced by multiple chemical, physical and biological factors, including pH, temperature, minerals and nutrients, water and redox potential (Sand, 2003; Sayeh et al., 2010; Gilbert et al., 2012). Despite research efforts, few of these factors have been directly linked to variations in the diversity and composition of microbial communities which inhabit geothermal systems (Sayeh et al., 2010; Briggs et al., 2014). The reason for this gap may be solely because the physicochemical conditions of geothermal springs were assumed to remain relatively stable over time (Lacap et al., 2007; Briggs et al., 2014). Consequently, few studies have investigated these cyclical changes of environmental factors in extreme-temperature environments in association with microbial communities (Briggs et al., 2014; Ward et al., 2017). Environmental conditions can influence microbial community dynamics due to changes in the conditions which support the optimum growth of each species. Communities can cluster in a consistent way with physicochemical parameters presented by the environment (Delgado-Serrano et al., 2014). Physicochemical factors can change over time or along an environmental gradient, which can be associated with shifts in community structure and metabolic capabilities (Jackson et al., 2001; Macur et al., 2004; Swingley et al., 2012; Ward et al., 2017). Specific species may adapt to these growth conditions, ensuring their survival and success within a new environmental niche (Norris et al., 2002). Although it is generally accepted that environmental factors can influence microbial communities, with a decrease in diversity in more extreme conditions, the relative importance of each of these environmental parameters is still debated (Cowan et al., 2012; Hreggvidsson et al., 2012; Sharp, Brady, et al., 2014). The top five physicochemical parameters known to affect microbial life (i.e. temperature, pH, water source, elements/minerals/nutrients and redox potential) will now be discussed in more detail (Sand, 2003; Sayeh et al., 2010; Gilbert et al., 2012).

1.5.1 Temperature

Temperature is an important driving factor for the growth and survival of microorganisms (Normand et al., 2015). At high temperatures, microbial enzymes begin to denature which can ultimately lead to cell death, while at low temperatures, cell activity slows until dormancy, before reactivation with increasing temperature (Normand et al., 2015). Depending on the microbial species, the optimal temperature range varies, for example, psychrophiles from 8-15 °C and thermophiles from 40-65 °C (Normand et al., 2015). It is generally accepted that as temperature increases, community diversity declines (Cowan et al., 2012; Sharp, Brady, et al., 2014), and although microbes have the capacity to survive at temperatures of >120 °C, certain phyla, such as cyanobacteria, have an upper limit of 74 °C in order to carry out photosynthesis (due to thermal instability of intermediates in the Calvin-Benson-Bassham Cycle) (Castenholz, 1969; Lacap et al., 2007; Boothroyd, 2009; Sharp, Brady, et al., 2014; Madigan et al., 2015). Several studies have revealed temperature as the dominant factor influencing microbial diversity in geothermal systems (Lacap et al., 2007; Mackenzie et al., 2013; Alsop et al., 2014; Sharp, Brady, et al., 2014; Ward et al., 2017), while others have revealed that temperature in association with other factors, such as the level of oxygen solubility, can be more influential. In high temperature environments, oxygen is less soluble in water, resulting in development of anoxic environments which are favoured by methanogenic Archaea (Coman et al., 2013). Another study found different communities can inhabit geochemically distinct regions of geothermal springs, with their distribution based on temperature as well as geochemical conditions and oxygen availability (Childs et al., 2008). Precipitate samples taken at the sub-aerial, sub-aqueous and water/air interface showed communities dominated by thermophilic and moderately acidophilic microorganisms, whereas samples taken from the surrounding orange biofilm revealed communities of eukaryotic and prokaryotic acidophiles (Childs et al., 2008). It may be that as temperature increases, other factors, such as chemical composition become more important in determining microbial community composition (Purcell et al., 2007; Sharp, Brady, et al., 2014).

1.5.2 pH

Hotspring pH is determined by the source and quantity of the geothermal fluid, as well as gas constituents (Hreggvidsson et al., 2012). Seasonal weather patterns can therefore alter water chemistry over short and long temporal scales (Cowan et al., 2012). Generally, hot springs are split into two categories; acid springs (pH 0-6), and neutral to slightly alkaline springs (pH 7-9). Acidic springs form when hydrogen sulphide (H_2S) is oxidised to sulfur (S) then sulfuric acid (H_2SO_4) by microorganisms. In this process, H_2S forms numerous sulfur species (elemental sulfur, sulfate, sulphite, thiosulfate and polythionates) which is dependent on the availability of complementary physicochemistry. These springs are commonly found in the central region of active geothermal systems. Neutral to alkaline hot springs form when the H_2S level in the fluid is lower and CO_2 becomes concentrated. This reduces acidity to within the range of pH 7 to 10 (Cayol et al., 2015). Other components including HCO_3^- , CO_3^{2-} and SiO_2 are the main chemical compounds that control pH in these environments (Hreggvidsson et al., 2012) These hot springs are located at the edges and surrounding the active geothermal zones (Cayol et al., 2015).

Some studies have indicated that pH is the main driver of microbial community structure in global soil studies, as well as in extreme environments, such as hot springs and acid mine drains (Fierer & Jackson, 2006; Boothroyd, 2009; Chu et al., 2010; Jun Liu et al., 2014). Certain species of microorganisms can be restricted by pH. For example, cyanobacteria are restricted from environments which are highly acidic ($\text{pH} < 4.0$) as this degree of acidity does not support their growth which is optimised above pH 6 (Lacap et al., 2007). Two categories of extremophiles, thermoacidophiles and thermoalkaliphiles, are adapted to these hot acidic and alkaline environments at $\sim\text{pH} 2$ and $\sim\text{pH} 8$, respectively (Stan-Lotter, 2012; Cayol et al., 2015). An example of an acidophilic species is *Picrophilus torridus* which grows optimally at pH 0.06 (Rampelotto, 2013). Alterations to pH have also been linked to changes in community dynamics independent of other factors, including temperature. Some trends, such as higher alpha diversity, have been observed for slightly alkaline springs compared to acidic springs, as well as grouping of acid springs separately from neutral-alkaline spring, independent of temperature (Briggs et al., 2014; Sharp, Brady, et al., 2014). This indicates that pH

is an important driver of microbial community dynamics in geothermal environments.

1.5.3 Water

The origin of geothermal water can be atmospheric rainwater, groundwater or snow melt (Hreggvidsson et al., 2012). This water penetrates deep into the Earth, circulates and becomes concentrated in minerals and gases before resurfacing via heat and pressure (Cayol et al., 2015). Seasonally, temperatures and weather patterns can rapidly change, which alters the amount of water input into the underlying aquifer (Cowan et al., 2012). At the surface, this can lead to alterations in the chemical composition of geothermal waters and the inclusion of external environmental constituents, such as non-thermophilic species which can change the overall community composition (Cowan et al., 2012; Hreggvidsson et al., 2012; Briggs et al., 2014).

1.5.4 Elements, minerals and nutrient availability

The mechanisms which drive the formation of springs can be inferred through the relative concentrations of dissolved elements, such as chloride (Cl^-), bicarbonate (HCO_3^-) and sulfate (SO_4^{2-}) (Pope & Brown, 2014). As geothermal fluids ascend, Cl^- remains dissolved in the liquid body throughout boiling, dilution and mixing processes, therefore pools with a high concentration of Cl^- harbour fluids which have rapidly ascended and include little dilution from local groundwater (Pope & Brown, 2014). Chloride is an example of a conservative component of geothermal fluids. These pools are generally characterised by their deep and clear nature at the surface. During this ascent process, CO_2 and H_2S also dissociate into the steam fraction, and can interact with oxygen. If these reduced sulfur gases are oxidised, acid-sulfate springs form, whereas if this interaction does not occur, bicarbonate springs can form (Pope & Brown, 2014). Other components known as non-conservatives are influenced by the precipitation of alteration minerals and host rock interactions. An example is iron (Fe), which leaches out of host rocks in acid-sulfate springs. Generally, the relative concentrations of major components which reflect the reservoir conditions are stable over time, whereas components which are influenced by shallow processes, such as boiling and mixing, are less stable over time (Pope & Brown, 2014). Alterations to the chemical composition of these environments can cause shifts in the dominant species

observed; for example, the filamentous cyanobacterium, *Oscillatoria ampigranulata*, prefers warm, sulfide-rich waters compared to the sulfide-intolerant species, *Mastigocladus laminosus* (Boothroyd, 2009). The presence of substances such as arsenic can also lead to inhibition of enzymatic activity, with trivalent species inhibiting methanogenic organisms (Hetzer et al., 2007). Elements, especially sulfur or sulfur compounds such as thiosulfate, are commonly required for the growth of microbial species. Many *Aquificae*, *Proteobacteria* and *Crenarchaeota* species require sulfur, sulfur monoxide or thiosulfate as a sulfur source for growth (Shima & Suzuki, 1993; Kelly & Wood, 2000; Hetzer et al., 2008; Albers & Siebers, 2014; Greene, 2014; Nakagawa & Takai, 2014; Orlygsson & Kristjansson, 2014; Takai & Nakagawa, 2014). The chemistry of geothermal water can therefore be a controlling factor for the type of microorganisms found within different systems due to the requirement of certain elements for microbial growth. Certain elements, such as chloride and iron, can also provide insight into the stability and mechanisms driving the formation of geothermal hotspots (due to their participation in different processes as conservative and non-conservative elements).

1.5.5 Redox potential

A microbial cell is subject to the harsh geochemical conditions which are present in geothermal fluid. In order to remain functionally viable, an extremophile must thrive in these conditions or maintain the internal cell environment in a reduced state via chemical and phototrophic reactions (Matheron & Caumette, 2015). Redox potential (E_h) is the measure of a compound's ability to reduce (gain electrons) or oxidise (lose electrons) (Sand, 2003; Madigan et al., 2015). This is measured in millivolts and provides a value in reference to standards, H_2 and O_2 at neutral pH (Madigan et al., 2015). A redox reaction is formed of two components, known as a couple; the electron donor (low redox potential) donates electrons to the electron acceptor (high redox potential) (Madigan et al., 2015; Matheron & Caumette, 2015). The electron donor is thereby oxidised and the electron acceptor is reduced. During the transfer of electrons, energy is lost. This can be recovered and used to synthesize ATP through the phosphorylation of ADP (Matheron & Caumette, 2015). Therefore, the greater the difference between the electron donor

and acceptor (redox potential), the more energy is produced. Microorganisms are able to use oxidants (electron acceptors) for growth (Sand, 2003).

Microbial activity occurs between the range of -500 mV to +800 mV, which is split into narrower ranges for different types of microorganisms (Sand, 2003). Microorganisms are able to change the redox potential of fluid via the consumption of certain electron acceptors, such as oxygen (McArthur, 2006). In geothermal fluids, they are responsible for the oxidation of iron and arsenic and important in the oxidation of elemental sulfur to sulfuric acid (Nordstrom et al., 2005).

1.6 Taupō Volcanic Zone

1.6.1 Setting and formation

New Zealand is home to a multitude of geothermal features scattered across the Taupō Volcanic Zone (TVZ) in the North Island, which hosts a wide range of the physicochemical conditions discussed in the previous section (Boothroyd, 2009). The TVZ, located in the central North Island of New Zealand, includes more than 20 active geothermal systems which formed approximately one million years ago, and now contains over 4000 individual active geothermal features (Boothroyd, 2009; Wilson et al., 2012). This zone spans from Mt. Ruapehu in the Central Plateau, to White Island in the Bay of Plenty, and is approximately 300 km long (200 km land) and up to 60 km wide, as defined by vent positions and caldera structure boundaries (Figure 1.4) (Wilson et al., 1995; Boothroyd, 2009; Wilson et al., 2012). The TVZ is the dominant locus of late Pliocene to Quaternary volcanic activity resulting from subduction of the oceanic Pacific plate from the East, under the Australasian plate, on the East Coast of the North Island (Houghton et al., 1995; Wyering et al., 2014). As the Australian plate is pulled over the Pacific plate, an already weakened zone in the middle of the North Island is being stretched, allowing input of volcanic and geothermal activity to this area. The estimated heat output from the TVZ is approximately 4200 MW, with most of this energy concentrated along the eastern boundary within the Waikato region, which includes the longest river in New Zealand, the Waikato River and associated catchments (Bibby et al., 1995; Boothroyd, 2009). Individual geothermal features and microorganisms have already been studied and isolated from within the TVZ,

showing novel taxonomy and function (Hetzer et al., 2007; Stott et al., 2008; Ullrich et al., 2013).

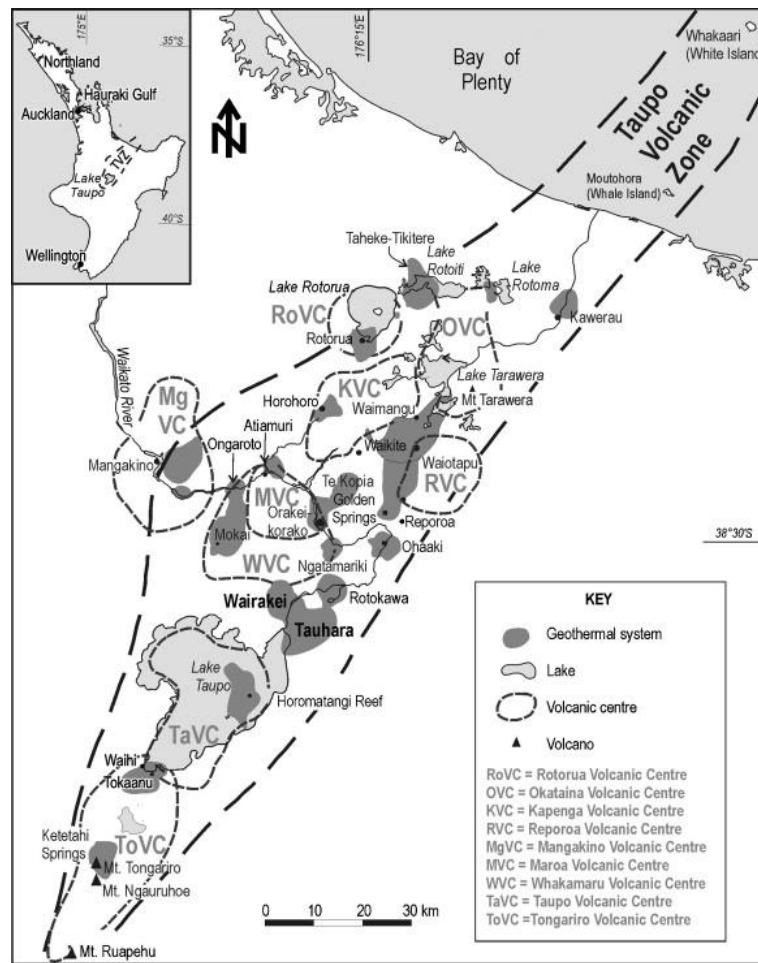


Figure 1.4: Taupō Volcanic Zone

Location of the TVZ within the North Island (top left insert) and enlarged overview of the locations of the geothermal systems within the TVZ. Sourced from Boothroyd, 2009.

1.6.2 TVZ temporal microbial studies

Several studies have been undertaken in the Waikite – Waiotapu – Waimangu geothermal system focusing on the microbial life and temporal variations in pool chemistry (Pope et al., 2004; Hetzer et al., 2007). Pope & Brown (2014) analysed temporal chemical data from 11 springs at Waiotapu and noted that depending on the nature of elements in geothermal fluid, whether they are conserved in the liquid state (e.g. Cl) or affected by shallow reservoir processes (e.g. Mg), indicates the likelihood of whether pool chemistry will change temporally. Conservative elements which are determined by the reservoir characteristics are unlikely to change over a two to eight-year period, compared to other elements

which participate in boiling, mixing and host rock interaction processes (Pope & Brown, 2014).

A focus site at Waiotapu is Champagne Pool, the largest geothermal feature within this field (~65 m in diameter), which formed over 900 years ago via a hydrothermal eruption (Hetzer et al., 2007). The temperature of the pool is approximately 75 °C with a pH of 5.5. The geothermal body is rich in CO₂, trace elements and sulfide minerals which form white silica sinter rims around the pool edges, also known as the Artist's Palette (Pope et al., 2004; Hetzer et al., 2007). No seasonal variations in temperature and pH were noted from 2004 to 2006 in a study by Hetzer et al. (2007), where water levels also remained stable. Although this pool has relatively low microbial diversity and biomass, species from the genera *Sulfolobus*, *Sulfurihydrogenibium* and *Paracoccus*, representing archaeal and bacterial domains, are present in this system (Hetzer et al., 2007; Kaur et al., 2015). Due to the high level of dissolved gases, including CO₂, H₂ and O₂, this is an ideal environment for hydrogen-oxidizing microorganisms such as *Sulfurihydrogenibium* species (Hetzer et al., 2007).

Diverse microbial communities are found on the sinter rims surrounding Champagne Pool (Pope et al., 2004). Several studies have shown that diurnal variations in chemistry are present, and possibly driven by microbial activity (Pope et al., 2004; Ullrich et al., 2013). Changes were typically noted during the night and early morning when antimony (Sb) and arsenic (As) concentrations were high during the daytime and low at night (Ullrich et al., 2013). It was suggested that alterations to fluid oxidation and chemistry occur downstream in a diurnal pattern due to the addition of oxygen via photosynthesis by microorganisms, as well as the metabolizing of thiosulfate and sulfide to form sulfate by sulfur-oxidizing bacteria (Pope et al., 2004; Ullrich et al., 2013). These studies outline the importance of combining ecological and geochemical investigations of geothermal environments, and demonstrate that diurnal variations in chemistry are present in the discharge of Champagne Pool (Pope et al., 2004).

A recent study by Ward et al. (2017) was undertaken at Inferno Crater Lake, Waimangu. Inferno Crater Lake has a thermal cycle which varies between 30-80 °C over a 40-60 day period, while pH remains stable (pH 2.0-2.5). Multiple processing methods including qPCR and 16S rRNA gene amplicon pyrosequencing were used to quantify and characterize the microbial community in parallel with geochemical

analyses (Ward et al., 2017). When the temperature exceeded 65 °C, the community was dominated by archaeal *Sulfolobus* species, while at lower temperatures the community was mixed. Temperature was the only significant variable associated with community dynamics (Ward et al., 2017). This study, unlike previous studies, was able to monitor microbial community dynamics in a natural model environment. It is a challenge in such an environment to interpret microbial community response with the variation in environmental factors linked or covariable, such as temperature and pH. This study was able to focus on temperature as the driving factor due to the stability of pH, which is important in temporal microbial research.

So far, these temporal microbial studies in the TVZ have focused on a single site, either Waiotapu or Waimangu (Hetzer et al., 2007; Ullrich et al., 2013; Pope & Brown, 2014; Ward et al., 2017). At Waiotapu, seasonal variations in physicochemical variables and microbial communities are not apparent, with an exception being the discharge from Champagne Pool (Pope et al., 2004; Ullrich et al., 2013). Sites at Waiotapu display a bimodal pH range from 2-4 and 5-8.5, with a gap between pH 4-5 (Pope & Brown, 2014). This pH range limits the microbial environments available to study at this site. At Inferno Crater Lake, the natural thermal cycle and constant pH provides an ideal environment to study the microbial community's response to temperature, while removing pH as a driving factor for temporal variations. Considering these studies, there is still a large knowledge gap in our understanding of microbial dynamics within the TVZ, with over 4000 active geothermal features to categorise. Many studies, like those described above, focus on temporal changes at single sites, or a limited number of sites within a single geothermal system. This removes the ability to study biogeographical patterns in microbial communities. Further temporal research needs to be focused on a range of geothermal systems in the TVZ with emphasis on varying pH.

1.7 Research aims

The aim of this Master's research was to investigate the temporal dynamics of microbial communities in association with physicochemical parameters of geothermal hotsprings of the TVZ, with an emphasis on varying pH. This research was part of a larger project established in 2012 called the "1,000 Springs Project" which was a collaborative project between GNS Science and the University of

Waikato, with the aim of studying the physicochemical and microbial diversity of 1,000 geothermal features within the TVZ (<http://1000springs.org.nz/>). This project was undertaken as part of the PhD of Jean Power at GNS Science Taupō. The information derived from this large-scale study is publicly available on the 1,000 Springs website (www.1000springs.org.nz), and provides the background for my thesis. The hypothesis of this research was; “temporal changes in physicochemical variables will elicit changes in the microbial communities inhabiting each of the target pools”. The aims of this Master’s research include; firstly, the selection and temporal sampling of target pools from the 1,000 Springs project database at a set temperature range and varied pH levels; secondly, the quantification and sequencing of microbial DNA and geochemical analysis from temporal samples, and finally, the comparison of geochemical and microbial community data at each site to determine any temporal shifts present, and if present, the investigation of the driving factors facilitating changes to microbial community composition and structure. The temperature range from which the target hotsprings were selected was 60-70 °C, while pH was at 3, 5, 7, and 9. These conditions were chosen to reduce the complexity of the system, in terms of reducing microbial diversity, and removing diurnal cycles from photosynthesis which occur at 50 °C and below.

The methods used in this thesis were developed for the 1,000 Springs project including field methods and laboratory protocols. Field sampling was undertaken by myself with the aid of Dr. Matthew Stott (Scientist), Jean Power (PhD student/Advanced Research Assistant) and Hanna Peach (Technician) from GNS Science Taupō. I prepared the microbial samples for sequencing that was run by John Longmore (University of Waikato). Geochemical analyses were processed at the Extremophile Research Group laboratory at GNS Science by myself, Jean Power, Karen Houghton and Hanna Peach, the New Zealand Geothermal Analytical laboratory, and at the University of Waikato by Steve Cameron and Ronald Ram.

Chapter Two:

Temporal dynamics of microbial communities in geothermal hotsprings of the Taupō Volcanic Zone

2.1 Introduction

A central goal of microbial ecology is to understand how environmental conditions can shape community composition and function. Different species exhibit optimal growth under different environmental conditions, and thus changes in these conditions can influence community dynamics. Communities can cluster in a consistent way, both temporally and spatially, with physicochemical parameters presented by the environment, which can elicit a shift in the community structure and function (Jackson et al., 2001; Macur et al., 2004; Swingley et al., 2012; Delgado-Serrano et al., 2014; Ward et al., 2017). In the past decade, a large number of studies in non-geothermal environments have explored this trend in regards to microbial biogeography at both spatial and temporal scales, and have identified the presence of geographically isolated communities based on local environmental conditions (Fierer & Jackson, 2006; Chu et al., 2010; Bahl et al., 2011; Griffiths et al., 2011; Fortunato et al., 2012; Pasternak et al., 2013; Zheng et al., 2013; Livermore & Jones, 2015; Salazar et al., 2015). Although limited, the few studies that have explored biogeographical patterns in geothermal systems also suggest that thermophilic communities are subject to harsh physiological conditions and historical dispersal limitation events, which can cause the formation of geographically isolated populations, both regionally and globally (Fenchel, 2003; Whitaker et al., 2003; Takacs-Vesbach et al., 2008; Herbold et al., 2014). One reason why few studies have explored temporal patterns in geothermal microbial communities (relative to spatial patterns), may be that the physicochemical conditions of geothermal systems were assumed to remain relatively stable over time (due to the consistent depth from which the source waters are derived). This assumption is supported by a number of geothermal studies (Ferris & Ward, 1997; Norris et al., 2002; Siering et al., 2013), while other studies highlight the presence

of temporal physicochemical and microbial community patterns (Lacap et al., 2007; Havig et al., 2011; Mackenzie et al., 2013). These opposing findings demonstrate the difficulty of forming a consensus on the presence of temporal microbial community dynamics at geothermal sites, highlighting the need for more research in this area.

The Taupō Volcanic Zone (TVZ) is an iconic feature of New Zealand's natural landscape, presenting a wide range of geothermal features ideal for improving our understanding of how microbial communities respond to changing physicochemical variables. Several geothermal features and microorganisms have already been studied and isolated from the TVZ, demonstrating novel taxonomy and function (Hetzer et al., 2007; Stott et al., 2008; Ullrich et al., 2013). However, temporal studies in the TVZ are limited and only focus on single sites. For example, Ullrich et al. (2013) reported diurnal variations in chemistry in the surrounding sinter rims of Champagne Pool, Waiotapu, where antimony and arsenic concentrations were highly concentrated during daytime and typically low at night - possibly driven by fluid oxidation and metabolic processes of sulfur-oxidizing bacteria (Ullrich et al., 2013; Pope & Brown, 2014). An additional study by Ward et al. (2017) explored the temporal fluctuations of Inferno Crater Lake, Waimangu, which has a thermal cycle from 30-80 °C over a 40-60 day period. They found that the community was dominated by archaea at temperatures above 65 °C, while at lower temperatures a mixed community of archaea and bacteria was present. Temperature was the only significant variable associated with community change in this study (Ward et al., 2017). These studies demonstrate the presence of dynamic physicochemical and microbial communities in the TVZ, however they did not explore the potential variation observed across multiple sites and varied pH. To investigate this, a more extensive temporal sampling of 12 hotsprings at consistent temperature (60-70 °C) and varied pH groups (3, 5, 7 and 9) was undertaken in four geothermal systems of the TVZ (Rotorua, Waiotapu, Atiamuri, Ohaaki). In this study, we tested two hypotheses surrounding the microbial community's response to changing physicochemical variables. The first hypothesis, based on previously published studies (Lacap et al., 2007; Briggs et al., 2014), was that temporal changes in physicochemical variables would drive changes to microbial community composition and structure. Further, we hypothesized that seasonal patterns in rainfall would influence changes in pool chemistry based on variable water input.

We tested the first hypothesis by combining microbial community (16S rRNA, Ion Torrent) and physicochemical analyses of water samples collected bimonthly (December 2015 to October 2016) from the target hotsprings. The physicochemical variables were correlated with changes observed in community abundances at both phylum and genus level to determine the primary physicochemical drivers at each site. The second hypothesis was tested by analysing and correlating rainfall and geothermal bore water datasets with the physicochemical variations at the target hotsprings. Together, these data can enhance our understanding of how temporal physicochemical patterns influence microbial community composition and structure in geothermal environments.

2.2 Materials and methods

2.2.1 Site selection and description

Hotsprings were chosen based on set criteria; within a temperature range of 60-70 °C and at a pH of 3, 5, 7, or 9; ease of access for sample collection over a two-day period and within a range of geothermal systems (<http://www.1000springs.org.nz/>). For this study, four geothermal systems within the TVZ were targeted for temporal analysis; Rotorua, Waiotapu, Ohaaki and Atiamuri (Figure 2.1).

The Rotorua geothermal system is located in the southern section of the Rotorua caldera which formed via the Mamaku ignimbrite eruption 220,000 – 230,000 years ago (Wood, 1992; Milner et al., 2003). The surface area of the geothermal field spans approximately 31 km² including Lake Rotorua (8 km²) (Bibby et al., 1995). Two of the primary geothermally active sites within the Rotorua geothermal system are Whakarewarewa/Te Puia and Kuirau Park. The geothermal fluids at these sites are generally alkaline, high chloride and low sulfate in chemistry and ascend through shallow rock units, where hydrology is highly influenced by the rock permeability (Wood, 1992; Scott & Cody, 2000). Kuirau Park is in the SE corner of the Rotorua geothermal field within the central Rotorua district (Wood, 1992; Glover & Mroczek, 1998; Scott & Cody, 2000). Whakarewarewa is located south east of Kuirau Park where upflow fluids of 250 °C are derived from fractured ignimbrites (Wood, 1992; Glover & Mroczek, 1998). The largest geyser in the southern hemisphere, Pohutu, is located at

Whakarewarewa/Te Puia and is part of the wider sinter terrace known as Geyser flat (Scott & Cody, 2000).

Waiotapu is part of the Waikite – Waiotapu – Waimangu geothermal system located 27 km south of Rotorua (Figure 2.1). The Waiotapu geothermal field has a surface area of approximately 17 km² encompassing a collection of geothermal features legally protected within the Waiotapu Thermal Wonderland tourist park (Hetzer et al., 2007; Pope & Brown, 2014; Waikato Regional Council, n.d; Waiotapu Thermal Wonderland, n.d). Geochemical analyses of the system's fluids indicate chloride-rich discharges, mostly controlled by the dissolution of basement rock and mineral interactions within the reservoir (Giggenbach et al., 1994; Pope & Brown, 2014). Hotspring pH across the Waiotapu geothermal field displays a bimodal distribution, with peaks at both pH 2-4, and pH 5-8.5, with a gap in the pH 4-5 range (Pope & Brown, 2014). This distribution pattern is also observed at YNP, USA, and reflects the different mechanisms governing spring formation and maintenance, possibly influenced by microbial metabolic activity (Fouke, 2011; Pope & Brown, 2014).

The Ohaaki geothermal system (Figure 2.1) is located 20 km north of Lake Taupō and spans approximately 14 km² (Bibby et al., 1995; New Zealand Geothermal Association, 2010b). Exploitation since the 1990's after the completion of the Ohaaki power station (Contact Energy) has led to impairment or destruction of the existing hot springs and geysers due to widespread surface flooding (New Zealand Geothermal Association, 2010b, 2010a; Waikato Regional Council, 2012). The main pool in this field is known as Ohaaki Ngawha, and is now classified as a significant feature within a developed geothermal system. Due to the disruption of input flow, Ngawha is now fed by a bore water system (Waikato Regional Council, 2012).

Atiamuri is the smallest of the selected geothermal systems spanning approximately 8 km² and located 40 km north of Lake Taupō (Figure 2.1) (New Zealand Geothermal Association, 2010b; Ratouis & Zarrouk, 2016). There are two main pools, the largest known as Whangapaoa, located in this field which produce dilute chloride water of up to 73 °C from deep sources of approximately 200 °C (New Zealand Geothermal Association, 2010b; Waikato Regional Council, 2012). Atiamuri is classed as a limited development geothermal system under the Waikato Region Plan (Waikato Regional Council, 2012).

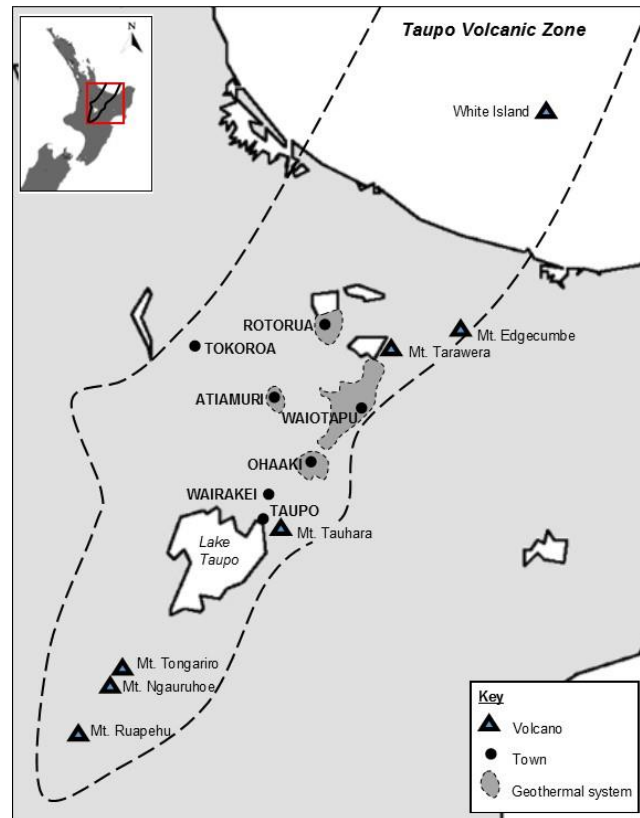


Figure 2.1 Taupō Volcanic Zone

Smaller inset map at top left shows relative position of TVZ in the North Island. Full map provides spatial context and relative size of target geothermal systems.

2.2.2 Field sampling and processing

Water samples were obtained from target hotspots every two months from December 2015 to October 2016. All equipment including the sampling pole and thermocouple were sprayed with 70 % v/v ethanol/water and aired before sampling to reduce cross contamination between sites. All vessels that would contain a microbiological sample were subject to stringent washing procedures, namely with detergent (Extran MA 05, Merck Millipore) and bleach (20% v/v bleach/water solution using 5% sodium hypochlorite), followed by a final autoclave step (122 °C for 20 min). At each site, temperature was first taken using a thermocouple probe attached to a sampling pole. All bottles (2 L and 500 mL polypropylene (PP) Nalgene bottles (Thermo Fisher), 250 mL PP Corning centrifuge tubes (Sigma Aldrich) and a 330 mL rubber-necked glass bottle) were triple rinsed with spring water prior to final water collection. Geothermal water was collected from deep springs using a custom-made 316 stainless steel water column sampler (Figure 2.2).

Shallow pools were sampled using a sterile 500 mL PP Nalgene bottle connected to a clamped sampling pole. At each site, a 2 L PP Nalgene bottle was collected for microbial diversity analysis, a 500 mL PP Nalgene bottle for physical parameters (pH, redox potential, conductivity, total dissolved solids, turbidity, and dissolved oxygen), 250 mL PP Corning tube for soil analysis, a 330 mL rubber-necked glass bottle for geochemical analysis (hydrogen sulfide (H₂S), bicarbonate (HCO₃⁻) and chloride (Cl⁻)) and a 50 mL syringe sample (Terumo) for dissolved gas content. The syringes were first rinsed with spring water before ~60 mL water was filtered *in situ* into a sterile syringe via a three-way stopcock. Five millilitres of nitrogen gas (N₂) was then added to the syringe (dispensed to 50 mL, ensuring no air bubbles present) and left to equilibrate. Sediment samples from each spring were also collected using the clamped sampling pole and 250 mL PP Corning tube and placed in an insulated bin with ice packs for transport back to the laboratory. Metadata was collected using a custom-made application for the 1,000 Springs Project (<http://1000springs.org.nz/methodologies>). Metadata included feature name, location details (including GPS coordinates), description, photographs and sketches, with each entry automatically linked to the corresponding sample identification. This allowed for zero errors in transcribing data.



Figure 2.2: Sampling procedure using specialized water column sampler and personal protective equipment at Ohaaki geothermal field

2.2.3 Post-sampling laboratory processing

In the laboratory, syringe gas volumes were recorded immediately before the gas was pushed into a vented gas bag for downstream analysis. The 2L Nalgene samples were filtered through a 0.22 μm Sterivex-GP PES column filter (Millipore) via a battery operated Masterflex peristaltic pump system (Cole-Parmer, NZ). Multiple filters were used for the more turbid samples to ensure adequate biomass was collected from the water columns. Filters were stored at $-20\text{ }^{\circ}\text{C}$ until DNA extraction. Filtered water was collected into three 50 mL centrifuge tubes and two 15 mL centrifuge tubes, one of which was acidified with 300 μL conc. analytical grade nitric acid (HNO_3) and the other alkalified with 500 μL 2.4 M sodium hydroxide (NaOH). Two 50 mL tubes, both 15 mL tubes and the sediment tube for each spring were stored at $4\text{ }^{\circ}\text{C}$, and the remaining 50 mL tube was stored at $-20\text{ }^{\circ}\text{C}$. Physical properties including pH, redox potential, conductivity, total dissolved solids, turbidity, and dissolved oxygen were measured using the 500 mL Nalgene sample with a multiparameter field meter (Hanna Instruments) in the laboratory. The 330 mL rubber-sealed bottles were stored at $4\text{ }^{\circ}\text{C}$ until processing (within 24 h).

2.2.4 Geochemical analyses

Geochemical analyses were undertaken to examine potential correlations between environmental parameters and microbial communities at each site. Analyses were performed at either the New Zealand Geothermal Analytical Laboratory (NZGAL) or the Extremophile Research Group (ERG) laboratory, both located at GNS Science Taupō, or at the University of Waikato (UoW) Hamilton. Gases stored in the vented gas bags were analysed using a Peak Performer gas chromatograph with a flame ionization detector (Peak Laboratories, CA, USA) for methane (CH_4) and a Peak Performer gas chromatograph with a reducing compound photometer (Peak Laboratories, CA, USA) for hydrogen (H_2) and carbon monoxide (CO). Ferrous iron (Fe^{2+}) was analysed by colorimetric spectroscopy, using a Halo VIS-10 visible spectrophotometer (Dynamica, Clayton, Australia) (Wilson, 1960). The 330 mL rubber-necked bottles were used to analyse H_2S by an iodometric method, using a Halo DB-30 ultraviolet-visible double beam spectrophotometer (Dynamica, Clayton, Australia), and sulfate (SO_4^{2-}) on a Dionex ICS-5000+ ion chromatograph (ThermoFisher, Auckland). HCO_3^- was measured through

automated titration (Mettler Toledo, Hamilton), while Cl⁻ was analysed by potentiometry (Mettler Toledo, Hamilton). (<https://www.gns.cri.nz/Home/Services/Laboratories-Facilities/New-Zealand-Geothermal-Analytical-Laboratory/Analytical-Methods>). Filtered and acidified water samples (15 mL) were diluted 1/50 by weight using 1 g of sample, 48 g reverse osmosis (RO) water, and 1 g of HNO₃. Diluted samples were used for elemental analysis by inductively coupled plasma mass spectrometry (ICP-MS) on a PerkinElmer ELAN DRCII model (PerkinElmer, USA). NH₄⁺, PO₄³⁻, NO₂⁻, NO₃⁻ were analysed by Flow Injection Analysis on a Lachat 8500 Series II analyser (DKSH, Auckland) using the filtered samples (-20 °C).

2.2.5 Extraction and quantification of microbial DNA

Genomic DNA was extracted from the Sterivex column filters (Millipore) following a modified CTAB protocol developed for the 1,000 Springs Project (<http://www.1000springs.org.nz/methodologies>). Briefly, the filters were thawed on ice, and 500 µL 0.8% skim milk powder added to the filter inlet (Takada-Hoshino & Matsumoto, 2004). Filters were recapped and incubated at 65 °C for 10 min at 150 RPM in an orbital mixer (Ratek). To the filter inlet, 0.4 mL of cetyl trimethylammonium bromide buffer, 0.2 mL phosphate-buffered saline (100 mM) and 0.1 mL sodium dodecyl sulfate (10%) lysis buffer was added. The CTAB buffer contained 2% cetyl trimethylammonium bromide, 1% polyvinyl pyrrolidone, 100 mM Tris-HCl, 1.4 M NaCl and 20 mM EDTA. Filters were recapped and glued, vortexed on low for 1 min and placed in a rack (Figure 2.3). Filters were then reincubated at 65 °C for 45 min in an orbital mixer at 150 RPM (turning filters several times). The CTAB extraction buffer was then pushed through the filter into a 1.5 mL centrifuge tube using an air-filled 10 mL luer-lok syringe. New CTAB buffer (0.7 mL) was then added to the filter inlet, and filters reincubated at 65 °C for an additional 15 min as before. The remaining CTAB buffer was collected in new 1.5 mL centrifuge tube using the same 10 mL luer-lok syringe. Equal volumes of chloroform: isoamyl alcohol (24:1) were added to each centrifuge tube, vortexed to form an emulsion and placed in the centrifuge at 10,000 RCF for 12 min at 4 °C. The aqueous layer was collected into a new tube. This step was repeated with 300 µL chloroform: isoamyl alcohol (24:1) and a final aqueous layer was collected into new 1.5 mL centrifuge tubes.

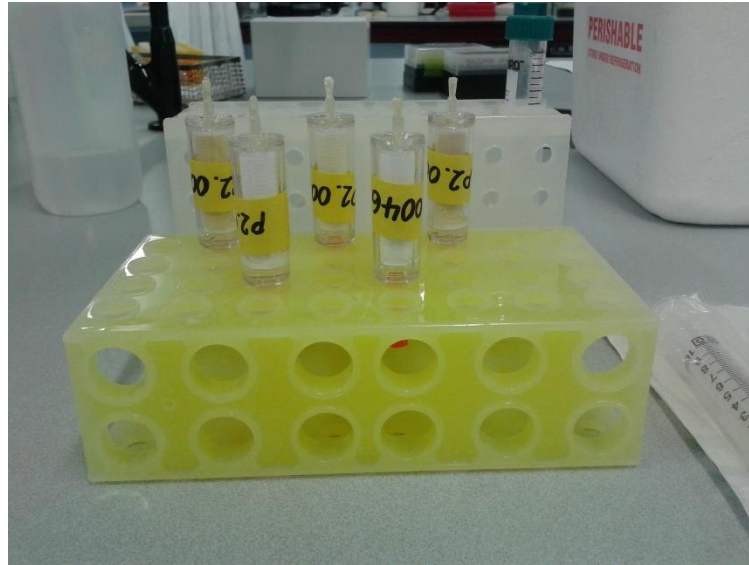


Figure 2.3: Labelled and recapped Sterivex column filters (Millipore) used in CTAB extraction protocol

To precipitate the DNA an equal volume of isopropanol (C_3H_8O) and 1:2 ratio of sodium chloride (5 M) were added to the tubes, mixed by 20 inversions and incubated overnight at $-20\text{ }^{\circ}\text{C}$. Samples were then placed in the centrifuge at 13,200 RCF for 20 min at $4\text{ }^{\circ}\text{C}$, the supernatant discarded, and the pellet left undisturbed. The pellet was then washed with 1 mL 70% AR grade ethanol and spun for 1 min at 13,200 RCF. Ethanol was pipetted off, avoiding the pellet, and the tubes were dried in a speed vacuum (Thermo Fisher Scientific, USA) for 4 – 15 min (checking samples every two min). Finally, pellets were re-suspended in $30\text{ }\mu\text{L}$ sterile 1X TE (10 mM Tris, 1mM EDTA) by pipetting up and down and vortexing. The two centrifuge tubes per sample were pooled into a single tube. DNA was quantified using a HS Qubit 2.0 (Life Technologies, Auckland) and stored at $-20\text{ }^{\circ}\text{C}$ until amplification.

2.2.6 Ion Torrent preparation

Polymerase chain reaction (PCR) and the Ion PGM System for Next-Generation-Sequencing (Ion Torrent) (Thermo Fisher) pipeline were used to generate the DNA sequence needed to categorise microbial taxa present in each sample. The V4 region of the 16S rRNA gene was amplified using the Ion Torrent primer set F515 (5'-GTGCCAGCMGCCGCGGTAA-3') and R926 (5'-CCACTACGCCTCCGCTTTCCTCTCTATGGGCAGTCGGTGATCCGYCAAT

TYMTTTRAGTTT-3') (Caporaso et al., 2011). PCR reactions (25 μ L) were performed in triplicate on each sample using 0.2 μ M of both forward and reverse primers, 0.048 μ g/ μ L BSA, 0.24 mM dNTPs, 1.2X PCR buffer, 3 mM MgCl₂, 0.6 U TAQ and 1 ng DNA. Prior to DNA addition, the PCR master mix was treated with ethidium monoazide bromide (EMA, 1 mg/mL stock) to remove reagent introduced exogenous DNA contamination following the method of Ruekert & Morgan, 2007. The amount of EMA added varied for each batch of the reagent made. This was determined by serial dilution and the resultant highest concentration that did not inhibit PCR (a 1/100 dilution was typical). One minute dark and light incubations on ice followed. Thermocycler conditions were held at 94 °C for 3 min, followed by 30 cycles of 94 °C for 45 sec, 53 °C for 1 min, and 72 °C for 1.5 min, with a final incubation at 72 °C for 10 min (Caporaso et al., 2011).

The resulting amplicons for each sample were pooled and the concentration normalized using a SequelPrep Normalization Kit (Life Technologies, Auckland). Briefly, 25 μ L of the pooled PCR product was added to a plate well with an equal volume of binding buffer, and incubated at room temperature for 1 h. Amplicon/binding buffer mixture was removed, and plate wells were washed with 50 μ L of wash buffer to remove residual PCR product. The wash buffer was discarded and amplicons eluted with 20 μ L of normalized Elution buffer and incubated at room temperature for 5 min. Samples were collected into final centrifuge tubes, before pooling 2 μ L of each sample and storing at 4 °C until sequencing.

2.2.7 Next Generation Sequencing

Next-Generation sequencing (NGS) using the Ion PGM System allowed multiple samples to be sequenced and run in parallel. Sequencing was undertaken at the DNA Sequencing Facility at UoW Hamilton using the Ion PGM system with a Ion 318v2 chip (Life Technologies). Raw sequences were trimmed and quality filtered through a pipeline using mothur and USEARCH (Schloss et al., 2009; Edgar, 2010). Raw sequences were first filtered in mothur to remove short and long reads and homopolymers. This range was set between 375 and 425 bp and homopolymer limit set to 6 bases. A total of 4,303,543 reads were processed in this initial filtering step with 2,134,446 reads being retained. Strict primer matching was enforced in mothur using a python script which returned 2,074,253 reads (Schloss

et al., 2009). Sequences were then quality filtered using USEARCH (ver 9) with a maximum expected error of 1%. Sequences were further truncated to 350 bp, dereplicated to find duplicated (replicated) sequences before removing all unique sequences. Reads were then clustered (97% similarity) followed by chimera detection using uchime_ref based against the SILVA 128 SSURef Nr99 database (Quast et al., 2013). A total of 1189 OTU's were identified and 188 chimeras discarded. Reads were then mapped to OTU's (97%) and an OTU table generated (Edgar, 2010). The final read count was 1,621,964, with an average of 25,745 (mean) reads per sample.

2.2.8 Data analyses

Sequence data were processed using a combination of QIIME (Caporaso, 2010) and R for statistical analysis (R Core Team, 2016). Taxonomic summaries for each site were generated and plotted in QIIME (Caporaso, 2010). Sequencing and physicochemical databases were brought together in R Studio using the "phyloseq" package (McMurdie & Holmes, 2013). Covariance and Pearson's correlation tests were completed in R to assess the relative variation between physicochemical variables and dominant phyla at each hotspring across the temporal samples (R Core Team, 2016).

2.2.9 Meteoric data analyses

Rainfall and geothermal bore water datasets were obtained for the time course of this study to associate with patterns observed in the physicochemical conditions of the sampled hotsprings. Geothermal bores from Rotorua were selected based on their proximity to the sampling areas. Rainfall data were downloaded from the NIWA website and geothermal bore water data were downloaded from the Bay of Plenty Regional Council website (Bay of Plenty Regional Council, 2015; NIWA, 2016). Daily rainfall and bore water level measurements were processed in Microsoft Excel. Links between physicochemical variables and rainfall were determined by observation only, not based on statistical measures.

2.3 Results

2.3.1 Hotspring selection and sampling

Temporal sampling was undertaken for 12 target springs (every two months) from the TVZ between December 2015 and October 2016 (Supplementary Table 4.1 and Table 2.2). Sites were chosen based on temperature, pH and accessibility using the 1,000 Springs Project (<http://1000springs.org.nz>). All target springs selected were within the temperature range of 60-70 °C. This was to provide consistency between sites and to reduce the overall diversity of the microbial communities (as diversity often decreases with increasing temperature). It was hypothesized that community changes would be more apparent in less complex community structures. By selecting this temperature range we could also remove photosynthesis as a driver for community composition variation. Three springs were chosen at each of the following groupings; pH 3, 5, 7, and 9. The initial selection of candidate springs was conducted using the 1,000 Springs Database. The candidate springs were then measured in the field to ensure the final spring selection was based on *in situ* pH values that were as close to the target values as possible. By selecting hotsprings at a consistent temperature and varied pH it allowed us to examine temporal changes of community composition with emphasis on varying pH. The hotsprings were categorized into pH groups (Table 2.1). Locations included Rotorua, Atiamuri, Waitapu and Ohaaki geothermal systems. Eight target springs were selected in the Rotorua geothermal field (Figure 2.4). These hotsprings were inclusive of all pH's. Two target springs were selected in the Waitapu geothermal field (pH 5 group), and one spring in each of the Atiamuri (pH 7 group) and Ohaaki (pH 9 group) geothermal fields (Figure 2.5). One of the target springs in Kuirau Park (Kui2) was sampled but unable to be processed for sequencing due to time constraints (the physicochemical conditions for this spring are presented in Appendix 4.2). Field sketches and photos of sampling points are presented in Supplementary Figures 4.1 and 4.2.

Table 2.1: Target hotsprings within pH Groups

Spring	Geothermal field	Location	pH Group	Initial temperature (°C)
Whkr1	Whakarewarewa Village	Rotorua	3	60.1
Whkr3	Whakarewarewa Village	Rotorua	3	71
TeP	Te Puia (Te Whakarewarewa Village)	Rotorua	3	71.6
Wai01	Waiotapu Thermal Wonderland	Waiotapu	5	64.9
Wai02	Waiotapu Thermal Wonderland	Waiotapu	5	59.4
Kui3	Kuirau Park	Rotorua	5	59.2
Whgpa	Atiamuri General	Atiamuri	7	63.3
Kui1	Kuirau Park	Rotorua	7	62.2
Kui2	Kuirau Park	Rotorua	7	70.6
Whkr2	Whakarewarewa Village	Rotorua	9	69.5
Whkr4	Whakarewarewa Village	Rotorua	9	63.4
Ohaaki	Ohaaki General	Ohaaki	9	70

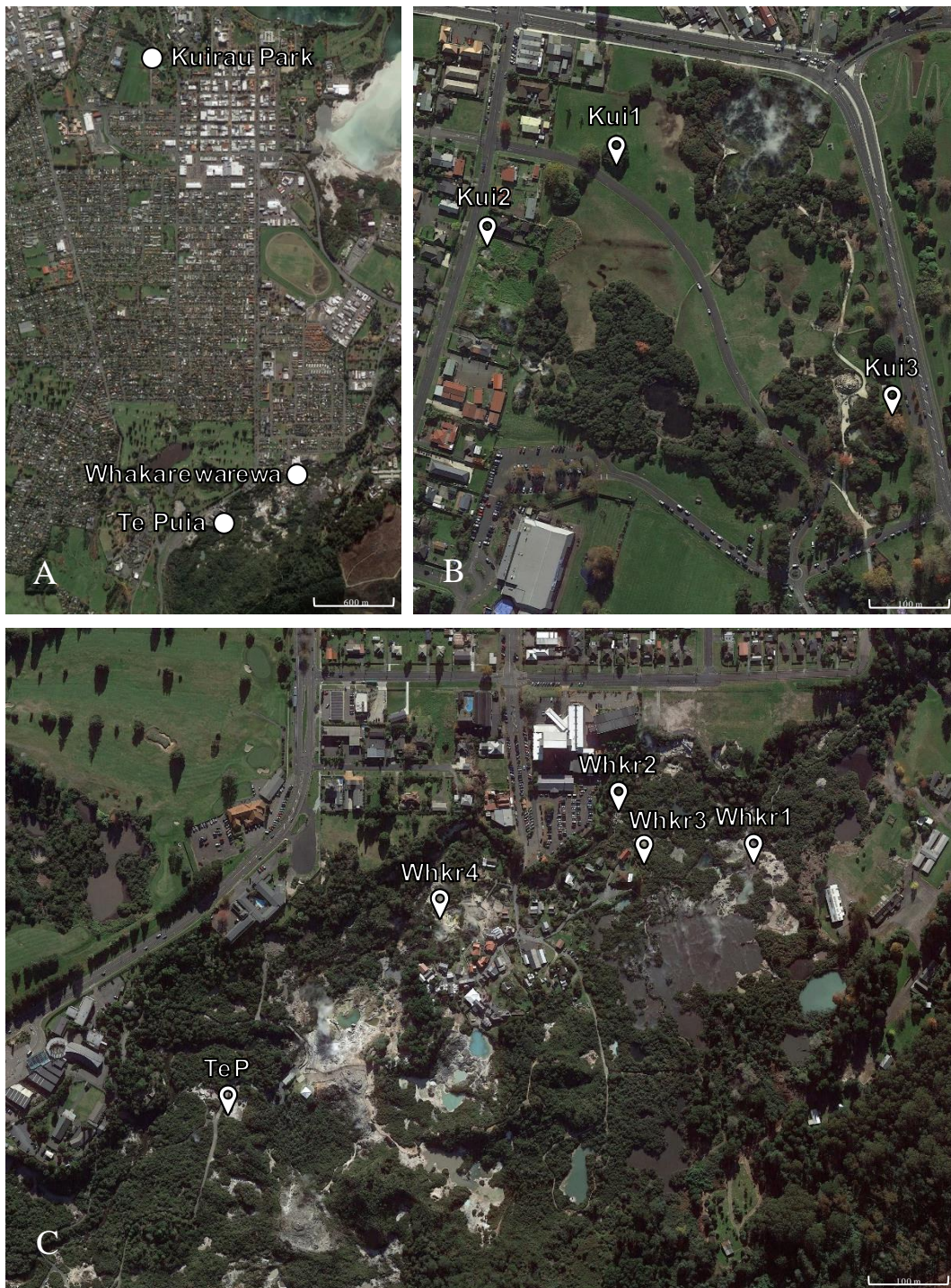


Figure 2.4: Location of geothermal springs within the Rotorua geothermal system

(A) Relative positions of Rotorua geothermal locations (B) Kuirau Park springs (C) Te Puia and Whakarewarewa Village springs. (Source: Google Earth)



Figure 2.5: Location of geothermal springs within Waiotapu, Ohaaki and Atiamuri geothermal systems

(D) Waiotapu springs; (E) Ohaaki spring; (F) Atiamuri spring. (Source: Google Earth)

Table 2.2: Overview of spring locations and descriptions

Spring	Location	pH Group	Geothermal System	Location Latitude	Location Longitude	Description	Sampling dates
Whkr1	Whakarewarewa Village	3	Rotorua	38° 9'42.02"S	176°15'34.92"E	Small stream into V-notch catchment overflowing into lower spring. Grey/brown sediment at bottom. Foam on surface and multiple inputs. Public, paid entry site.	Feb, April, June, Aug, Oct
Whkr3	Whakarewarewa Village	3	Rotorua	38° 9'42.03"S	176°15'29.62"E	Small grey spring in hollow with sinter embankment on one side with overhanging manuka and kanuka trees. Dead branches visible in and around spring. Public, paid entry site.	Dec, Feb, April, June, Aug, Oct
TeP	Te Puia (Te Whakarewarewa Village)	3	Rotorua	38° 9'51.28"S	176°15'9.71"E	Medium, turbid grey spring with several islands in the middle. Most edges surrounded by hard sinter and vegetation. Public, paid entry site.	Feb, April, June, Aug, Oct
Wai01	Waiotapu Thermal Wonderland	5	Waiotapu	38°21'42.58"S	176°22'10.59"E	Oyster springs at Waiotapu. Light green cloudy spring with slight overflow onto surrounding sinter terrace. No surrounding vegetation. Public, paid entry site.	Dec, Feb, April, June, Aug, Oct
Wai02	Waiotapu Thermal Wonderland	5	Waiotapu	38°21'30.23"S	176°22'10.42"E	Large, yellow/green spring at the edge of Artist's Palette. Yellow precipitate around edges and overflow onto surrounding sinter. No overhanging vegetation. Public, paid entry site.	Dec, Feb, April, June, Aug, Oct
Kui3	Kuirau Park	5	Rotorua	38° 7'54.95"S	176°14'44.07"E	Small, stagnant spring in hollow surrounded by a small patch of vegetation fenced and overhanging the spring. Leaf matter at bottom of spring with intermittent bubbling and sheen formed on surface. Free, public access site.	Dec, Feb, April, June, Aug, Oct
Whgpa	Atiamuri General	7	Atiamuri	38°21'46.8"S	176°03'00.0"E	Large, deep blue/green spring with thick sinter rims covered in orange biofilm. Scattered manuka and kanuka bushes around edges. Outflow to the West. Free, public access site.	Dec, Feb, April, June, Aug, Oct
Kui1	Kuirau Park	7	Rotorua	38° 7'48.13"S	176°14'34.46"E	Large spring surrounded by small patch of manuka and kanuka vegetation. Small outflow into an adjacent spring. Build-up of brown biomass throughout and surrounding the spring. Free, public access site.	Dec, Feb, April, June, Aug, Oct
Kui2	Kuirau Park	7	Rotorua	38° 7'50.84"S	176°14'29.94"E	Large clear blue spring with the remains of a house within it. Fence and long grass surrounding the spring. No visible outputs. Physicochemical dataset complete (see Appendix 4.2). Sequencing not complete.	Dec, Feb, April, June, Aug, Oct
Whkr2	Whakarewarewa Village	9	Rotorua	38° 9'40.04"S	176°15'28.40"E	Long spring in rocky crevasse that flows into Puarenga stream. Input from medium hot spring above. Overhanging manuka bushes and white foam on surface of spring. Public, paid entry site.	Dec, Feb, April, June, Aug, Oct
Whkr4	Whakarewarewa Village	9	Rotorua	38° 9'44.15"S	176°15'19.90"E	Waipuru Spring at Whakarewarewa. Small clear blue/green spring with surrounding hard sinter. Manuka and kanuka on one side with some dead vegetation and rocks at the bottom and surrounding the spring. Public, paid entry site.	Dec, Feb, April, June, Aug, Oct
Ohaaki	Ohaaki General	9	Ohaaki	38°31'0.48"S	176°18'36.36"E	Large blue silica-rich spring with thick white sinter rims. Outflow from spring joins Waikato river. Some sparse manuka bushes surround the edges. Spring fed by bore water input. Privately owned site.	Feb, April, June, Aug, Oct

2.3.2 Observed patterns in spring temperature and pH

Although hotsprings were selected to be as close as possible to the temperature and pH windows based on the 1,000 Springs database, variations in these parameters were observed across the temporal samples (Figure 2.6 and Supplementary Table 4.2). General observations of the four different pH Groups are given below:

pH 3 GROUP

Two out of three springs (TeP, Whkr1) in the pH 3 group had consistent pH across temporal samples at pH ~2.5 and pH 3, while temperature dropped by 9.8 °C and 9.3 °C between February and August, respectively. Whkr3 showed the largest increase in pH over the temporal samples, from pH 3.37 to pH 4.77. Temperature at this site steadily decreased by 10.4 °C from December to October.

pH 5 GROUP

Wai01 and Wai02 had similar and consistent pH and temperature measurements across the temporal samples at ~pH 4.8 and 66 °C. The pH at Kui3 was consistent at ~pH 5.2 across December to April before decreasing across June and August to pH 4.47 in October. Temperature at this site decreased significantly between February and August (15.2 °C).

pH 7 GROUP

pH at Whgpa was the same in December and October (pH 7.55) with small fluctuations between pH 7.3 and pH 7.08 across February to August. Temperature was ~62.8 °C across the temporal samples, with an increase in February (65.3 °C) and decrease in August (60.8 °C). Kui1 and Kui2 pH and temperature measurements were consistent across the temporal samples (pH ~6.7 and ~61°C, pH ~7.1 and ~70 °C, respectively).

pH 9 GROUP

Temperature at Whkr2 was higher across the first two temporal samples at ~69.6 °C before decreasing to ~65 °C across the final three samples. Following a similar trend to temperature, pH was higher across the first three temporal samples (December – April) at pH ~8.95 before declining to ~pH 8.75 across the final three samples. Temperature at Whkr4 initially decreased from 63.4 °C in December to 61.1 °C in April before increasing significantly (19.5 °C) to 80.6 °C in October. pH was consistent at ~pH 8.35 across December, February, April and October, with

lower measurements (pH 7.98, pH 7.76) recorded in June and August. Temperature and pH at Ohaaki followed similar trends. Temperature was stable across February and April (70, 70.3 °C) then declined to 65 °C in August before increasing to 67.9 °C in October. pH increased from pH 8.84 – 9.04 (March to April) before declining to pH 8.84 in August and increasing to pH 9.0 in October.

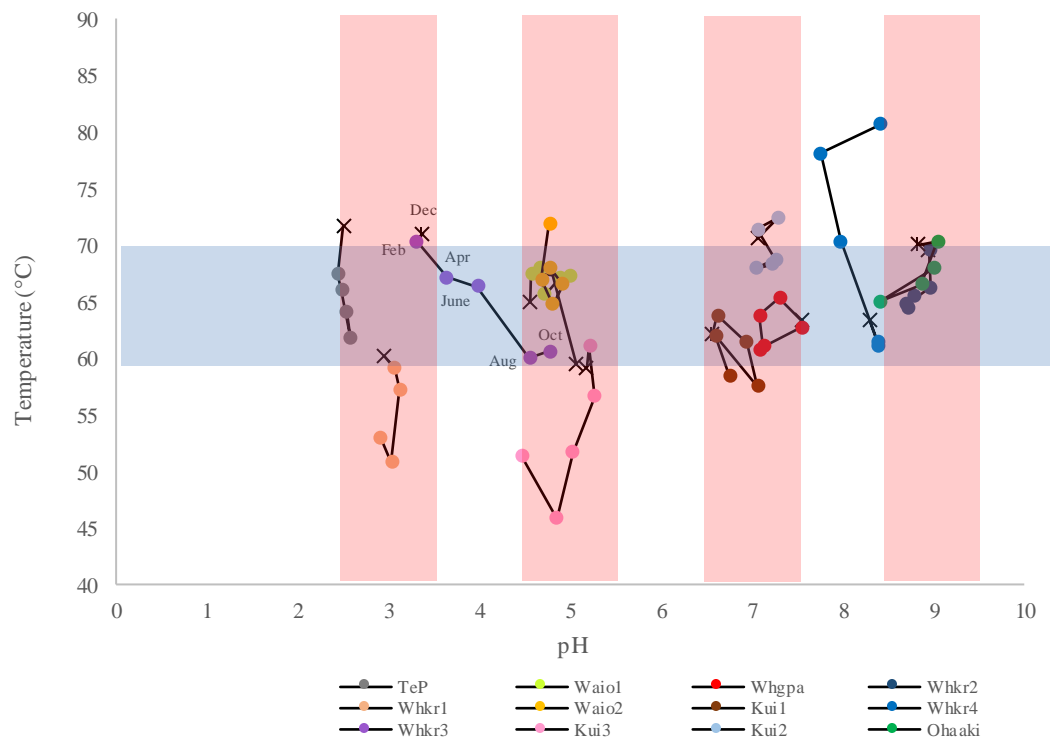


Figure 2.6: Temperature vs. pH scatterplot of target hotsprings across temporal samples

Black crosses indicate the first samples taken. Each subsequent dot represents the next sample collected in temporal order. Lines show connections between temporal samples across the study period (Whkr3 for example). Targeted temperature window indicated by blue shading and pH Groups highlighted by pink shading.

2.3.3 Relating spring community variation to physicochemical conditions

To assess the variation in microbial community structure and how it relates to the observed physicochemical conditions, changes in the relative abundances (%) of phyla across temporal samples were firstly determined at each site and significant temporal changes in community composition highlighted. Pearson’s correlation coefficient tests were then implemented between dominant phyla (>2% of reads) and the typical physicochemical conditions of each hotspring (Table 2.3). Of the 43

chemical elements, nutrients and gases measured in each sample, eight chemical components and gases (plus temperature and pH) were assessed (Appendix 4.2). The selection of these eight variables was based on; their variance and observational changes in concentrations across temporal samples as well as their covariance and correlation with the dominant phyla at each site. See Appendix 4.2 for raw chemical datasets. The results of individual spring analyses are presented below in their respective pH groups.

Table 2.3: Summary table of Pearson’s correlation coefficient association test between dominant phyla and environmental variables at target springs

Green highlighted squares indicate positive correlation (>0.7) and pink highlighted squares indicate negative correlation (>-0.7)

P values less than 0.05 are in bold text. Black squares highlight sites where variables were below detection limits across the temporal samples

Site	pH Group	Dominant phyla	Temperature		pH		Sodium		Sulfate		Potassium		Total sulfur		Silica		Methane		Chloride		Bicarbonate	
			Corr	P test	Corr	P test	Corr	P test	Corr	P test	Corr	P test	Corr	P test	Corr	P test	Corr	P test	Corr	P test	Corr	P test
Whkr1	3	<i>k_Bacteria;p_Aquificae</i>	0.767	0.13	-0.268	0.66	0.834	0.08	0.443	0.46	0.907	0.03	0.815	0.09	0.381	0.53	-0.643	0.24	-0.008	0.99	-	-
		<i>k_Bacteria;p_Proteobacteria</i>	-0.747	0.15	0.278	0.65	-0.731	0.16	-0.395	0.51	-0.824	0.09	-0.707	0.18	-0.343	0.57	0.545	0.34	0.139	0.82	-	-
		<i>k_Bacteria;p_Thermotogae</i>	-0.502	0.39	0.235	0.70	-0.910	0.03	-0.594	0.29	-0.876	0.05	-0.939	0.02	-0.490	0.40	0.758	0.14	-0.615	0.27	-	-
Whkr3	3	<i>k_Archaea;p_Crenarchaeota</i>	0.928	0.01	-0.946	0.004	-0.110	0.84	0.759	0.08	0.906	0.01	0.380	0.46	-0.643	0.17	-0.601	0.21	0.585	0.22	0.396	0.44
		<i>k_Bacteria;p_Aquificae</i>	-0.852	0.03	0.899	0.02	0.018	0.97	-0.686	0.13	-0.895	0.02	-0.426	0.40	0.526	0.28	0.557	0.25	-0.510	0.30	-0.541	0.27
TeP	3	<i>k_Archaea;p_Crenarchaeota</i>	-0.167	0.79	0.689	0.20	-0.093	0.88	0.069	0.91	-0.126	0.84	-0.684	0.20	-0.032	0.96	-0.186	0.76	0.525	0.36	-0.775	0.12
		<i>k_Archaea;p_Euryarchaeota</i>	0.030	0.96	-0.662	0.22	-0.058	0.93	-0.004	1.00	-0.029	0.96	0.562	0.32	-0.101	0.87	0.198	0.75	-0.504	0.39	0.700	0.19
		<i>k_Bacteria;p_Aquificae</i>	-0.250	0.69	-0.250	0.69	-0.319	0.60	-0.322	0.60	-0.290	0.64	0.389	0.52	-0.326	0.59	-0.163	0.79	-0.844	0.07	0.872	0.05
Wao1	5	<i>k_Bacteria;p_Aquificae</i>	-0.571	0.24	-0.547	0.26	0.430	0.40	-0.184	0.73	0.555	0.25	0.044	0.93	0.260	0.62	-0.840	0.04	0.212	0.69	0.476	0.34
Wao2	5	<i>k_Bacteria;p_Aquificae</i>	0.859	0.03	-0.569	0.24	-0.438	0.38	0.688	0.13	-0.351	0.50	0.497	0.32	-0.255	0.63	-0.660	0.15	-0.356	0.49	-0.815	0.05
Kui3	5	<i>k_Bacteria;p_Aquificae</i>	0.476	0.34	-0.024	0.96	0.441	0.38	0.901	0.01	0.523	0.29	0.282	0.59	0.583	0.23	-0.098	0.85	0.377	0.46	-0.487	0.33
		<i>k_Bacteria;p_Proteobacteria</i>	-0.438	0.39	0.050	0.93	-0.420	0.41	-0.916	0.01	-0.496	0.32	-0.273	0.60	-0.555	0.25	0.124	0.81	-0.357	0.49	0.455	0.36
Whgpa	7	<i>k_Bacteria;p_Armatimonadetes</i>	0.450	0.37	0.929	0.01	0.426	0.40	-0.945	0.004	0.383	0.45	-	-	0.576	0.23	-0.073	0.89	0.678	0.14	-0.570	0.24
		<i>k_Bacteria;p_Deinococcus-Thermus</i>	0.566	0.24	-0.485	0.33	0.453	0.37	0.330	0.52	0.456	0.36	-	-	-0.826	0.04	0.915	0.01	-0.301	0.56	0.560	0.25
Kui1	7	<i>k_Bacteria;p_Aquificae</i>	0.182	0.73	0.331	0.52	0.213	0.69	-0.035	0.95	0.186	0.72	-0.186	0.72	0.041	0.94	-0.262	0.62	0.586	0.22	-0.385	0.45
Whkr2	9	<i>k_Bacteria;p_Aquificae</i>	0.815	0.05	0.731	0.10	0.539	0.27	-0.750	0.09	0.717	0.11	-0.245	0.64	0.168	0.75	0.137	0.80	-0.109	0.84	-0.487	0.33
		<i>k_Bacteria;p_Proteobacteria</i>	-0.953	0.003	-0.851	0.03	-0.440	0.38	0.808	0.05	-0.790	0.06	0.411	0.42	0.102	0.85	-0.446	0.38	-0.032	0.95	0.657	0.16
Whkr4	9	<i>k_Bacteria;p_Aquificae</i>	0.935	0.01	-0.390	0.44	-0.713	0.11	0.356	0.49	-0.730	0.10	-	-	0.673	0.14	-0.106	0.84	0.251	0.63	-0.561	0.25
		<i>k_Bacteria;p_Deinococcus-Thermus</i>	-0.896	0.02	0.340	0.51	0.774	0.07	-0.388	0.45	0.792	0.06	-	-	-0.628	0.18	0.060	0.91	-0.132	0.80	0.618	0.19
		<i>k_Bacteria;p_Thermodesulfobacteria</i>	0.903	0.01	-0.331	0.52	-0.975	0.001	0.020	0.97	-0.980	0.001	-	-	0.501	0.31	0.132	0.80	0.409	0.42	-0.817	0.05
Ohaaki	9	<i>k_Bacteria;p_Aquificae</i>	0.015	0.98	-0.359	0.55	0.664	0.22	0.221	0.72	-0.147	0.81	-	-	-0.376	0.53	0.201	0.75	0.037	0.95	0.665	0.22
		<i>k_Bacteria;p_Deinococcus-Thermus</i>	0.025	0.97	0.377	0.53	-0.673	0.21	-0.185	0.77	0.113	0.86	-	-	0.418	0.48	-0.167	0.79	-0.069	0.91	-0.633	0.25

pH 3 GROUP

Whkr1 community

The *Whkr1* community (pH 3 group) was dominated at phylum-level by *Proteobacteria*, *Aquificae*, and *Thermotogae*. *Proteobacteria* 16S rRNA gene sequences increased from 3.4% of the total reads in February to 83.5% in June and then remained at high read count for August and October 2016. Conversely, sequences grouping to *Aquificae* decreased temporally from 94.5% in February to 2.3% in October. The percentage of sequences grouping to *Thermotogae* varied across the samples but was always below 20% (Figure 2.7 and Table 2.4).

Assessment of the temporal chemical concentrations from this site indicated a decrease in the concentration of the majority of elements, nutrients and gases across the temporal samples (Appendix 4.2). Based on a $P < 0.05$ significance level, three of the selected variables, total sulfur, sodium and potassium were significantly associated with variation observed in the microbial community at *Whkr1*. The concentrations (ppm) of these variables displayed similar trends (decreasing across the temporal samples, spiking in April) (Figure 2.8 and Appendix 4.2). The trends observed in total sulfur and sodium negatively correlated with *Thermotogae* ($P < 0.03$, $P < 0.02$), while *Aquificae* significantly correlated with potassium ($P < 0.03$). There was no significant correlation between *Proteobacteria* abundance and the measured variables (Table 2.3).

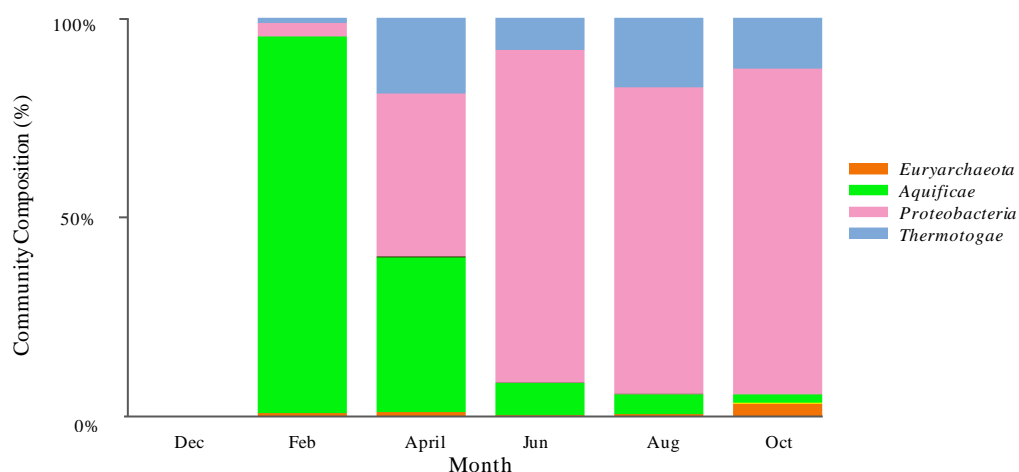


Figure 2.7: *Whkr1* phylum-level community composition (%) based upon the relative abundances of 16S rRNA gene sequence reads

Table 2.4: Whkr1 community percentage of 16S rRNA gene sequence reads grouping to genera

Table representing the percentages of sequences grouped to the most abundant genera observed at Whkr1.

<i>Taxonomy</i>	<i>Feb</i>	<i>April</i>	<i>June</i>	<i>Aug</i>	<i>Oct</i>
<i>k_Archaea;p_Euryarchaeota;c_Thermoplasmata;o_Thermoplasmatales;f_unknown;g_unknown</i>	0.7%	0.9%	0.2%	0.5%	3.2%
<i>k_Bacteria;p_Aquificae;c_Aquificae;o_Aquificales;f_Aquificaceae;g_Aquifex</i>	4.7%	23.7%	5.5%	3.4%	0.0%
<i>k_Bacteria;p_Aquificae;c_Aquificae;o_Aquificales;f_Aquificaceae;g_Hydrogenobaculum</i>	89.7%	14.5%	2.4%	1.5%	2.3%
<i>k_Bacteria;p_Aquificae;c_Aquificae;o_Aquificales;f_Hydrogenothermaceae;g_Venenivibrio</i>	0.1%	0.4%	0.4%	0.1%	0.0%
<i>k_Bacteria;p_Proteobacteria;c_Deltaproteobacteria;o_Desulfurellales;f_Desulfurellaceae;g_Desulfurella</i>	0.1%	2.1%	2.2%	6.0%	2.4%
<i>k_Bacteria;p_Proteobacteria;c_Gammaproteobacteria;o_Acidithiobacillales;f_Acidithiobacillaceae;g_Acidithiobacillus</i>	3.1%	38.6%	81.3%	70.8%	79.1%
<i>k_Bacteria;p_Thermotogae;c_Thermotogae;o_Thermotogales;f_Thermotogaceae;g_Mesoaciditoga</i>	1.3%	18.9%	7.9%	17.5%	12.8%

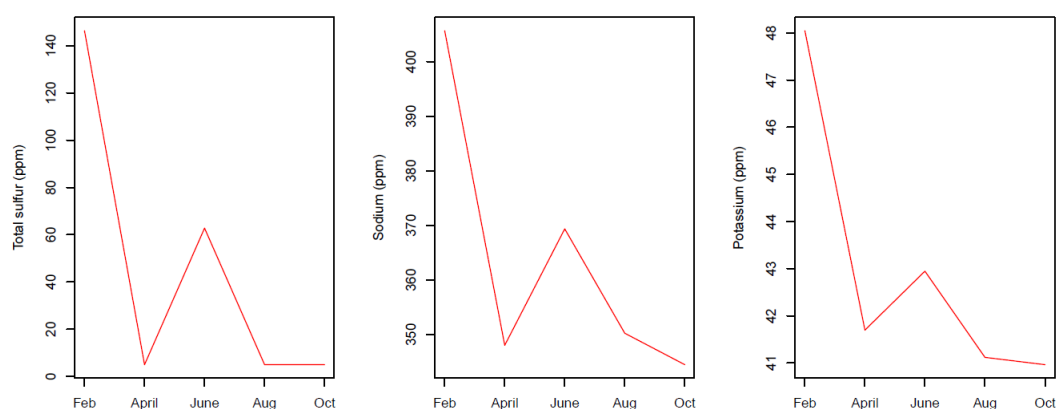


Figure 2.8: Total sulfur, sodium and potassium trend observed at Whkr1

Significant correlations measured between total sulfur, sodium and potassium (ppm) and dominant phyla *Aquificae*, *Proteobacteria* and *Thermotogae* across the temporal samples at Whkr1. *Thermotogae* correlated with total sulfur ($P < 0.03$) and sodium ($P < 0.02$), *Aquificae* with potassium ($P < 0.03$).

Whkr3 community

The Whkr3 community (pH 3 group) was dominated at phylum-level by *Aquificae*, *Crenarchaeota* and *Euryarchaeota*. The percentage of sequences grouping to *Aquificae* increased between December and October from 60% to 84.6%. Sequences grouping to *Crenarchaeota* decreased from 33.1% to 1.1%, and sequences grouping to *Euryarchaeota* increased from 6.2% to 12% between December and October (Figure 2.9). *Aquificae* was represented by two families;

Aquificaceae and *Hydrogenothermaceae*, represented by the genera *Hydrogenobaculum* and *Venenivibrio*, respectively, which were present across all six temporal samples. The percentage of sequence reads grouping to *Hydrogenobaculum* decreased significantly between June and August from 81% to 2.8%, while *Venenivibrio* increased from 0.1% to 74.3% (Table 2.5). See Supplementary Table 4.3 for full genus-level analysis.

Based on a $P < 0.05$ significance level, three of the monitored variables, temperature, pH and potassium correlated with the dominant phyla *Crenarchaeota* and *Aquificae*, most significantly with pH which increased across the temporal samples (pH 3.37-4.77). pH significantly correlated with *Crenarchaeota* ($P < 0.01$) and negatively correlated with *Aquificae* ($P < 0.02$) (Figure 2.10 and Table 2.3).

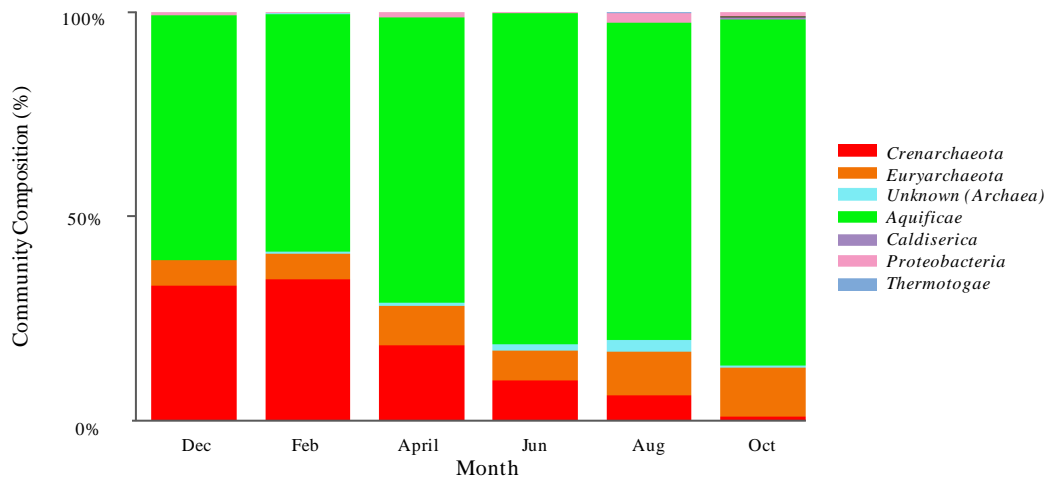


Figure 2.9: Whkr3 phylum-level community composition (%) based upon the relative abundances of 16S rRNA gene sequence reads

Table 2.5: Whkr3 community percentage of 16S rRNA gene sequence reads grouping to *Aquificae*

Community composition of families *Aquificaceae* and *Hydrogenothermaceae* (phylum *Aquificae*) at Whkr3. Highlighted columns represent the largest genus-level shift in the dominant genera.

<i>Taxonomy</i>	<i>Dec</i>	<i>Feb</i>	<i>April</i>	<i>June</i>	<i>Aug</i>	<i>Oct</i>
<i>Aquificaceae</i> ;g_ <i>Hydrogenobaculum</i>	50.8%	56.9%	69.7%	81.0%	2.8%	0.0%
<i>Hydrogenothermaceae</i> ;g_ <i>Venenivibrio</i>	3.1%	1.1%	0.1%	0.1%	74.3%	84.1%

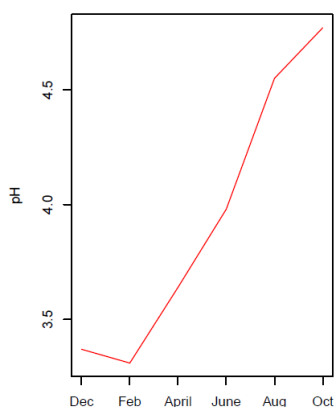


Figure 2.10: pH trend observed at Whkr3

Significant correlations measured between pH and dominant phyla *Aquificae* and *Crenarchaeota* across the temporal samples at Whkr3. *Crenarchaeota* and *Aquificae* significantly correlated with pH ($P < 0.01$, $P < 0.02$).

***TeP* community**

The *TeP* community (pH 3 group) was dominated at phylum-level by *Crenarchaeota*, *Aquificae* and *Euryarchaeota*. The percentage of sequences grouping to *Crenarchaeota* was consistent at ~80% in the February, June, August and October samples. A decrease in *Crenarchaeota* sequences to 50.2% was observed in the April sample. Sequences grouping to *Aquificae* were constant (<10%) except for an increase observed in April (23.7%) and August (14.5%). The phylum *Euryarchaeota* was not observed in February. Sequences grouping to this phylum decreased from 18.3% in April to 1.0% in October (Figure 2.11 and Table 2.6).

There was no significant correlation between the microbial community and physicochemical variables at this site (Table 2.3). Assessment of the physicochemical variables revealed no large variations in concentration across the temporal samples (Appendix 4.2).

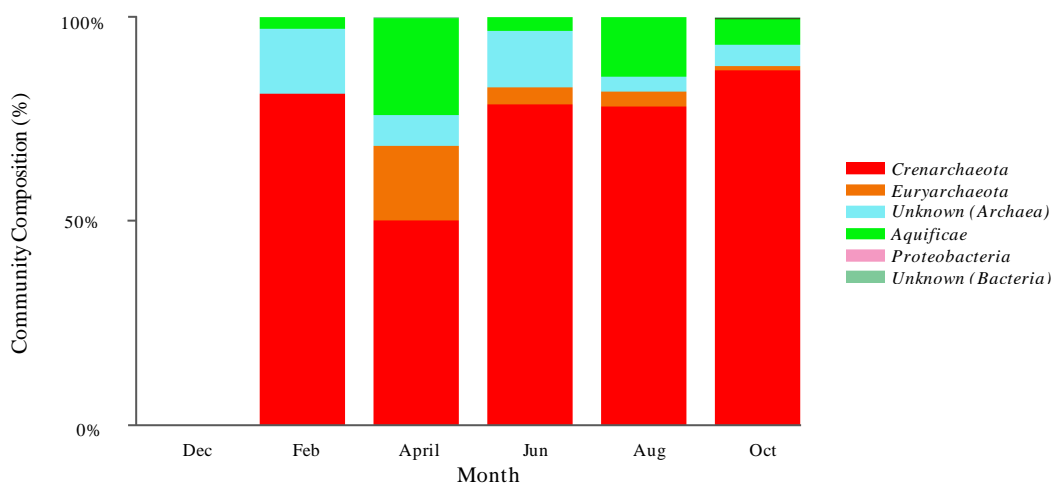


Figure 2.11: *TeP* phylum-level community composition (%) based upon the relative abundances of 16S rRNA gene sequence reads

Table 2.6: TeP community percentage of 16S rRNA gene sequence reads grouping to genera

<i>Taxonomy</i>	<i>Feb</i>	<i>April</i>	<i>June</i>	<i>Aug</i>	<i>Oct</i>
<i>k_Archaea;p_Crenarchaeota;c_Thermoprotei;o_Sulfolobales;f_Sulfolobaceae;g_unknown</i>	81.4%	50.2%	78.7%	78.1%	86.9%
<i>k_Archaea;p_Euryarchaeota;c_Thermoplasmata;o_Thermoplasmatales;f_unknown;g_unknown</i>	0.0%	18.3%	4.2%	3.8%	1.0%
<i>k_Archaea;p_unknown;c_unknown;o_unknown;f_unknown;g_unknown</i>	15.7%	7.5%	13.6%	3.5%	5.2%
<i>k_Bacteria;p_Aquificae;c_Aquificae;o_Aquificales;f_Aquificaceae;g_Hydrogenobacter</i>	0.0%	0.4%	0.0%	0.0%	0.0%
<i>k_Bacteria;p_Aquificae;c_Aquificae;o_Aquificales;f_Aquificaceae;g_Hydrogenobaculum</i>	0.0%	22.6%	3.2%	14.5%	6.2%
<i>k_Bacteria;p_Aquificae;c_Aquificae;o_Aquificales;f_Hydrogenothermaceae;g_Venenivibrio</i>	2.9%	0.7%	0.1%	0.0%	0.0%
<i>k_Bacteria;p_unknown;c_unknown;o_unknown;f_unknown;g_unknown</i>	0.0%	0.4%	0.0%	0.0%	0.2%

pH 5 GROUP

Waio1 and Waio2 communities

Both communities at Waio1 and Waio2 (pH 5 group) were dominated at phylum-level by *Aquificae* at 99.4% and 97.5%, respectively (Figure 2.12), which was almost exclusively represented by the genus *Venenivibrio*. The percentage of sequences grouping to *Aquificae* were consistent across the temporal samples at both springs (Table 2.7). For full genus-level analysis see Supplementary Tables 4.4 and 4.5.

Assessment of the monitored physicochemical variables across the temporal samples revealed no large variations in concentrations at both sites (Appendix 4.2). Based on a $P < 0.05$ significance level, three of the variables, methane (Waio1), bicarbonate and temperature (Waio2) were significantly correlated with *Aquificae* community abundance respective to the sites indicated (Table 2.3). Methane levels which were consistent across the temporal samples at ~3 ppm significantly correlated with *Aquificae* community abundance ($P < 0.04$) at Waio1. Bicarbonate levels declined over the study period from 271 to 111 ppm at Waio2 which significantly correlated with *Aquificae* community abundance ($P < 0.05$).

Temperature (as described above) significantly correlated ($P < 0.03$) with *Aquificae* community abundance at Waio2 (Figure 2.13).

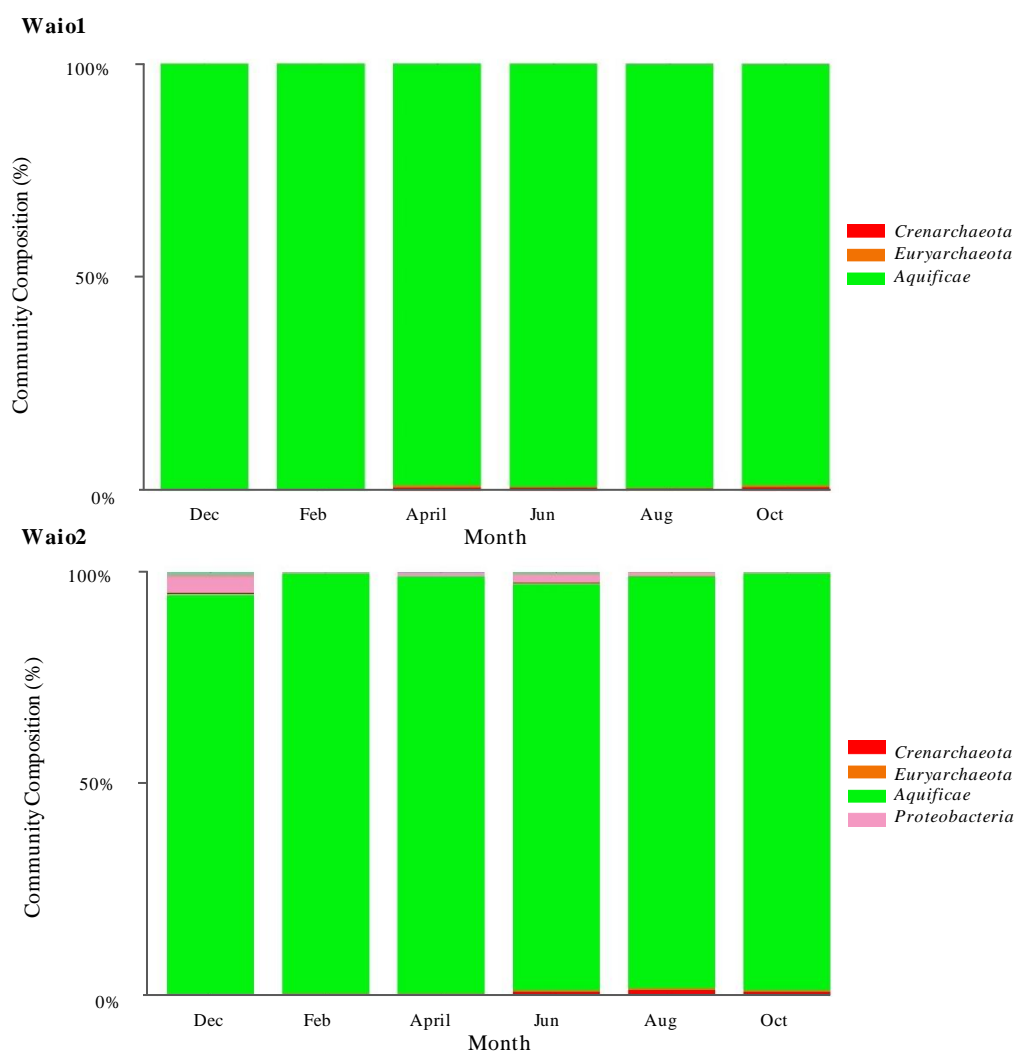


Figure 2.12: Waiotapu springs phylum-level community composition (%) based upon the relative abundances of 16S rRNA gene sequence reads

Table 2.7: Waio1 and Waio2 community percentage of sequences grouping to *Aquificae*

<i>Taxonomy</i>	<i>Dec</i>	<i>Feb</i>	<i>April</i>	<i>June</i>	<i>Aug</i>	<i>Oct</i>
Waio1						
<i>Aquificae:g_Venenivibrio</i>	99.6%	99.6%	98.8%	99.2%	99.3%	98.6%
Waio2						
<i>Aquificae:g_Venenivibrio</i>	94.2%	99.1%	98.5%	95.9%	97.3%	98.5%

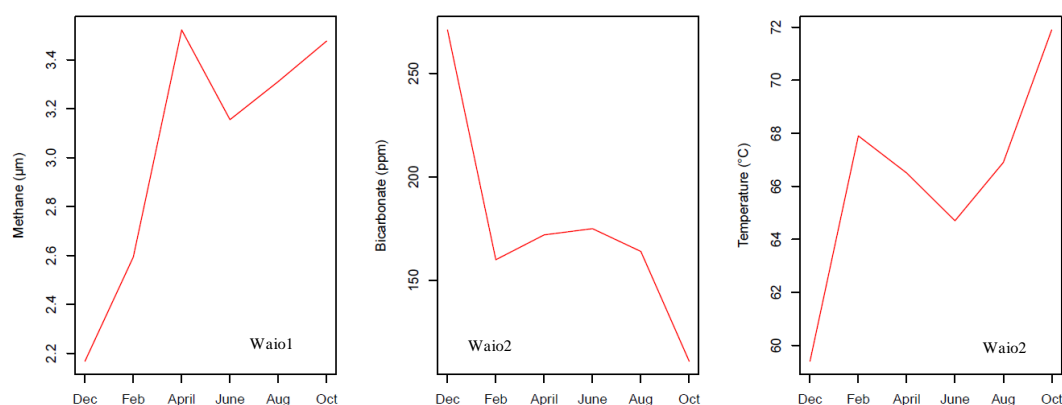


Figure 2.13: Methane trend observed at Waio1 and bicarbonate and temperature trends observed at Waio2

Significant correlations measured between methane (μm) and *Aquificae* ($P < 0.04$) at Waio1. Significant correlation observed between *Aquificae* and bicarbonate ($P < 0.05$) and temperature ($P < 0.03$) at Waio2.

***Kui3* community**

The *Kui3* community (pH 5 group) was dominated at phylum-level by *Aquificae* and *Proteobacteria*. The community in December was evenly dispersed with sequences grouping to *Aquificae* and *Proteobacteria* at 45.4% and 53.7%, respectively. An increase in *Aquificae* was observed in February to 85.1% which coincided with a decrease in *Proteobacteria* (12.4%), with community composition consistent until June. *Aquificae* abundance significantly decreased to 4.2% in August before returning to 95.1% in October, while *Proteobacteria* increased in August to 91.2% and returned to 1.3% in October (Figure 2.14).

Aquificae was exclusively represented by two families *Aquificaceae* and *Hydrogenothermaceae*. The genus *Venenivibrio* (family *Hydrogenothermaceae*) accounted almost exclusively for the sequences grouping to *Aquificae*. Dominant proteobacterial genera *Thiomonas* (*Betaproteobacteria*), *Nitratiruptor* (*Epsilonproteobacteria*) and *Thiovirga* (*Gammaproteobacteria*) almost exclusively accounted for the changes observed in community composition of the phylum. The genus *Thiomonas* (*Betaproteobacteria*) decreased over the study period from 43.3% in December to 0.7% in October. The genera *Nitratiruptor* (*Epsilonproteobacteria*) and *Thiovirga* (*Gammaproteobacteria*) both spiked in August at 68.3% and 18.7% respectively and were unrepresented in the February and October samples (Table 2.8). For full genus-level analysis see Supplementary Table 4.6.

Assessment of the chemical dataset indicated consistency in concentrations across the majority of variables between December and February, with

concentrations decreasing subsequently in the August sample (Appendix 4.2). The association test (based on a $P < 0.05$ significance level) indicated a significant correlation ($P < 0.01$) between sulfate and the community abundance of the dominant phyla (*Aquificae* and *Proteobacteria*) (Table 2.3). The concentration of sulfate increased from 71 ppm in December to 89 ppm in April which was consistent across June before decreasing to 70 ppm in August and returning to 92 ppm in October (Figure 2.15).

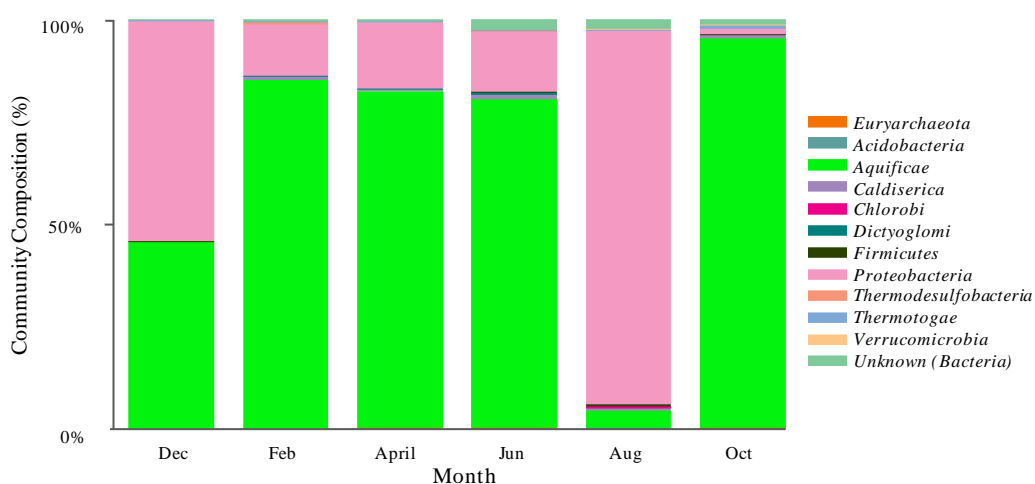


Figure 2.14: Kui3 phylum-level community composition (%) based upon the relative abundances of 16S rRNA gene sequence reads

Table 2.8: Kui3 community percentage of 16S rRNA gene sequence reads grouping to *Aquificae* and *Proteobacteria*

Highlighted rows show the shift in dominant genera representing *Aquificae* and *Proteobacteria*. For full genus-level analysis see Supplementary Table 4.6

<i>Taxonomy</i>	<i>Dec</i>	<i>Feb</i>	<i>April</i>	<i>June</i>	<i>Aug</i>	<i>Oct</i>
<i>Aquificae</i> ;g_ <i>Venenivibrio</i>	44.4%	79.3%	81.5%	79.3%	4.1%	94.4%
<i>Proteobacteria</i> ;g_ <i>Thiomonas</i>	43.3%	12.3%	1.9%	3.4%	2.3%	0.7%
<i>Proteobacteria</i> ;g_ <i>Nitratiruptor</i>	10.3%	0.0%	0.0%	6.4%	68.3%	0.0%
<i>Proteobacteria</i> ;g_ <i>Thiovirga</i>	0.1%	0.0%	13.3%	0.6%	18.7%	0.0%

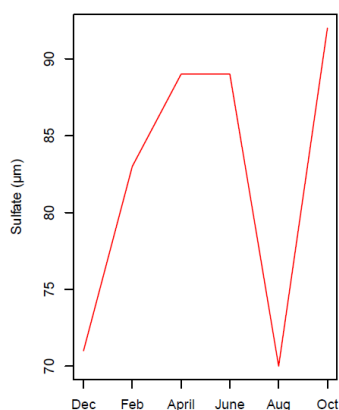


Figure 2.15: Sulfate (ppm) trend observed across temporal samples at Kui3

Significant correlations measured between sulfate (ppm) and *Aquificae* and *Proteobacteria* ($P < 0.01$)

pH 7 GROUP

***Whgpa* community**

The *Whgpa* community (pH 7 group) was dominated at phylum-level by *Deinococcus-Thermus* and *Armatimonadetes* (Figure 2.16). The percentage of sequences grouping to *Deinococcus-Thermus* increased from 39.9% in December to 63.6% in April and returned to 21.7% in October. The inverse trend was observed in the other dominant sequence group, *Armatimonadetes*. The percentage of sequences grouping to *Armatimonadetes* decreased from 39% in December to 15.7% in June returning to 45.7% in October (Table 2.9). For full genus-level analysis, see Supplementary Table 4.7.

Assessment of the temporal variations in chemistry at this site indicated consistency across the majority of elements, nutrients and gases (Appendix 4.2). The association test indicated significant correlations between two variables, pH and methane and the dominant phyla *Armatimonadetes* and *Deinococcus-Thermus*, respectively ($P < 0.01$) (Table 2.3). Methane concentrations fluctuated across the temporal samples, spiking in April (18.2 ppm) and dropping in August (0.6 ppm). pH levels followed the trend as described above (Figure 2.17).



Figure 2.16: Whgpa phylum-level community composition (%) based upon the relative abundances of 16S rRNA gene sequence reads

Table 2.9: Whgpa community percentage of 16S rRNA gene sequence reads grouping to genera

For full genus-level analysis see Supplementary Table 4.7

<i>Taxonomy</i>	<i>Dec</i>	<i>Feb</i>	<i>April</i>	<i>June</i>	<i>Aug</i>	<i>Oct</i>
<i>Armatimonadetes</i> ;_gp6	0.1%	0.1%	0.1%	0.1%	0.4%	0.2%
<i>Armatimonadetes</i> ;_gp7	38.9%	30.8%	24.4%	15.6%	20.5%	45.4%
<i>Deinococcus- Thermus</i> ;g_Thermus	39.9%	56.7%	63.6%	45.1%	30.6%	21.6%

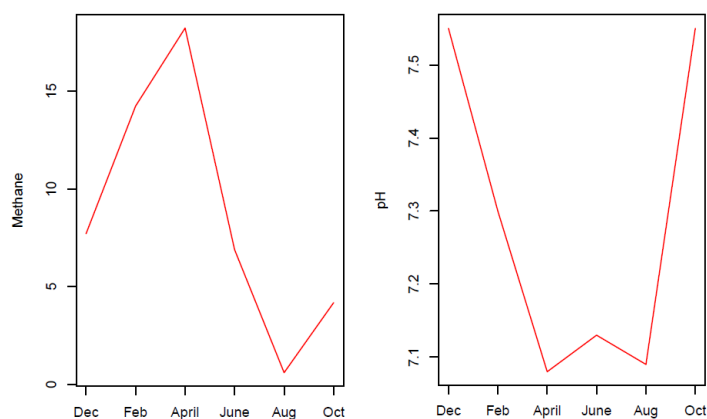


Figure 2.17: Methane (μm) and pH trends observed across temporal samples at Whgpa

Significant correlations measured between methane (ppm) and *Deinococcus-Thermus* ($P < 0.01$) and pH and *Armatimonadetes* ($P < 0.01$)

***Kui1* community**

The *Kui1* community (pH 7 group) was dominated at phylum-level by *Aquificae*. Other phyla present in lower abundances included *Proteobacteria* and *Thermodesulfobacteria* (Figure 2.18). The percentage of sequences grouping to *Aquificae* was constant (~75%) across the December, February, June, August and October samples. An increase in *Aquificae* was observed in April sample (91.9%) which coincided with a decrease in the percentage of the other phyla present (Table 2.10). For full genus-level analysis see Supplementary Table 4.8.

Physicochemical variables were stable across the temporal samples at this site (Appendix 4.2). There was no significant correlation between the physicochemical variables assessed and *Aquificae* community abundance (Table 2.3).

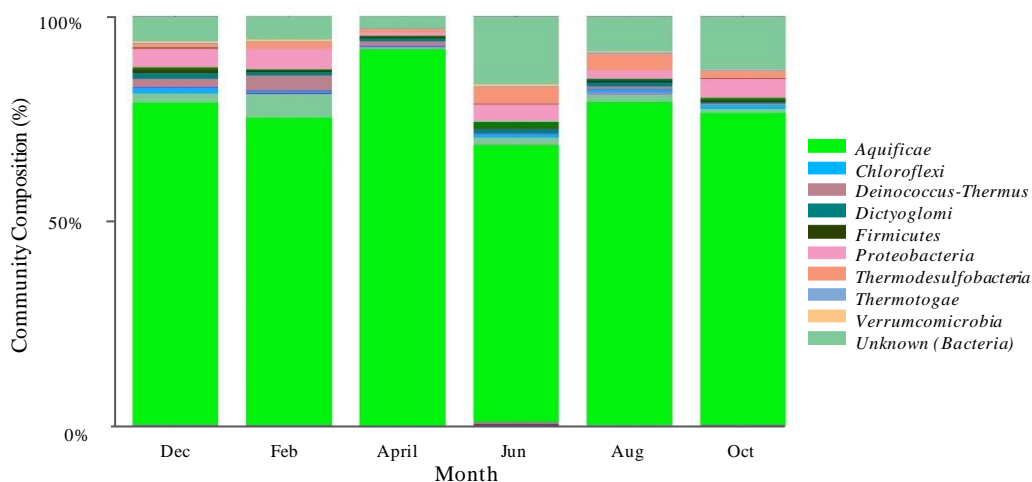


Figure 2.18: *Kui1* phylum-level community composition (%) based upon the relative abundances of 16S rRNA gene sequence reads

Table 2.10: *Kui1* community percentage of 16S rRNA gene sequence reads grouping to *Aquificae*

Percentages of sequences grouped to the genus *Venenivibrio* at *Kui1*. For full genus-level analysis see Supplementary Table 4.8.

<i>Taxonomy</i>	<i>Dec</i>	<i>Feb</i>	<i>April</i>	<i>June</i>	<i>Aug</i>	<i>Oct</i>
<i>Aquificae</i>:g_<i>Venenivibrio</i>	78.1%	74.6%	91.6%	67.4%	78.5%	75.8%

pH 9 GROUP

Whkr2 community

The Whkr2 community (pH 9 group) consisted of sequences grouping to the phyla *Aquificae*, *Proteobacteria*, *Thermodesulfobacteria* and *Deinococcus-Thermus* (Figure 2.19). The percentage of sequences grouping to *Aquificae* was consistent at ~35% over the study period, with a single increase to 63.8% observed in February. Sequences grouping to *Proteobacteria* remained at ~25% across the study period, dropping to 6.8% in February following an inverse trend observed in *Aquificae*.

Aquificae was represented by the families *Aquificaceae* and *Hydrogenothermaceae*. The percentage of sequences grouping to the family *Aquificaceae* increased from December (37.1%) to February (60.1%) before declining to October (23.9%). The inverse trend was observed for sequences grouping to *Hydrogenothermaceae* with the percentage of sequences increasing from December (5.9%) to August (20.6%) and declining in October (10.8%) (Table 2.11). See Supplementary Table 4.9 for full genus-level analysis.

Aquificae and *Proteobacteria* community variations correlated with several physicochemical variables, including pH, sulfate and potassium, with the most significant correlation with temperature. Temperature at Whkr2 decreased from 69.5 °C in December to 64.5 °C in August before increasing to 65.5 °C in October (Figure 2.20 and Appendix 4.2). This trend significantly correlated with *Aquificae* ($P < 0.05$) and negatively correlated with *Proteobacteria* ($P > 0.01$) (Table 2.3).

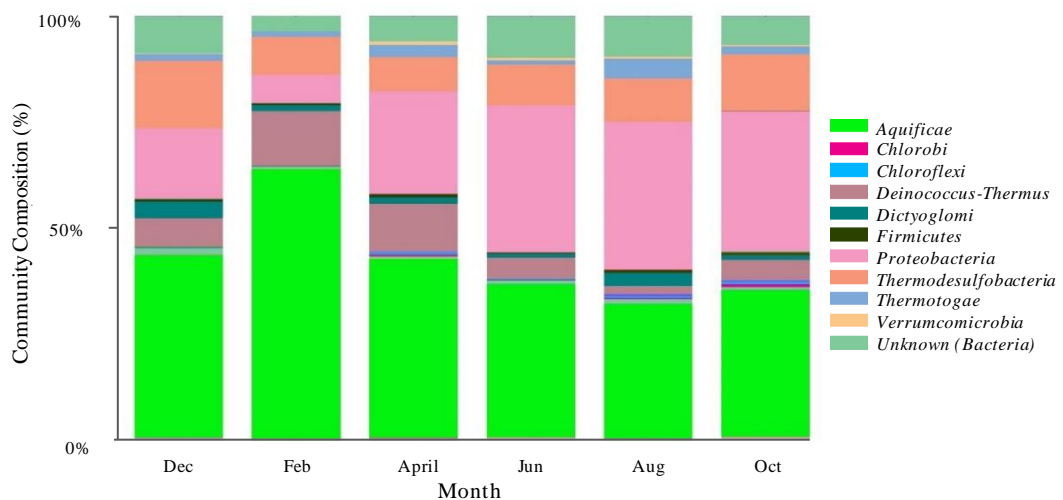


Figure 2.19: Whkr2 phylum-level community composition (%) based upon the relative abundances of 16S rRNA gene sequence reads

Table 2.11: Whkr2 community percentage of 16S rRNA gene sequence reads grouping to *Aquificae*

Percentage of sequence reads grouping to the *Aquificaceae* and *Hydrogenothermaceae* (phylum *Aquificae*) at genus-level. Highlighted columns represent the month with the largest observed community percentage of the respective families. See Supplementary Table 4.9 for full genus-level analysis.

<i>Taxonomy</i>	<i>Dec</i>	<i>Feb</i>	<i>April</i>	<i>June</i>	<i>Aug</i>	<i>Oct</i>
<i>Aquificaceae</i> ;g_ <i>Aquifex</i>	9.4%	19.1%	11.0%	3.2%	4.1%	1.3%
<i>Aquificaceae</i> ;g_ <i>Hydrogenobacter</i>	27.5%	39.6%	18.5%	25.0%	6.9%	22.5%
<i>Aquificaceae</i> ;g_ <i>Hydrogenobaculum</i>	0.2%	1.4%	0.0%	0.0%	0.2%	0.1%
<i>Hydrogenothermaceae</i> ; g_ <i>Sulfurihydrogenibium</i>	0.0%	0.1%	0.1%	0.0%	12.6%	6.4%
<i>Hydrogenothermaceae</i> ; g_ <i>Venenivibrio</i>	5.9%	3.5%	12.5%	8.0%	7.9%	4.3%
<i>Hydrogenothermaceae</i> ;g_ <i>unknown</i>	0.0%	0.1%	0.1%	0.1%	0.1%	0.1%

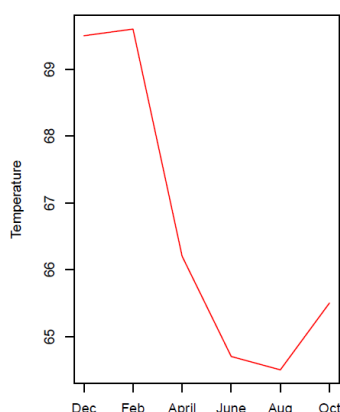


Figure 2.20: Temperature (°C) trend observed across temporal samples at Whkr2

Significant correlations measured between temperature and *Aquificae* ($P < 0.05$) and *Proteobacteria* ($P < 0.01$).

Whkr4 community

The Whkr4 community (pH 9 group) was dominated at phylum-level by *Deinococcus-Thermus*, *Aquificae* and *Thermodesulfobacteria*. The percentage of sequences grouping to *Deinococcus-Thermus* and *Aquificae* were consistent across the first four sampling points (at ~60% and 20%, respectively). A shift in community dominance was observed between June and August with the percentage of sequences grouping to *Deinococcus-Thermus* decreasing to 3.5%, and *Aquificae* increasing to 74% which was consistent into October. The percentage of sequence reads grouping to *Thermodesulfobacteria* increased over the study period from 3% to 14.9% (Figure 2.21 and Table 2.12). See Supplementary Table 4.10 for full genus-level analysis.

Hotsprings chemistry at this site was variable across the temporal samples, with no apparent pattern observed (Appendix 4.2). The association test indicated significance between temperature and both dominant phyla (*Aquificae* and *Deinococcus-Thermus*). Temperature (as described above) significantly correlated with *Aquificae* ($P < 0.01$) and *Thermodesulfobacteria* ($P < 0.02$) and negatively with *Deinococcus-Thermus* ($P < 0.02$) (Figure 2.22 and Table 2.3).

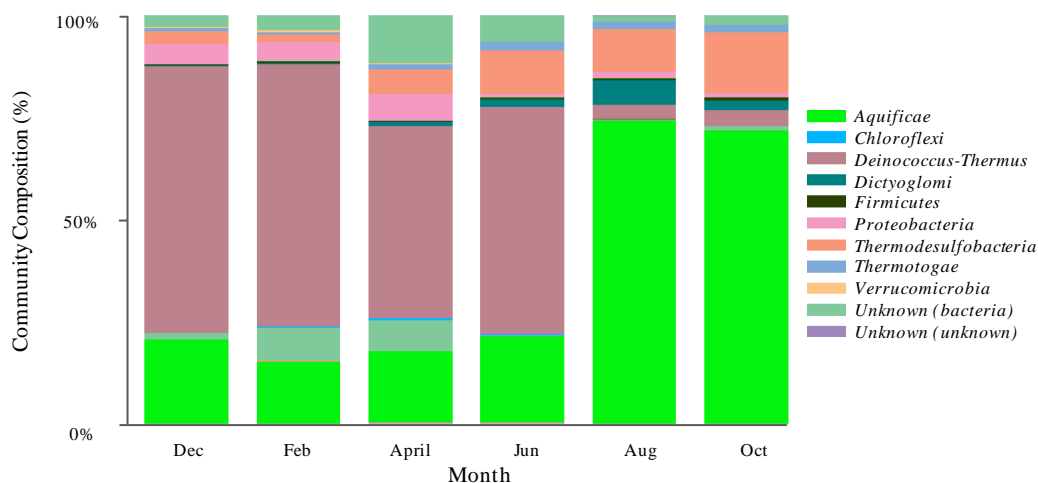


Figure 2.21: Whkr4 phylum-level community composition (%) based upon the relative abundances of 16S rRNA gene sequence reads

Table 2.12: Whkr4 community percentage of 16S rRNA gene sequence reads grouping to genera

Highlighted columns show the largest shift observed in the genus representing the most dominant phyla (*Deinococcus-Thermus* and *Aquificae*). See Supplementary Table 4.10 for full genus-level analysis.

<i>Taxonomy</i>	<i>Dec</i>	<i>Feb</i>	<i>April</i>	<i>June</i>	<i>Aug</i>	<i>Oct</i>
<i>Aquificae</i> ;g_ <i>Aquifex</i>	1.0%	1.8%	2.7%	2.0%	8.0%	7.5%
<i>Aquificae</i> ;g_ <i>Hydrogenobacter</i>	17.8%	11.6%	10.0%	12.1%	53.3%	59.0%
<i>Aquificae</i> ;g_ <i>Venenivibrio</i>	1.8%	1.8%	4.4%	6.4%	12.3%	4.9%
<i>Aquificae</i> ;g_ <i>unknown</i>	0.0%	0.0%	0.0%	0.1%	0.2%	0.1%
<i>Deinococcus-Thermus</i> ;g_ <i>Thermus</i>	64.9%	63.9%	46.7%	55.5%	3.5%	3.9%
<i>Thermodesulfobacteria</i> ;g_ <i>Caldimicrobium</i>	3.0%	1.7%	6.0%	10.8%	10.5%	14.8%

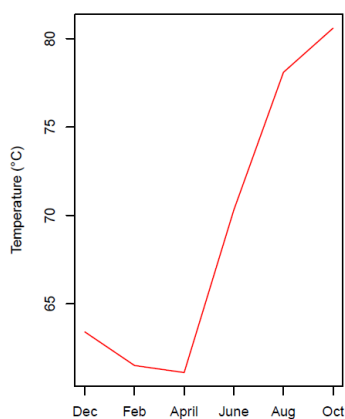


Figure 2.22: Temperature (°C) trend observed across temporal samples at Whkr4

Significant correlations measured between temperature and *Aquificae* ($P < 0.01$), *Thermodesulfobacteria* ($P < 0.02$) and *Deinococcus-Thermus* ($P < 0.02$)

Ohaaki community

The Ohaaki community (pH 9 group) was dominated at phylum-level by *Aquificae* and *Deinococcus-Thermus*. The percentages of sequences grouping to *Aquificae* and *Deinococcus-Thermus* were consistent across the first four samples (February to August) at ~90% and ~4%, respectively. In October, *Aquificae* community composition significantly decreased to 9.5%, while *Deinococcus-Thermus* increased to 73.2% (Figure 2.23 and Table 2.13). See Supplementary Table 4.11 for full genus-level analysis.

Physicochemical variables were relatively stable across the temporal samples at this site (Appendix 4.2). There was no significant correlation between the dominant phyla and the physicochemical variables at this site (Table 2.3).

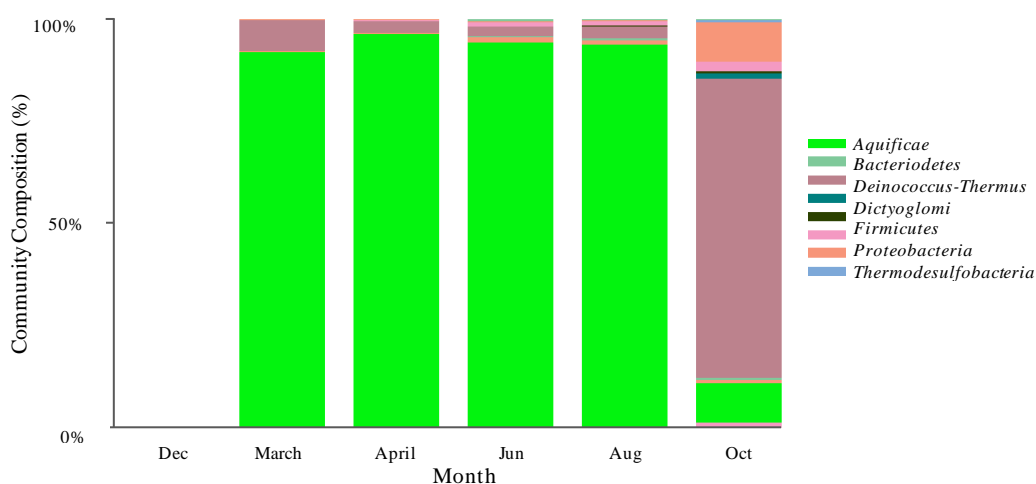


Figure 2.23: Ohaaki phylum-level community composition (%) based upon the relative abundances of 16S rRNA gene sequence reads

Table 2.13: Ohaaki community percentage of 16S rRNA gene sequence reads grouping to *Aquificae* and *Deinococcus-Thermus*

Highlighted columns show the largest shift observed in the genus representing the most dominant phyla (*Deinococcus-Thermus* and *Aquificae*). See Supplementary Table 4.11 for full genus-level analysis.

<i>Taxonomy</i>	<i>March</i>	<i>April</i>	<i>June</i>	<i>Aug</i>	<i>Oct</i>
<i>Aquificae</i> ;g_ <i>Hydrogenobacter</i>	92.0%	96.1%	94.1%	93.7%	9.5%
<i>Deinococcus-Thermus</i> ;g_ <i>Thermus</i>	7.6%	2.8%	2.2%	3.1%	73.2%

2.3.4 Determining primary and secondary physicochemical drivers

Based on the significance association test between the physicochemical variables and microbial community composition (Table 2.13), the primary and secondary physicochemical drivers were determined (Table 2.14). These drivers are described at each of the pH groups below.

pH 3 GROUP

A combination of chemical drivers (total sulfur, potassium and sodium) influenced the microbial community at Whkr1, while pH and temperature were the primary and secondary physicochemical drivers at Whkr3. No significant associations between the dominant phyla and the physicochemical variables at TeP were determined.

pH 5 GROUP

Temperature and chemical variables were the main driver at the three pH 5 Group hotsprings. Methane was the primary physicochemical driver at Waio1, while temperature and bicarbonate were at Waio2. Sulfate and temperature were the primary and secondary physicochemical drivers at Kui3.

pH 7 GROUP

pH and methane were the primary and secondary physicochemical drivers at Whgpa. No significant associations/physicochemical drivers were determined at Kui1.

pH 9 GROUP

Temperature was the primary physicochemical driver at two of pH 9 hotsprings, Whkr2 and Whkr4. pH and sodium were the secondary drivers at these sites, respectively. No significant associations/physicochemical drivers were determined at Ohaaki.

Table 2.14: Summary table of target hotspring temporal dynamics

Summary table outlining the dominant phyla and primary and secondary physicochemical variable influencing the community at each target spring.

Spring	Temperature/pH range/group	Sample Months	Location	Description	Dominant phyla	Primary physicochemical driver	Secondary physicochemical driver	Observable trends
Whkr1	pH 3 53 - 60.1 °C pH 2.91 - 3.12	Feb, April, June, Aug, Oct	Whakarewarewa Village, Rotorua	Small pool with foamy surface at edge of flowing stream over v-catchment to spring below.	<i>p_Proteobacteria</i> <i>p_Aquificae</i> <i>p_Thermotogae</i>	Total sulfur	Potassium/Sodium	Covariance observed between total sulfur and <i>Aquificae</i> . Increased water level observed in August which decreased in October.
Whkr3	pH 3 60 - 71 °C pH 3.37 - 4.77	Dec, Feb, April, June, Aug, Oct	Whakarewarewa Village, Rotorua	Acidic grey spring with surrounding hard sinter	<i>p_Aquificae</i> <i>p_Crenarchaeota</i> <i>p_Euryarchaeota</i>	pH	Temperature	Variation in both pH and temperature covaried with dominant phyla <i>Aquificae</i> and <i>Crenarchaeota</i> . The largest increase in pH was observed at this site. pH increased from pH 3.37 to 4.77 from December (2015) to October (2016). The largest incremental increase was observed between June and August (2016) from pH 3.98 to 4.55
TeP	pH 3 61.8 - 71.6 °C pH 2.44 - 2.58	Feb, April, June, Aug, Oct	Te Puia, Rotorua	Long grey spring surrounded by sinter with thick grey sediment island in centre	<i>p_Crenarchaeota</i>	-	-	No large variation observed in physicochemical variables or microbial community phyla. Weak associations between variables and dominant community phyla. Observed increase in water level in August and October
Wai01	pH 5 64.9 - 68 °C pH 4.66 - 5	Dec, Feb, April, June, Aug, Oct	Waiotapu Thermal Wonderland	Small creamy yellow/green spring (Oyster pool) with hard sinter covered in thick yellow sulfur film	<i>p_Aquificae</i>	Methane	-	Stable physicochemical conditions and microbial community. No observable change in hot spring over study period
Wai02	pH 5 59.4 - 71.9 °C pH 4.68 - 5.07	Dec, Feb, April, June, Aug, Oct	Waiotapu Thermal Wonderland	Large creamy yellow/green spring at edge of Artist's Palette covered in thick yellow sulfur film	<i>p_Aquificae</i>	Temperature	Bicarbonate	Stable physicochemical conditions and microbial community. No observable change in hot spring over study period
Kui3	pH 5 45.8 - 61 °C pH 4.47 - 5.27	Dec, Feb, April, June, Aug, Oct	Kuirau Park, Rotorua	Small stagnant shallow pool in hollow of vegetation thicket with thick leave matter at bottom	<i>p_Aquificae</i> <i>p_Proteobacteria</i>	Sulfate	Temperature	Weak association between sulfate and <i>Aquificae</i> . Genus-level shift in <i>Proteobacteria</i> associated with temperature. Increase in water level observed in August and October
Whgpa	pH 7 60.8 - 65.3 °C pH 7.08 - 7.55	Dec, Feb, April, June, Aug, Oct	Atiamuri General	Large deep blue spring with surrounding orange biomass	<i>p_Deinococcus-Thermus</i> <i>p_Armatimonadetes</i>	pH	Methane	Cyclical trend in physicochemical variables, pH and methane associated with <i>Deinococcus-Thermus</i> and <i>Armatimonadetes</i> community composition. No observable change noted in the spring description. Same temperature (~63 °C) and pH (7.55) recorded in December (2015) and October (2016)
Kui1	pH 7 57.5 - 63.8 °C pH 6.57 - 7.06	Dec, Feb, April, June, Aug, Oct	Kuirau Park, Rotorua	Large spring in vegetation thicket with brown biomass	<i>p_Aquificae</i>	-	-	No large variation observed in physicochemical variables or microbial community phyla. Spring water level increased in August.
Whkr2	pH 9 64.5 - 69.6 °C pH 8.7 - 8.97	Dec, Feb, April, June, Aug, Oct	Whakarewarewa Village, Rotorua	Small pool with input from above hot spring which flows into Puarenga stream below	<i>p_Aquificae</i> <i>p_Proteobacteria</i>	Temperature	pH	No large variations in physicochemical variables and community composition and structure. Microbial community significantly associated with temperature. Vegetation surrounding spring cleared between June and August
Whkr4	pH 9 61.1 - 80.6 °C pH 7.76 - 8.41	Dec, Feb, April, June, Aug, Oct	Whakarewarewa Village, Rotorua	Medium light blue hot spring (Waipuru) surrounded by hard white sinter rims	<i>p_Deinococcus-Thermus</i> <i>p_Aquificae</i>	Temperature	Sodium	Largest recorded increase in temperature (19.5 °C) observed from April (61.1 °C) to October (80.6 °C) associated with shift in the relative community abundance of <i>Aquificae</i> and <i>Deinococcus-Thermus</i> . Substantial drop in water level (~60cm) between August and October
Ohaaki	pH 9 65 - 70.3 °C pH 8.41 - 9.04	Mar, April, June, Aug, Oct	Ohaaki General	Large creamy white spring with blue centre surrounded by thick white sinter	<i>p_Aquificae</i> <i>p_Deinococcus-Thermus</i>	-	-	Shift in dominant phyla observed in October. Physicochemical variables stable across the study period. No significant association between physicochemical variables and dominant phyla.

2.3.5 Meteoric and field observations

Rainfall and geothermal bore water measurements were collected for the course of study (November 2015 - October 2016) (Bay of Plenty Regional Council, 2015; NIWA, 2016). Four geothermal bores were selected in the Rotorua town district based on their proximity to the sampled geothermal fields. These datasets were used to monitor seasonal changes in precipitation and associated hydrological changes to the underlying aquifer that could be correlated with physicochemical changes in the Rotorua hotsprings. Two geothermal bores, M25 and M26, were located in close proximity to the sites, Te Puia and Whakarewarewa, while M27 and M28 were located near Kuirau Park (Figure 2.24).

Rainfall was on average higher during the austral winter (376.6 mm) than summer (312.6 mm) months. Geothermal bore water levels were overlaid onto the rainfall data to link the observed rainfall with fluctuations in groundwater (Figure 2.25). The water levels in geothermal bores M25 and M26 were consistent over the study period at 285 m and 282 m, respectively. The water level in M26 dropped to 278 m in November, February and August. Geothermal bores M27 and M28 water levels fluctuated 0.47 m across the study period in association with rainfall. The largest rainfall peaks observed in March and June were associated with an average increase of 0.06 m and 0.1 m at M27 and M28 bores, respectively. The water levels of M27 and M28 remained unchanged until August after the largest rainfall recorded in June (72 mm). A reduction in rainfall in mid-August was associated with a decrease of 0.34 m and 0.27 m in bore water level at M27 and M28, respectively.

Observational notes were taken at each site during each temporal sampling. The water levels of the Rotorua hotsprings remained stable between December and June. A visible increase in water level was observed at all these sites during the August sampling after a night of heavy rainfall (Figure 2.25). Water levels remained consistent at Whkr2, Whkr3, and Kui1 during October, while water levels decrease at TeP, Whkr1 and Whkr4 and increased at Kui3.

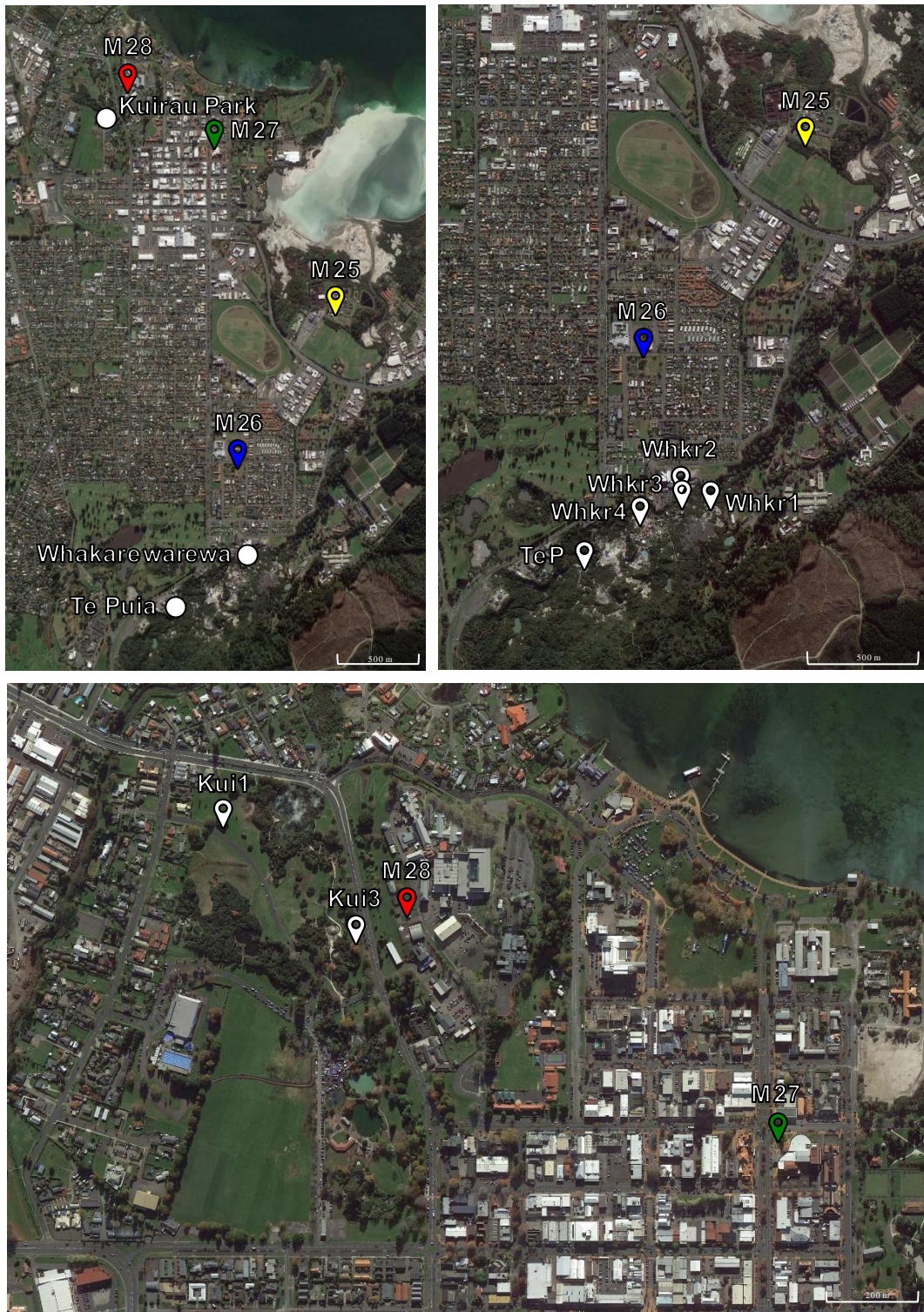


Figure 2.24: Location of geothermal bores in association with target geothermal sites in Rotorua (A) Position of geothermal bores M25 and M26 in proximity to Te Puia and Whakarewarewa hot springs (B) and M27 and M28 with Kuirau Park hot springs (C)

(Source: Google Earth)

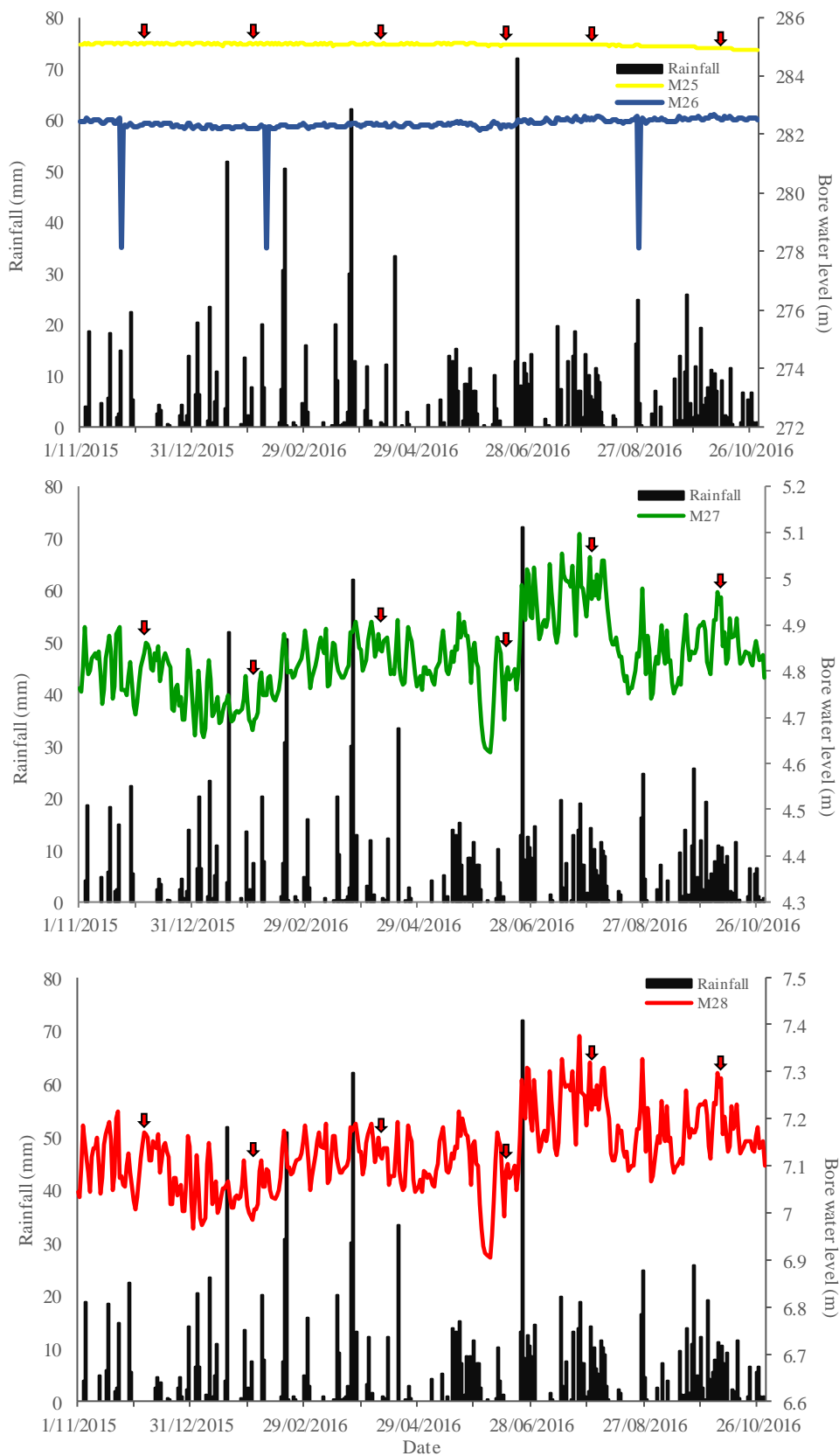


Figure 2.25: Daily rainfall in Rotorua and geothermal bore water level

Red arrows indicate sampling timepoints. Rainfall data sourced from the NIWA database (NIWA, 2016). Geothermal bore water level data sourced from the Bay of Plenty Regional Council website (Bay of Plenty Regional Council, 2015).

2.4 Discussion

Geothermal environments are natural systems that present a range of extreme physicochemical variables ideal for addressing central questions to microbial ecology. The diversity of physicochemical parameters presented by the geothermal hotsprings in the Taupo Volcanic Zone (TVZ) made them ideal study sites for investigating temporal chemical variations at set temperature and pH ranges.

Temporal dynamics in physicochemical variables and microbial communities

The focus of this study was to link temporal changes in physicochemical conditions to patterns in microbial community composition (i.e. to analyse temporal dynamics). By selecting hotsprings within the 60-70 °C range, it was anticipated from past experience that microbial communities would be simplified, in terms of overall diversity and the removal of photosynthesis as a primary driver. The selection of springs at different pH groups allowed comparisons across pH levels. Of the 43 chemical elements, nutrients and gases measured in each sample, eight chemical components and gases (plus temperature and pH) were association tested, based on their variance and observational changes in concentrations across temporal samples as well their covariance and correlation with the dominant phyla at each site (Table 2.3). The primary and secondary physicochemical variables associated with temporal microbial dynamics at each hotspring are discussed in detail below (Table 2.14).

pH

pH was the primary physicochemical driver at two sites, Whkr3 and Whgpa (Table 2.14). It was interesting to note that pH was a primary driver at hotsprings representing both acidic and neutral pH groups. The largest pH increase across the temporal samples was observed at the Whakarewarewa hotspring, Whkr3. pH at this site increased from pH 3.37 in December to pH 4.77 in October, with the most significant increase between June and August (pH 3.98-4.55). When pH changes along an environmental gradient or temporally, it introduces a selection pressure (based on optimal pH of different species), which can cause shifts in the relative abundance of microbial species in a community (Jackson et al., 2001; Macur et al., 2004; Delgado-Serrano et al., 2014). This was observed at Whkr3, where the increasing pH was associated with an increase in the relative abundance of

Aquificae and a decrease in *Crenarchaeota* (Figure 2.26). When the pH exceeded pH 3.5 in April and kept increasing, the relative community abundance of *Crenarchaeota* started declining. This observation is supported by the optimum pH of representative order *Sulfolobales* (pH 1-3.5) (Albers & Siebers, 2014). In contrast to *Crenarchaeota*, the relative abundance of *Aquificae* increased respective to the increase in pH. This observation is supported by the optimal pH of the representative genera, *Hydrogenobaculum* and *Venenivibrio* at pH 3-4 and pH 4.8-5.8, respectively (Hetzler et al., 2008). Additionally, between the June and August samples, a genus-level shift was observed in *Aquificae* (Figure 2.26). When pH reached pH 4.55 in August a significant shift was observed in genus-level dominance of *Hydrogenobaculum* to *Venenivibrio*. This observation again is supported by the known optimal pH of *Hydrogenobaculum* and *Venenivibrio* at pH 3-4 and pH 4.8-5.8, respectively (Hetzler et al., 2008). These findings demonstrate pH as the primary physicochemical driver shaping the microbial community at Whkr3 and highlight temporal dynamics in both the physicochemical conditions and microbial community at this site.

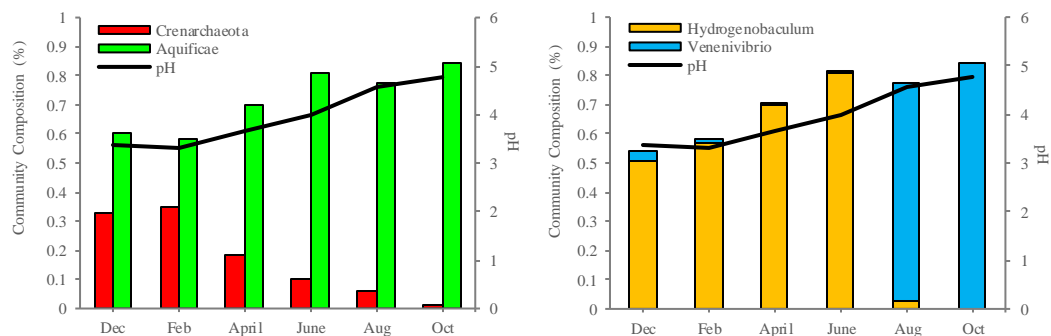


Figure 2.26: *Aquificae* and *Crenarchaeota* community composition in association with pH at Whkr3

Phylum level community composition of *Aquificae* and *Crenarchaeota* at Whkr3 with pH (left) *Aquificae* genus-level community composition of *Hydrogenobaculum* and *Venenivibrio* with pH (right)

At the Atiamuri hot spring (Whgpa), representing the pH 7 group, a cyclical pattern was observed in pH. pH measurements were the same in the December and October samples (pH 7.55), with lower values measured across the April and June samples. The community composition of *Armatimonadetes* significantly correlated with pH at this site (Figure 2.27 and Table 2.3). This phylum (*Armatimonadetes*) was only recently reclassified from the candidate division OP10 with limited phylogenetic data to date describing strains as soil dwelling aerobic oligotrophs.

Temperature for optimal growth of this phylum ranges from -3 °C to 79 °C, while optimal pH is between pH 4.5 to pH 8.6 (Tamaki et al., 2011; Lee et al., 2014). Strains from this phylum have been isolated from geothermal systems in the TVZ (Stott et al., 2008; Lee et al., 2011). pH at Whgpa ranged between pH 7.08 and pH 7.55, which supports the presence of at least some members of the *Armatimonadetes*, however, is unable to justify the temporal pattern observed in response to the change in pH (due to limited phylogenetic data) (Supplementary Table 4.2). Interestingly, *Deinococcus-Thermus* community abundance also significantly correlated with methane levels at this site (Figure 2.27). Research to date on this phylum, however, has not described an association between methane concentration and microbial growth, which may suggest that a combination of these variables influenced the observed cyclical pattern of the community composition. Together, these findings show that the microbial community follows the same cyclical trend displayed by the physicochemical conditions.

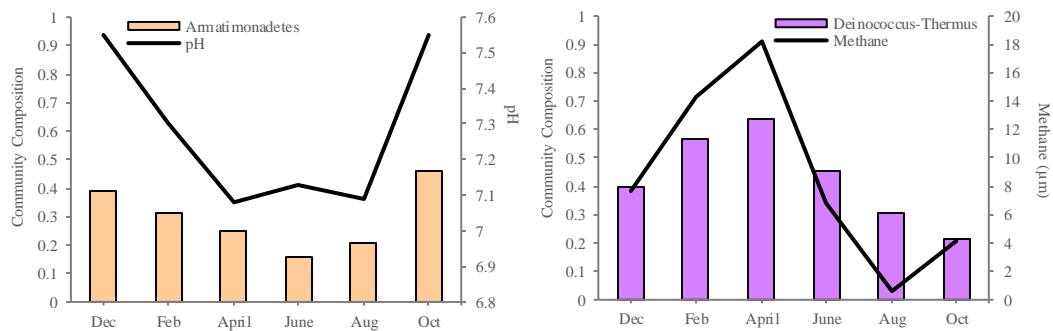


Figure 2.27: Trend observed in community composition in association with pH and methane at Whgpa

Community composition of *Armatimonadetes* in association with pH (left) Community composition of *Deinococcus-Thermus* in association with methane (right)

Temperature

Temperature was the primary physicochemical variable associated with microbial community dynamics at two of the Whakarewarewa Village hotsprings, Whkr2 and Whkr4 (Table 2.14). Both hotsprings were part of the pH 9 group. Temperature in geothermal environments is an important driver of microbial community composition and structure and can be linked with other environmental factors, such as oxygen solubility (Lacap et al., 2007; Mackenzie et al., 2013; Alsop et al., 2014; Sharp, Brady, et al., 2014). Certain microorganisms are restricted by temperature (based on their optimal growth temperature) which can cause shifts in

microbial community composition and structure over time (Boothroyd, 2009; Normand et al., 2015). This trend was observed at Whkr4, which had the largest increase in temperature across the study period. Temperature initially decreased at this site from 63.4 °C in December to 61.1 °C in April before increasing significantly (19.5 °C) to 80.6 °C in October (Supplementary Table 4.2). The largest incremental step in temperature was from 70.3 °C to 78.1 °C which occurred between the June and August samples. This significant temperature increase coincided with a switch in community dominance from *Deinococcus-Thermus* to *Aquificae* (Figure 2.28). This observation is supported by the optimal growth temperatures of each phyla, at 73 °C and 85 °C, respectively (Albuquerque & da Costa, 2014; Gupta, 2014). As temperature exceeded 73 °C between the June and August samples, the relative abundance of *Deinococcus-Thermus* significantly decreased in respect to *Aquificae*. Additionally, an increase in the relative abundance of *Thermodesulfobacteria* was also observed at this site. The optimal growth temperature of the representative genus *Caldimicrobium* is 75 °C, thus supporting the increase in relative abundance observed in association with increasing temperature (Mori, 2014). Together, we can conclude that temperature (based on the optimal growth conditions) was the primary physicochemical parameter driving the observed temporal change in the microbial community at Whkr4.

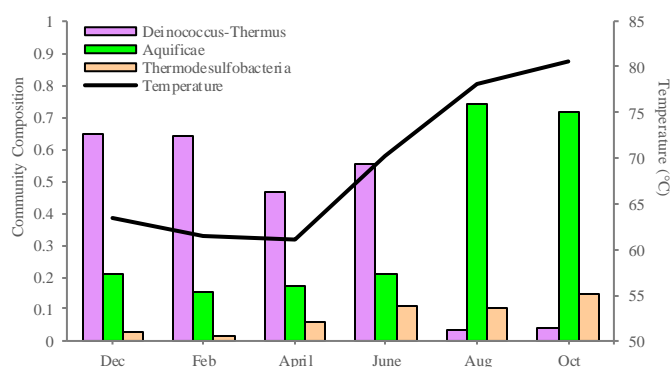


Figure 2.28: Trend observed in community composition in association with temperature at Whkr4

Community composition percentages over temporal samples of *Deinococcus-Thermus*, *Aquificae*, and *Thermodesulfobacteria* with temperature.

At the other Whakarewarewa Village site, Whkr2, temperature was consistent at 69.5 °C across December and February before decreasing to 65.5 °C

in October. This temperature range was relatively stable in comparison to the trend observed at Whkr4. Across the temporal samples, the relative abundance of *Aquificae* declined while *Proteobacteria* abundance increased (relative to the temperature decrease) (Figure 2.29). This observation can be supported by the optimal growth temperature of the dominant genera *Hydrogenobacter* (*Aquificae*) and *Hydrogenophilus* (*Proteobacteria*) at 60-85 °C and <65 °C, respectively (Gupta, 2014; Orlygsson & Kristjansson, 2014). Although variation observed in the community composition of the dominant phyla was low, temperature as an explanatory variable may have favoured the growth of *Proteobacteria* over *Aquificae* in the later samples. Notably, a shift in family-level dominance of *Aquificae* was also observed in February and August (Figure 2.29). This trend may be explained by the optimal growth temperature for the two families. The community composition of the family *Aquificaceae* spiked in February (69.6 °C) while *Hydrogenothermaceae* spiked in August (64.5 °C) (Table 2.11). *Aquificaceae* has a higher optimal growth temperature at 76 °C, compared to *Hydrogenothermaceae*. The three dominant *Aquificaceae* genera, *Aquifex*, *Hydrogenobacter* and *Hydrogenobaculum* all grow optimally above 65 °C, while *Hydrogenothermaceae* genera (*Sulfurihydrogenibium* and *Venenivibrio*) can survive at temperatures as low as 40 °C (Gupta, 2014). This switch in family dominance during August may also be associated with the increase in rainfall and surface flooding at this site (discussed in further section). Together, these observations conclude (based on optimal growth conditions) that temperature was the primary driver influencing community composition at Whkr2.

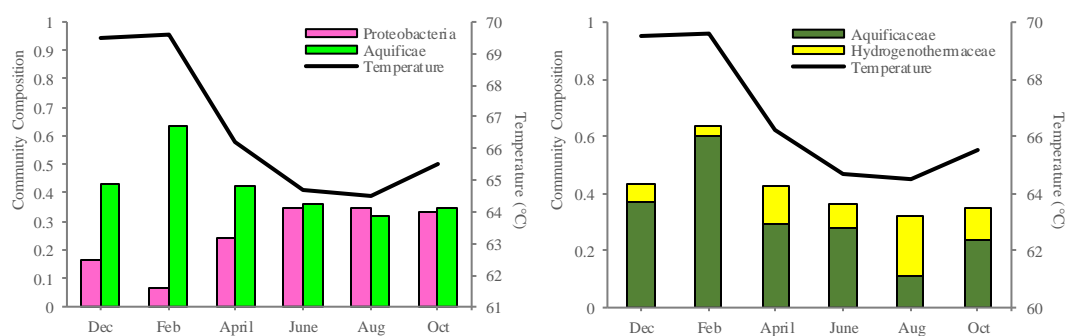


Figure 2.29: Trend observed in community composition in association with temperature at Whkr2

Phylum-level community composition of *Proteobacteria* and *Aquificae* with temperature (left)
 Family-level community composition of phylum *Aquificae* and temperature (right)

Chemistry

Alterations to the chemical composition of geothermal environments can cause shifts in the dominant species within a community (based on the relative concentrations of components required for microbial growth). Major components of geothermal hotsprings, such as chloride and sulfate can reflect the aquifer conditions and are relatively stable over time (in regards to non-conservatives e.g. (iron) which are influenced by shallow processing including boiling and mixing) (Pope & Brown, 2014).

Sulfate was the primary physicochemical variable influencing the microbial community at Kui3 (pH 5 group) (Table 2.14). Increasing sulfate concentration was associated with an increase in the relative abundance of *Aquificae* and a decrease in *Proteobacteria* abundance (Figure 2.30). This observation is supported by the physiological requirement of sulfur compounds for the growth of the representative *Aquificae* genus *Venenivibrio* (Hetzer et al., 2008; Takai & Nakagawa, 2014). Additionally, temperature (although not correlated with *Proteobacteria* community composition change) could explain the observed increase of the phylum in the August sample. The lowest temperature of 45.8 °C was recorded during August which coincided with the increased rainfall (discussed in further section). This was associated with a spike in the community abundance of *Thiovirga* (*Gammaproteobacteria*) and *Nitratiruptor* (*Epsilonproteobacteria*) (Table 2.8 and Figure 2.30). This observation is supported by the hotsprings temperature decreasing to the upper optimal temperatures of these genera at 42 °C and 37 °C, respectively (Miroshnichenko et al., 2004; Miroshnichenko & Bonch-Osmolovskaya, 2006; Kelly & Wood, 2015). Together, we can conclude that hotspring chemistry (sulfate) and temperature influenced the temporal variations of the microbial community at Kui3.

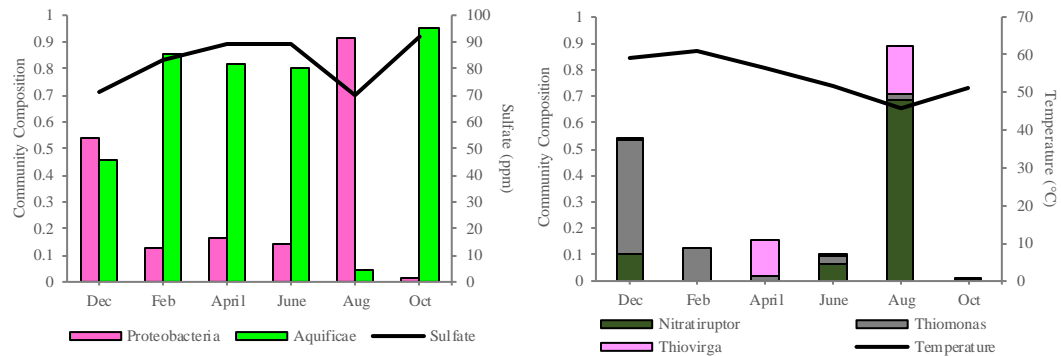


Figure 2.30: Trend observed in community composition in association with sulfate and temperature at Kui3

Phylum-level community composition of *Aquificae* and *Proteobacteria* with trend in sulfate at Kui3 (left) Genus-level community composition of the phylum *Proteobacteria* and temperature (right)

Hotspring chemical variables, total sulfur and potassium, were the primary physicochemical drivers at Whkr1 (pH 3 group) (Table 2.14). The structure of the Whkr1 community changed between February and October, where the community abundance of *Proteobacteria* increased respective to a decrease in *Aquificae*. Total sulfur decreased across temporal samples, spiking in June, which supports the change observed in the relative community abundance of *Aquificae* (Figure 2.31). The dominant genus representing *Aquificae* (*Hydrogenobaculum*) has a physiological requirement of sulfur for growth (Shima & Suzuki, 1993). This physiological property supports the observation of the decreasing *Aquificae* community abundance respective to decreasing total sulfur levels. The other dominant phylum *Proteobacteria*, represented by the class *Gammaproteobacteria*, and genus *Acidithiobacillus* are a genus of acidophilic species which can oxidize both Fe^{2+} and sulfide minerals at an optimal pH of <4.0 (Kelly & Wood, 2000). The abundance of this phylum increased relative to the decrease in *Aquificae* community abundance. No significant associations between *Proteobacteria* and the assessed elements, nutrients and gases were observed (Table 2.3). This may suggest that this community is driven by a combination of chemical variables. Significant conclusions could therefore not be made on the primary physicochemical driver at this site, however, it can be concluded that the physicochemical conditions and microbial community at Whkr1 are temporally dynamic. It should be noted that this site is fed by multiple inputs from surrounding features which could explain the variability in physicochemical drivers at this site.

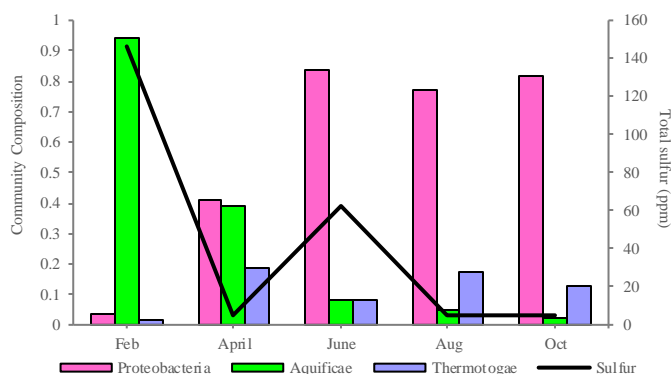


Figure 2.31: Trend observed in community composition in association with total sulfur at Whkr1

Community composition percentage of *Aquificae*, *Proteobacteria* and *Thermotogae* with total sulfur at Whkr1.

Variation in physicochemical variables and rainfall and microbial community composition

Physical changes to hot spring water levels were recorded for the duration of this study to link to rainfall and geothermal bore water datasets. It was hypothesized that changes to surface water levels caused by seasonal precipitation would influence the physicochemical variables and microbial community composition of target hot springs. The addition of rainfall over the winter months would hypothetically be linked to a decrease in temperature, a dilution in chemical components and a possible decrease in pH (increased O₂ associated with sulfur oxidation). These associations were based on observation only, and not statistical means. Associations were only made at the seven springs located in the Rotorua district where geothermal bore water and rainfall datasets were available.

Although there were increased levels of rainfall and surface flooding in Rotorua during August, only two of the four geothermal bores reflected trends associated with this increase (Figure 2.25). These geothermal bores, M27 and M28 were located in close proximity to Kuirau Park (Figure 2.24). The primary physicochemical changes at two Rotorua sites, Whkr2 and Kui3 could be anecdotally-linked with the increased rainfall during the August sampling. Temperature decreased over the winter months (June and August) at both hot springs which was associated with a genus-level shift in dominant phyla. At Whkr2 a genus-level shift in *Aquificae* was described, while at Kui3, a family-level

shift in *Proteobacteria* was described and associated with temperature (Tables 2.8 and 2.11).

Although a significant change in microbial community was associated with temperature and/or pH at Whkr3 and Whkr4, these observations did not reflect the idea that increased rainfall modified physicochemical conditions. Temperature at Whkr3 and Whkr4 increased across the winter months irrespective of the increase in rainfall. pH also increased at both sites (Whkr3 and Whkr4) with the largest increase in pH in this study observed at Whkr3 between June and August (Supplementary Table 4.2). These observations do not link in with the assumption of decreasing temperature and pH from rainfall during August. It was interesting to note however, as these sites (Whkr3, Whkr4) are in close proximity with the other Whakarewarewa spring Whkr2, which did display a decrease in temperature associated with the increased rainfall. This therefore, may highlight differences in the hydrology and source water of these springs which in turn may have influenced the observations noted in the physicochemical conditions.

Microbial community structure in response to stable physicochemical conditions

While this study focused on variations in community structure resulting from changes in environmental conditions, it is equally important that community structure remains stable where physicochemical conditions did not vary. This was observed at three of the target hotsprings in this study (Figure 2.14).

Two of these hotsprings were in the Waiotapu geothermal system, Waiol and Waiol2 (pH 5 group). These sites had the highest recorded levels of chloride, sodium, silica, potassium, calcium and ammonium making them chemically distinct from the other geothermal systems. There was no physical indication of change observed over the study period (i.e surface flooding). The geochemical conditions of these springs were relatively stable between December and October (Appendix 4.2), with temperature and pH (59.4-71.9 °C, pH 4.56-5.07) supporting the dominance of *Aquificae* (genus *Venenivibrio*). The representative species of this genus was isolated from Champagne Pool located within this geothermal park (Hetzer et al., 2007; Hetzer et al., 2008). These findings highlight the persistence of fixed microbial communities in response to stable physicochemical environments (see Figure 2.12).

The physicochemical conditions and microbial communities were also stable at the Kui1 (pH 7 Group) and TeP (pH 3 Group) hot springs. The Kui1 community was dominated by *Aquificae*, while archaeal phyla *Crenarchaeota* and *Euryarchaeota* were dominant at TeP (see Figure 2.18 and 2.11). There were no large variations observed in the physicochemical dataset, and no significant correlations between dominant phyla and variables at each site (Table 2.3). Primary and secondary driver could therefore not be concluded from this site, suggesting the presence of a stable physicochemical environment and microbial community.

While it is assumed that microbial communities would not change in the presence of stable physicochemical conditions, there was one pool in this study which did not follow this assumption. The Ohaaki hot spring (pH 9 Group) was highly concentrated in silica, potassium and chloride (Appendix 4.2). From March to August, the microbial community was dominated by *Aquificae* before a significant shift in community structure to *Deinococcus-Thermus* was observed in October. (see Figure 2.23). The presence of both *Aquificae* and *Deinococcus-Thermus* was supported by the temperature and pH conditions (~68 °C, pH 8.83) at this site (Albers & Siebers, 2014; Gupta, 2014), however, observations of the physicochemical dataset did not reveal any significant changes in the elements, nutrients, gases or temperature and pH during the October sampling which could account for the shift in community composition. Consequently, no significant correlations were noted between the dominant phyla and physicochemical variables assessed (Table 2.3). These findings indicate a change in microbial community in response to stable physicochemical conditions, suggesting the influence of an unmonitored variable at this site.

To summarize these findings, six of the target hot springs displayed temporal dynamics in physicochemical variables which were significantly associated with changes in the microbial communities. Temperature and pH were the primary physicochemical drivers across these hot springs, with the most dramatic community shifts observed between June and August. An increase in surface flooding with high rainfall was observed in August, however physicochemical and microbial community dynamics could only be associated with two Rotorua hot springs in this study (Whkr2 and Kui3). Of the six target hot springs where the primary physicochemical driver could not be determined, four did not display

temporal variations in either the physicochemical environment or microbial community.

Chapter Three

Conclusions and future directions

3.1 Conclusions

The aim of this research was to study the physicochemical and microbial dynamics of geothermal hotsprings of the Taupō Volcanic Zone (TVZ) through time. The over-arching hypothesis of this research was that temporal changes to physicochemical variables would influence microbial community composition and structure. We showed that physicochemical variables can be dynamic in geothermal hotsprings of the TVZ, which can influence the residing microbial communities. Importantly, temperature and pH were predominant factors influencing microbial community structure at both phylum and genus level of the communities. Chemical changes across the springs had weaker associations with the dominant phyla across the target hotsprings. To determine how subtle chemical changes can influence microbial composition, further in-depth analyses would be required with additional sampling time points. The temporal microbial community and physicochemical dynamics that were associated with rainfall added another layer of complexity to this study and were able to highlight possible differences in the hydrology at Whakarewarewa. This further emphasizes that these extreme ecosystems are not isolated from their surrounding environment.

This work provides an overview of the temporal physicochemical and microbial community dynamics at hotsprings within the TVZ. Importantly, this dataset will extend the resolution of the 1,000 Springs Project database by inferring the importance of temporal measurements.

3.2 Future directions

Widespread geochemical and microbial analysis at geothermal sites in the TVZ will be beneficial in furthering our understanding of how these complex and extreme environments vary over time and shape the composition and structure of the residing microbial communities. Long-term use of these economically important resources through geothermal power production has caused the destruction of many geothermal systems since the early 1900's. This is an issue

when considering the value these resources hold, not only for sustainable power production, but also as part of our biological and cultural heritage. This study alongside future studies can therefore provide a better understanding of the system to better inform policy and management decisions.

To extend this project, given additional funding and time, multiple intensive 24/7 studies at a range of pH's and TVZ systems, or a long-term study involving daily monitoring, would be ideal projects that would dramatically improve our understanding of these systems and ecological processes associated with time. By increasing sampling time points, subtle changes missed between time points in this study would be highlighted and would increase the statistical power in linking physicochemical changes with the microbial community. To add another layer to this project, a RNA-based functional study would be able to determine the community changes, as well as any changes to community function that occur temporally in association with physicochemical changes. Ultimately, the integration of multiple datasets (i.e. meteoric, physicochemical, microbial (DNA) and functional (RNA)) would provide an ideal dataset to thoroughly investigate (with increased statistical power) subtle changes in geothermal environments and their downstream effects on the geothermal microbial community.

References

- Albers, S.-V., & Siebers, B. (2014). The Family Sulfolobaceae. In E. Rosenberg, E. F. DeLong, S. Lory, E. Stackebrandt, & F. Thompson (Eds.), *The Prokaryotes: Other Major Lineages of Bacteria and The Archaea* (pp. 323-346). Berlin, Heidelberg: Springer Berlin Heidelberg.
- Albuquerque, L., & da Costa, M. S. (2014). The Family Thermaceae. In E. Rosenberg, E. F. DeLong, S. Lory, E. Stackebrandt, & F. Thompson (Eds.), *The Prokaryotes: Other Major Lineages of Bacteria and The Archaea* (pp. 955-987). Berlin, Heidelberg: Springer Berlin Heidelberg.
- Alsop, E. B., Boyd, E. S., & Raymond, J. (2014). Merging metagenomics and geochemistry reveals environmental controls on biological diversity and evolution. *BMC Ecology*, *14*, 16-16. doi:10.1186/1472-6785-14-16
- Auchtung, T. A., Shyndriayeva, G., & Cavanaugh, C. M. (2011). 16S rRNA phylogenetic analysis and quantification of Korarchaeota indigenous to the hot springs of Kamchatka, Russia. *Extremophiles*, *15*(1), 105-116. doi:10.1007/s00792-010-0340-5
- Auchtung, T. A., Takacs-Vesbach, C. D., & Cavanaugh, C. M. (2006). 16S rRNA Phylogenetic Investigation of the Candidate Division "Korarchaeota". *Applied and Environmental Microbiology*, *72*(7), 5077-5082. doi:10.1128/AEM.00052-06
- Bahl, J., Lau, M. C. Y., Smith, G. J. D., Vijaykrishna, D., Cary, S. C., Lacap, D. C., . . . Pointing, S. B. (2011). Ancient origins determine global biogeography of hot and cold desert cyanobacteria. *Nat Commun*, *2*, 163. doi:dx.doi.org/10.1038/ncomms1167
- Barns, S. M., Delwiche, C. F., Palmer, J. D., & Pace, N. R. (1996). Perspectives on archaeal diversity, thermophily and monophyly from environmental rRNA sequences. *Proceedings of the National Academy of Sciences of the United States of America*, *93*(17), 9188-9193.
- Bay of Plenty Regional Council. (2015). Telemetry Data for Groundwater. Retrieved from <http://monitoring.boprc.govt.nz/MonitoredSites/cgi-bin/hydwebserver.cgi/catchments/details?catchment=32>
- Bell, E. M., & Callaghan, T. V. (2012). What are extreme environments and what live in them? In E. Bell (Ed.), *Life at Extremes: Environments, Organisms, and Strategies for Survival*. Wallingford, Oxon, GBR: CABI Publishing.
- Bibby, H. M., Caldwell, T. G., Davey, F. J., & Webb, T. H. (1995). Geophysical evidence on the structure of the Taupo Volcanic Zone and its hydrothermal circulation. *Journal of Volcanology and Geothermal Research*, *68*(1-3), 29-58. doi:dx.doi.org/10.1016/0377-0273(95)00007-H
- Bokulich, N. A., Thorngate, J. H., Richardson, P. M., & Mills, D. A. (2014). Microbial biogeography of wine grapes is conditioned by cultivar, vintage, and climate. *Proceedings of the National Academy of Sciences*, *111*(1), E139-E148. doi:10.1073/pnas.1317377110
- Boothroyd, I. K. G. (2009). Ecological characteristics and management of geothermal systems of the Taupo Volcanic Zone, New Zealand. *Geothermics*, *38*(1), 200-209. doi:10.1016/j.geothermics.2008.12.010
- Briggs, B. R., Brodie, E. L., Tom, L. M., Dong, H., Jiang, H., Huang, Q., . . . Hungate, B. A. (2014). Seasonal patterns in microbial communities inhabiting the hot springs of Tengchong, Yunnan Province, China.

- Environmental Microbiology*, 16(6), 1579-1591. doi:10.1111/1462-2920.12311
- Brochier-Armanet, C., Forterre, P., & Gribaldo, S. (2011). Phylogeny and evolution of the Archaea: one hundred genomes later. *Current Opinion in Microbiology*, 14(3), 274-281. doi:dx.doi.org/10.1016/j.mib.2011.04.015
- Brochier, C., Gribaldo, S., Zivanovic, Y., Confalonieri, F., & Forterre, P. (2005). Nanoarchaea: representatives of a novel archaeal phylum or a fast-evolving euryarchaeal lineage related to Thermococcales? *Genome Biology*, 6(5), R42-R42. doi:10.1186/gb-2005-6-5-r42
- Brock, T. D. (1978). *Thermophilic Microorganisms and Life at High Temperatures*. New York: Springer.
- Brock, T. D. (1997). The Value of Basic Research: Discovery of *Thermus Aquaticus* and Other Extreme Thermophiles. *Genetics*, 146(4), 1207-1210.
- Caporaso, J. G. (2010). QIIME allows analysis of high-throughput community sequencing data: Nature Methods.
- Caporaso, J. G., Lauber, C. L., Walters, W. A., Berg-Lyons, D., Lozupone, C. A., Turnbaugh, P. J., . . . Knight, R. (2011). Global patterns of 16S rRNA diversity at a depth of millions of sequences per sample. *Proceedings of the National Academy of Sciences*, 108(Supplement 1), 4516-4522. doi:10.1073/pnas.1000080107
- Castelle, C. J., Wrighton, K. C., Thomas, B. C., Hug, L. A., Brown, C. T., Wilkins, M. J., . . . Banfield, J. F. (2015). Genomic Expansion of Domain Archaea Highlights Roles for Organisms from New Phyla in Anaerobic Carbon Cycling. *Current Biology*, 25(6), 690-701. doi:dx.doi.org/10.1016/j.cub.2015.01.014
- Castenholz, R. W. (1969). Thermophilic blue-green algae and the thermal environment. *Bacteriological Reviews*, 33(4), 476-504.
- Caumette, P., Brochier-Armanet, C., & Normand, P. (2015). Taxonomy and Phylogeny of Prokaryotes. In J.-C. Bertrand, P. Caumette, P. Lebaron, R. Matheron, P. Normand, & T. Sime-Ngando (Eds.), *Environmental Microbiology: Fundamentals and Applications: Microbial Ecology* (pp. 145-190). Dordrecht: Springer Netherlands.
- Cayol, J.-L., Ollivier, B., Alazard, D., Amils, R., Godfroy, A., Piette, F., & Prieur, D. (2015). The Extreme Conditions of Life on the Planet and Exobiology. In J.-C. Bertrand, P. Caumette, P. Lebaron, R. Matheron, P. Normand, & T. Sime-Ngando (Eds.), *Environmental Microbiology: Fundamentals and Applications: Microbial Ecology* (pp. 353-394). Dordrecht: Springer Netherlands.
- Childs, A. M., Mountain, B. W., O'Toole, R., & Stott, M. B. (2008). Relating Microbial Community and Physicochemical Parameters of a Hot Spring: Champagne Pool, Wai-o-tapu, New Zealand. *Geomicrobiology Journal*, 25(7-8), 441-453. doi:10.1080/01490450802413841
- Chu, H., Fierer, N., Lauber, C. L., Caporaso, J. G., Knight, R., & Grogan, P. (2010). Soil bacterial diversity in the Arctic is not fundamentally different from that found in other biomes H. Chu et al. Bacterial biogeography in arctic soils. *Environmental Microbiology*, 12(11), 2998-3006. doi:10.1111/j.1462-2920.2010.02277.x
- Clingenpeel, S., Kan, J., Macur, R. E., Woyke, T., Lovalvo, D., Varley, J., . . . McDermott, T. R. (2013). Yellowstone Lake Nanoarchaeota. *Frontiers in Microbiology*, 4, 274. doi:10.3389/fmicb.2013.00274

- Cole, J. K., Peacock, J. P., Dodsworth, J. A., Williams, A. J., Thompson, D. B., Dong, H., . . . Hedlund, B. P. (2013). Sediment microbial communities in Great Boiling Spring are controlled by temperature and distinct from water communities. *The ISME Journal*, 7(4), 718-729. doi:10.1038/ismej.2012.157
- Coman, C., Drugă, B., Hegedus, A., Sicora, C., & Dragoș, N. (2013). Archaeal and bacterial diversity in two hot spring microbial mats from a geothermal region in Romania. *Extremophiles*, 17(3), 523-534. doi:10.1007/s00792-013-0537-5
- Cowan, D., Tuffin, M., Mulako, I., & Cass, J. (2012). Terrestrial Hydrothermal Environments. In E. Bell (Ed.), *Life at Extremes: Environments, Organisms, and Strategies for Survival*. Wallingford, Oxon, GBR: CABI Publishing.
- Delgado-Serrano, L., López, G., Bohorquez, L. C., Bustos, J. R., Rubiano, C., Osorio-Forero, C., . . . Zambrano, M. M. (2014). Neotropical Andes hot springs harbor diverse and distinct planktonic microbial communities. *FEMS Microbiology Ecology*, 89(1), 56-66.
- DeLong, E. F., & Pace, N. R. (2001). Environmental Diversity of Bacteria and Archaea. *Systematic Biology*, 50(4), 470-478. doi:10.1080/10635150118513
- Edgar, R. C. (2010). Search and clustering orders of magnitude faster than BLAST. *Bioinformatics*, 26(19), 2460-2461. doi:10.1093/bioinformatics/btq461
- Elkins, J. G., Podar, M., Graham, D. E., Makarova, K. S., Wolf, Y., Randau, L., . . . Stetter, K. O. (2008). A korarchaeal genome reveals insights into the evolution of the Archaea. *Proceedings of the National Academy of Sciences of the United States of America*, 105(23), 8102-8107. doi:10.1073/pnas.0801980105
- Fenchel, T. (2003). Biogeography for Bacteria. *Science*, 301(5635), 925-926. doi:10.1126/science.1089242
- Ferris, M. J., & Ward, D. M. (1997). Seasonal distributions of dominant 16S rRNA-defined populations in a hot spring microbial mat examined by denaturing gradient gel electrophoresis. *Applied and Environmental Microbiology*, 63(4), 1375-1381.
- Fierer, N., & Jackson, R. B. (2006). The diversity and biogeography of soil bacterial communities. *Proceedings of the National Academy of Sciences of the United States of America*, 103(3), 626-631. doi:10.1073/pnas.0507535103
- Fortunato, C. S., Herfort, L., Zuber, P., Baptista, A. M., & Crump, B. C. (2012). Spatial variability overwhelms seasonal patterns in bacterioplankton communities across a river to ocean gradient. *The ISME Journal*, 6(3), 554-563. doi:dx.doi.org/10.1038/ismej.2011.135
- Fouke, B. W. (2011). Hot-spring Systems Geobiology: abiotic and biotic influences on travertine formation at Mammoth Hot Springs, Yellowstone National Park, USA. *Sedimentology*, 58(1), 170-219. doi:10.1111/j.1365-3091.2010.01209.x
- Giggenbach, W., Sheppard, D. S., Robinson, B. W., Stewart, M. K., & Lyon, G. L. (1994). Geochemical structure and position of the Waiotapu geothermal field, New Zealand. *Geothermics*, 23(5), 599-644. doi:dx.doi.org/10.1016/0375-6505(94)90022-1

- Gilbert, J. A., Steele, J. A., Caporaso, J. G., Steinbrück, L., Reeder, J., Temperton, B., . . . Field, D. (2012). Defining seasonal marine microbial community dynamics. *The ISME Journal*, 6(2), 298-308. doi:10.1038/ismej.2011.107
- Glover, R. B., & Mroczek, E. K. (1998). Changes in silica chemistry and hydrology across the Rotorua geothermal field, New Zealand. *Geothermics*, 27(2), 183-196. doi:dx.doi.org/10.1016/S0375-6505(97)10014-1
- Greene, A. C. (2014). The Family Desulfurellaceae. In E. Rosenberg, E. F. DeLong, S. Lory, E. Stackebrandt, & F. Thompson (Eds.), *The Prokaryotes: Deltaproteobacteria and Epsilonproteobacteria* (pp. 135-142). Berlin, Heidelberg: Springer Berlin Heidelberg.
- Griffiths, R. I., Thomson, B. C., James, P., Bell, T., Bailey, M., & Whiteley, A. S. (2011). The bacterial biogeography of British soils. *Environmental Microbiology*, 13(6), 1642-1654. doi:10.1111/j.1462-2920.2011.02480.x
- Gupta, R. S. (2014). The Phylum Aquificae. In E. Rosenberg, E. F. DeLong, S. Lory, E. Stackebrandt, & F. Thompson (Eds.), *The Prokaryotes: Other Major Lineages of Bacteria and The Archaea* (pp. 417-445). Berlin, Heidelberg: Springer Berlin Heidelberg.
- Guy, L., & Ettema, T. J. G. (2011). The archaeal 'TACK' superphylum and the origin of eukaryotes. *Trends in Microbiology*, 19(12), 580-587. doi:10.1016/j.tim.2011.09.002
- Havig, J., Hamilton, T., Boyd, E., Meyer-Dombard, D., & Shock, E. (2011). *Effects of geochemical changes on microbial community structure in a hot spring ecosystem*. Paper presented at the AGU Fall Meeting Abstracts.
- Herbold, C. W., Lee, C. K., McDonald, I. R., & Cary, S. C. (2014). Evidence of global-scale aeolian dispersal and endemism in isolated geothermal microbial communities of Antarctica. *Nature Communications*, 5, 3875. doi:dx.doi.org/10.1038/ncomms4875
- Hetzer, A., McDonald, I. R., & Morgan, H. W. (2008). *Venenivibrio stagnispumantis* gen. nov., sp. nov., a thermophilic hydrogen-oxidizing bacterium isolated from Champagne Pool, Waiotapu, New Zealand. *International Journal of Systematic and Evolutionary Microbiology*, 58(2), 398-403. doi:doi:10.1099/ijs.0.64842-0
- Hetzer, A., Morgan, H., McDonald, I., & Daughney, C. (2007). Microbial life in Champagne Pool, a geothermal spring in Waiotapu, New Zealand. *Extremophiles*, 11(4), 605-614. doi:10.1007/s00792-007-0073-2
- Houghton, B. F., Wilson, C. J. N., McWilliams, M. O., Lanphere, M. A., Weaver, S. D., Briggs, R. M., & Pringle, M. S. (1995). Chronology and dynamics of a large silicic magmatic system: Central Taupo Volcanic Zone, New Zealand. *Geology*, 23(1), 13-16. doi:10.1130/0091-7613(1995)023<0013:cadoal>2.3.co;2
- Hreggvidsson, G. O., Petursdottir, S. K., Björnsdottir, S. H., & Fridjonsson, O. H. (2012). Microbial speciation in the geothermal ecosystem. In H. Stan-Lotter & S. Fendrihan (Eds.), *Adaption of Microbial Life to Environmental Extremes: Novel Research Results and Application* (pp. 37-67). Vienna: Springer Vienna.
- Huber, H., Hohn, M. J., Reinhard, R., Fuchs, T., & et al. (2002). A new phylum of Archaea represented by a nanosized hyperthermophilic symbiont. *Nature*, 417(6884), 63-67. doi:dx.doi.org/10.1038/417063a
- Jackson, C. R., Langner, H. W., Donahoe-Christiansen, J., Inskeep, W. P., & McDermott, T. R. (2001). Molecular analysis of microbial community

- structure in an arsenite-oxidizing acidic thermal spring. *Environmental Microbiology*, 3(8), 532-542. doi:10.1046/j.1462-2920.2001.00221.x
- Jun Liu, Zheng-Shuang Hua, Lin-Xing Chen, Jia-Liang Kuang, Sheng-Jin Li, Wen-Sheng Shu, & Huang, L.-N. (2014). Correlating Microbial Diversity Patterns with Geochemistry in an Extreme and Heterogeneous Environment of Mine Tailings. *Applied and Environmental Microbiology*, 80(12), 3677-3686. doi:10.1128/AEM.00294-14
- Kan, J., Clingenpeel, S., Macur, R. E., Inskeep, W. P., Lovalvo, D., Varley, J., . . . Nealson, K. (2011). Archaea in Yellowstone Lake. *The ISME Journal*, 5(11), 1784-1795. doi:10.1038/ismej.2011.56
- Kaur, G., Mountain, B., Stott, M., Hopmans, E., & Pancost, R. (2015). Temperature and pH control on lipid composition of silica sinters from diverse hot springs in the Taupo Volcanic Zone, New Zealand. *Extremophiles*, 19(2), 327-344. doi:10.1007/s00792-014-0719-9
- Kelly, D. P., & Wood, A. P. (2000). Reclassification of some species of *Thiobacillus* to the newly designated genera *Acidithiobacillus* gen. nov., *Halothiobacillus* gen. nov. and *Thermithiobacillus* gen. nov. *International Journal of Systematic and Evolutionary Microbiology*, 50(2), 511-516.
- Kelly, D. P., & Wood, A. P. (2015). *Halothiobacillaceae* fam. nov. *Bergey's Manual of Systematics of Archaea and Bacteria*: John Wiley & Sons, Ltd.
- Lacap, D. C., Barraquio, W., & Pointing, S. B. (2007). Thermophilic microbial mats in a tropical geothermal location display pronounced seasonal changes but appear resilient to stochastic disturbance. *Environmental Microbiology*, 9(12), 3065-3076. doi:10.1111/j.1462-2920.2007.01417.x
- Lau, M. Y., Aitchison, J., & Pointing, S. (2009). Bacterial community composition in thermophilic microbial mats from five hot springs in central Tibet. *Extremophiles*, 13(1), 139-149. doi:10.1007/s00792-008-0205-3
- Lee, K. C., Dunfield, P. F., Morgan, X. C., Crowe, M. A., Houghton, K. M., Vyssotski, M., . . . Stott, M. B. (2011). *Chthonomonas calidirosea* gen. nov., sp. nov., an aerobic, pigmented, thermophilic micro-organism of a novel bacterial class, *Chthonomonadetes classis* nov., of the newly described phylum *Armatimonadetes* originally designated candidate division OP10. *Int J Syst Evol Microbiol*, 61(10), 2482-2490.
- Lee, K. C. Y., Dunfield, P. F., & Stott, M. B. (2014). The Phylum *Armatimonadetes*. In E. Rosenberg, E. F. DeLong, S. Lory, E. Stackebrandt, & F. Thompson (Eds.), *The Prokaryotes: Other Major Lineages of Bacteria and The Archaea* (pp. 447-458). Berlin, Heidelberg: Springer Berlin Heidelberg.
- Livermore, J. A., & Jones, S. E. (2015). Local-global overlap in diversity informs mechanisms of bacterial biogeography. *ISME J*. doi:10.1038/ismej.2015.51
- Mackenzie, R., Pedrós-Alió, C., & Díez, B. (2013). Bacterial composition of microbial mats in hot springs in Northern Patagonia: variations with seasons and temperature. *Extremophiles*, 17(1), 123-136. doi:10.1007/s00792-012-0499-z
- Macur, R. E., Langner, H. W., Kocar, B. D., & Inskeep, W. P. (2004). Linking geochemical processes with microbial community analysis: successional dynamics in an arsenic-rich, acid-sulphate-chloride geothermal spring. *Geobiology*, 2(3), 163-177. doi:10.1111/j.1472-4677.2004.00032.x

- Madigan, M., Martinko, J., Bender, K., Buckley, D., & Stahl, D. (2015). *Brock Biology of Microorganisms* (14 ed.). England: Pearson Education Limited
- Matheron, R., & Caumette, P. (2015). Structure and Functions of Microorganisms: Production and Use of Material and Energy. In J.-C. Bertrand, P. Caumette, P. Lebaron, R. Matheron, P. Normand, & T. Sime- Ngando (Eds.), *Environmental Microbiology: Fundamentals and Applications: Microbial Ecology* (pp. 25-71). Dordrecht: Springer Netherlands.
- McArthur, J. V. (2006). *Microbial Ecology : An Evolutionary Approach*. Burlington, US: Academic Press.
- McMurdie & Holmes (2013). phyloseq: An R package for Reproducible Interactive Analysis and Graphics of Microbiome Census Data. *PLoS One*, 8(4), e61217.
- Milner, D. M., Cole, J. W., & Wood, C. P. (2003). Mamaku Ignimbrite: a caldera-forming ignimbrite erupted from a compositionally zoned magma chamber in Taupo Volcanic Zone, New Zealand. *Journal of Volcanology and Geothermal Research*, 122(3-4), 243-264. doi:dx.doi.org/10.1016/S0377-0273(02)00504-8
- Miroshnichenko, M. L., Haridon, S., Schumann, P., Spring, S., Bonch-Osmolovskaya, E. A., . . . Stackebrandt, E. (2004). *Caminiibacter profundus* sp. nov., a novel thermophile of Nautiliales ord. nov. within the class ‘Epsilonproteobacteria’, isolated from a deep-sea hydrothermal vent. *International Journal of Systematic and Evolutionary Microbiology*, 54(1), 41-45. doi:doi:10.1099/ijs.0.02753-0
- Miroshnichenko, M. L., & Bonch-Osmolovskaya, E. A. (2006). Recent developments in the thermophilic microbiology of deep-sea hydrothermal vents. *Extremophiles*, 10(2), 85-96. doi:10.1007/s00792-005-0489-5
- Mori, K. (2014). The Family Thermodesulfobacteriaceae. In E. Rosenberg, E. F. DeLong, S. Lory, E. Stackebrandt, & F. Thompson (Eds.), *The Prokaryotes: Firmicutes and Tenericutes* (pp. 381-388). Berlin, Heidelberg: Springer Berlin Heidelberg.
- Munson-McGee, J. H., Field, E. K., Bateson, M., Rooney, C., Stepanauskas, R., & Young, M. J. (2015). Nanoarchaeota, Their Sulfolobales Host, and Nanoarchaeota Virus Distribution across Yellowstone National Park Hot Springs. *Applied and Environmental Microbiology*, 81(22), 7860-7868. doi:10.1128/aem.01539-15
- Nakagawa, S., & Takai, K. (2014). The Family Nautiliaceae: The Genera *Caminiibacter*, *Lebetimonas*, and *Nautilia*. In E. Rosenberg, E. F. DeLong, S. Lory, E. Stackebrandt, & F. Thompson (Eds.), *The Prokaryotes: Deltaproteobacteria and Epsilonproteobacteria* (pp. 393-399). Berlin, Heidelberg: Springer Berlin Heidelberg.
- New Zealand Geothermal Association. (2010a). Geothermal Energy & Electricity Generation. Retrieved from http://www.nzgeothermal.org.nz/elec_geo.html
- New Zealand Geothermal Association. (2010b). New Zealand Geothermal Fields. Retrieved from http://www.nzgeothermal.org.nz/nz_geo_fields.html
- New Zealand Institute of Chemistry. (2008). Geothermal Waters: A Source of Energy and Metals. Retrieved from <http://nzic.org.nz/ChemProcesses/water/index.html>
- NIWA. (2016). The National Climate Database. Retrieved from <https://cliflo.niwa.co.nz/>

- Nordstrom, D. K., Ball, J. W., & McCleskey, R. B. (2005). Ground Water to Surface Water: Chemistry of Thermal Outflows in Yellowstone National Park. In T. R. McDermott & W. P. Inskeep (Eds.), *Geothermal biology and geochemistry in Yellowstone National Park: proceeding of the Thermal Biology Institute workshop, Yellowstone National Park, WY, October 2003* (pp. xii, 352 p.). Bozeman, MT: Montana State University Publications.
- Normand, P., Caumette, P., Goulas, P., Pujic, P., & Wisniewski-Dyé, F. (2015). Adaptations of Prokaryotes to Their Biotopes and to Physicochemical Conditions in Natural or Anthropized Environments. In J.-C. Bertrand, P. Caumette, P. Lebaron, R. Matheron, P. Normand, & T. Sime-Ngando (Eds.), *Environmental Microbiology: Fundamentals and Applications: Microbial Ecology* (pp. 293-351). Dordrecht: Springer Netherlands.
- Norris, T. B., McDermott, T. R., & Castenholz, R. W. (2002). The long-term effects of UV exclusion on the microbial composition and photosynthetic competence of bacteria in hot-spring microbial mats. *FEMS Microbiology Ecology*, 39(3), 193-209. doi:dx.doi.org/10.1016/S0168-6496(01)00212-4
- Orlygsson, J., & Kristjansson, J. K. (2014). The Family Hydrogenophilaceae. In E. Rosenberg, E. F. DeLong, S. Lory, E. Stackebrandt, & F. Thompson (Eds.), *The Prokaryotes: Alphaproteobacteria and Betaproteobacteria* (pp. 859-868). Berlin, Heidelberg: Springer Berlin Heidelberg.
- Pagaling, E., Grant, W., Cowan, D., Jones, B., Ma, Y., Ventosa, A., & Heaphy, S. (2012). Bacterial and archaeal diversity in two hot spring microbial mats from the geothermal region of Tengchong, China. *Extremophiles*, 16(4), 607-618. doi:10.1007/s00792-012-0460-1
- Panosyan, H., & Birkeland, N.-K. (2014). Microbial diversity in an Armenian geothermal spring assessed by molecular and culture-based methods. *Journal of Basic Microbiology*, 54(11), 1240-1250. doi:10.1002/jobm.201300999
- Papke, R. T., Ramsing, N. B., Bateson, M. M., & Ward, D. M. (2003). Geographical isolation in hot spring cyanobacteria. *Environmental Microbiology*, 5(8), 650-659. doi:10.1046/j.1462-2920.2003.00460.x
- Pasternak, Z., Al-Ashhab, A., Gatica, J., Gafny, R., Avraham, S., Minz, D., . . . Jurkevitch, E. (2013). Spatial and Temporal Biogeography of Soil Microbial Communities in Arid and Semiarid Regions. *PLoS One*, 8(7), e69705. doi:10.1371/journal.pone.0069705
- Pester, M., Schleper, C., & Wagner, M. (2011). The Thaumarchaeota: an emerging view of their phylogeny and ecophysiology. *Current Opinion in Microbiology*, 14(3), 300-306. doi:dx.doi.org/10.1016/j.mib.2011.04.007
- Petitjean, C., Deschamps, P., López-García, P., & Moreira, D. (2015). Rooting the Domain Archaea by Phylogenomic Analysis Supports the Foundation of the New Kingdom Proteoarchaeota. *Genome Biology and Evolution*, 7(1), 191-204. doi:10.1093/gbe/evu274
- Pope, J., & Brown, K. L. (2014). Geochemistry of discharge at Waiotapu geothermal area, New Zealand - Trace elements and temporal changes. *Geothermics*, 51, 253-269. doi:10.1016/j.geothermics.2014.01.006
- Pope, J. G., McConchie, D. M., Clark, M. D., & Brown, K. L. (2004). Diurnal variations in the chemistry of geothermal fluids after discharge, Champagne Pool, Waiotapu, New Zealand. *Chemical Geology*, 203(3-4), 253-272. doi:dx.doi.org/10.1016/j.chemgeo.2003.10.004

- Purcell, D., Sompong, U., Yim, L. C., Barraclough, T. G., Peerapornpisal, Y., & Pointing, S. B. (2007). The effects of temperature, pH and sulphide on the community structure of hyperthermophilic streamers in hot springs of northern Thailand. *FEMS Microbiology Ecology*, *60*(3), 456-466. doi:10.1111/j.1574-6941.2007.00302.x
- Quast, C., Pruesse, E., Yilmaz, P., Gerken, J., Schweer, T., Yarza, P., . . . Glöckner, F. O. (2013). The SILVA ribosomal RNA gene database project: improved data processing and web-based tools. *Nucleic Acids Research*, *41*(D1), D590-D596. doi:10.1093/nar/gks1219
- R Core Team. (2016). R: A language and environment for statistical computing. R Foundation for Statistical Computing. Vienna, Austria.
- Rampelotto, P. H. (2013). Extremophiles and Extreme Environments. *Life*, *3*, 482-485. doi:10.3390/life3030482
- Ratouis, T. M. P., & Zarrouk, S. J. (2016). Factors controlling large-scale hydrodynamic convection in the Taupo Volcanic Zone (TVZ), New Zealand. *Geothermics*, *59, Part B*, 236-251. doi:dx.doi.org/10.1016/j.geothermics.2015.09.003
- Reigstad, L. J., Jorgensen, S. L., & Schleper, C. (2010). Diversity and abundance of Korarchaeota in terrestrial hot springs of Iceland and Kamchatka. *The ISME Journal*, *4*(3), 346-356. doi:dx.doi.org/10.1038/ismej.2009.126
- Rothschild, L. J., & Mancinelli, R. L. (2001). Life in extreme environments. *Nature*, *409*(6823), 1092-1101. Retrieved from dx.doi.org/10.1038/35059215
- Rueckert, A., & Morgan, H. W. (2007). Removal of contaminating DNA from polymerase chain reaction using ethidium monoazide. *Journal of Microbiological Methods*, *68*(3), 596-600. doi:dx.doi.org/10.1016/j.mimet.2006.11.006
- Salazar, G., Cornejo-Castillo, F. M., Benitez-Barrios, V., Fraile-Nuez, E., Alvarez-Salgado, X. A., Duarte, C. M., . . . Acinas, S. G. (2015). Global diversity and biogeography of deep-sea pelagic prokaryotes. *ISME J*. doi:10.1038/ismej.2015.137
- Sand, W. (2003). Microbial life in geothermal waters. *Geothermics*, *32*(4-6), 655-667. doi:dx.doi.org/10.1016/S0375-6505(03)00058-0
- Sayeh, R., Birrien, J., Alain, K., Barbier, G., Hamdi, M., & Prieur, D. (2010). Microbial diversity in Tunisian geothermal springs as detected by molecular and culture-based approaches. *Extremophiles*, *14*(6), 501-514. doi:10.1007/s00792-010-0327-2
- Schloss, P. D., Westcott, S. L., Ryabin, T., Hall, J. R., Hartmann, M., Hollister, E. B., . . . Weber, C. F. (2009). Introducing mothur: Open-Source, Platform-Independent, Community-Supported Software for Describing and Comparing Microbial Communities. *Applied and Environmental Microbiology*, *75*(23), 7537-7541. doi:10.1128/AEM.01541-09
- Scott, B. J., & Cody, A. D. (2000). Response of the Rotorua geothermal system to exploitation and varying management regimes. *Geothermics*, *29*(4-5), 573-592. doi:dx.doi.org/10.1016/S0375-6505(00)00023-7
- Sharp, C. E., Brady, A. L., Sharp, G. H., Grasby, S. E., Stott, M. B., & Dunfield, P. F. (2014). Humboldt's spa: microbial diversity is controlled by temperature in geothermal environments. *The ISME Journal*, *8*(6), 1166-1174. doi:10.1038/ismej.2013.237
- Sharp, C. E., Smirnova, A. V., Graham, J. M., Stott, M. B., Khadka, R., Moore, T. R., . . . Dunfield, P. F. (2014). Distribution and diversity of

- Verrucomicrobia methanotrophs in geothermal and acidic environments. *Environmental Microbiology*, 16(6), 1867-1878. doi:10.1111/1462-2920.12454
- Shima, S., & Suzuki, K.-I. (1993). Hydrogenobacter acidophilus sp. nov., a Thermoacidophilic, Aerobic, Hydrogen-Oxidizing Bacterium Requiring Elemental Sulfur for Growth. *International Journal of Systematic and Evolutionary Microbiology*, 43(4), 703-708. doi:10.1099/00207713-43-4-703
- Siering, P. L., Wolfe, G. V., Wilson, M. S., Yip, A. N., Carey, C. M., Wardman, C. D., . . . Zhou, J. (2013). Microbial biogeochemistry of Boiling Springs Lake: a physically dynamic, oligotrophic, low-pH geothermal ecosystem. *Geobiology*, 11(4), 356-376. doi:10.1111/gbi.12041
- Spang, A., Saw, J. H., Jørgensen, S. L., Zaremba-Niedzwiedzka, K., Martijn, J., Lind, A. E., . . . Ettema, T. J. G. (2015). Complex archaea that bridge the gap between prokaryotes and eukaryotes. *Nature*, 521(7551), 173-179E. doi:10.1038/nature14447
- Stan-Lotter, H. (2012). Physico-chemical boundaries of life. In H. Stan-Lotter & S. Fendrihan (Eds.), *Adaption of Microbial Life to Environmental Extremes: Novel Research Results and Application* (pp. 1-19). Vienna: Springer Vienna.
- Stott, M. B., Crowe, M. A., Mountain, B. W., Smirnova, A. V., Hou, S., Alam, M., & Dunfield, P. F. (2008). Isolation of novel bacteria, including a candidate division, from geothermal soils in New Zealand. *Environmental Microbiology*, 10(8), 2030-2041. doi:10.1111/j.1462-2920.2008.01621.x
- Swingley, W. D., Meyer-Dombard, D., Shock, E. L., Alsop, E. B., Falenski, H. D., Havig, J. R., & Raymond, J. (2012). Coordinating environmental genomics and geochemistry reveals metabolic transitions in a hot spring ecosystem. *PLoS One*, 7(6). doi:dx.doi.org/10.1371/journal.pone.0038108
- Takacs-Vesbach, C., Mitchell, K., Jackson-Weaver, O., & Reysenbach, A.-L. (2008). Volcanic calderas delineate biogeographic provinces among Yellowstone thermophiles. *Environmental Microbiology*, 10(7), 1681-1689. doi:10.1111/j.1462-2920.2008.01584.x
- Takada-Hoshino, Y., & Matsumoto, N. (2004). An Improved DNA Extraction Method Using Skim Milk from Soils That Strongly Adsorb DNA. *Microbes and environments*, 19(1), 13-19. doi:10.1264/jisme.2.19.13
- Takai, K., & Nakagawa, S. (2014). The Family Hydrogenothermaceae. In E. Rosenberg, E. F. DeLong, S. Lory, E. Stackebrandt, & F. Thompson (Eds.), *The Prokaryotes: Other Major Lineages of Bacteria and The Archaea* (pp. 689-699). Berlin, Heidelberg: Springer Berlin Heidelberg.
- Tamaki, H., Tanaka, Y., Matsuzawa, H., Muramatsu, M., Meng, X.-Y., Hanada, S., . . . Kamagata, Y. (2011). Armatimonas rosea gen. nov., sp. nov., of a novel bacterial phylum, Armatimonadetes phyl. nov., formally called the candidate phylum OP10. *International Journal of Systematic and Evolutionary Microbiology*, 61(6), 1442-1447. doi:10.1099/ijs.0.025643-0
- Ullrich, M. K., Pope, J. G., Seward, T. M., Wilson, N., & Planer-Friedrich, B. (2013). Sulfur redox chemistry governs diurnal antimony and arsenic cycles at Champagne Pool, Waiotapu, New Zealand. *Journal of Volcanology and Geothermal Research*, 262, 164-177. doi:dx.doi.org/10.1016/j.jvolgeores.2013.07.007
- Waikato Regional Council. (2012). *Environment Waikato Policy Series: Waikato Regional Plan: Geothermal Module (7)*. Hamilton.

- Waikato Regional Council. (n.d). Waiotapu. Retrieved from <http://www.waikatoregion.govt.nz/Environment/Natural-resources/Geothermal-resources/Geothermal-systems-map/Waiotapu/>
- Waiotapu Thermal Wonderland. (n.d). Location. Retrieved from <http://www.waiotapu.co.nz/location/>
- Wang, S., Hou, W., Dong, H., Jiang, H., Huang, L., Wu, G., . . . Zhang, L. (2013). Control of Temperature on Microbial Community Structure in Hot Springs of the Tibetan Plateau. *PLoS One*, 8(5). doi:10.1371/journal.pone.0062901
- Ward, L., Taylor, M. W., Power, J. F., Scott, B. J., McDonald, I. R., & Stott, M. B. (2017). Microbial community dynamics in Inferno Crater Lake, a thermally fluctuating geothermal spring. *ISME J*. doi:10.1038/ismej.2016.193
- Whitaker, R. J., Grogan, D. W., & Taylor, J. W. (2003). Geographic Barriers Isolate Endemic Populations of Hyperthermophilic Archaea. *Science*, 301(5635), 976-978. doi:10.1126/science.1086909
- Wilson, A. D. (1960). The micro-determination of ferrous iron in silicate minerals by a volumetric and a colorimetric method. *Analyst*, 85(1016), 823-827. doi:10.1039/AN9608500823
- Wilson, C. J. N., Houghton, B. F., McWilliams, M. O., Lanphere, M. A., Weaver, S. D., & Briggs, R. M. (1995). Volcanic and structural evolution of Taupo Volcanic Zone, New Zealand: a review. *Journal of Volcanology and Geothermal Research*, 68(1-3), 1-28. doi:10.1016/0377-0273(95)00006-G
- Wilson, N., Webster-Brown, J., & Brown, K. (2012). The behaviour of antimony released from surface geothermal features in New Zealand. *Journal of Volcanology and Geothermal Research*, 247-248, 158-167. doi:10.1016/j.jvolgeores.2012.08.009
- Wood, C. P. (1992). Geology of the rotorua geothermal system. *Geothermics*, 21(1), 25-41. doi:dx.doi.org/10.1016/0375-6505(92)90066-I
- Wurch, L., Giannone, R. J., Belisle, B. S., Swift, C., Utturkar, S., Hettich, R. L., . . . Podar, M. (2016). Genomics-informed isolation and characterization of a symbiotic Nanoarchaeota system from a terrestrial geothermal environment. *Nature Communications*, 7, 12115. doi:10.1038/ncomms12115
- Wyering, L. D., Villeneuve, M. C., Wallis, I. C., Siratovich, P. A., Kennedy, B. M., Gravley, D. M., & Cant, J. L. (2014). Mechanical and physical properties of hydrothermally altered rocks, Taupo Volcanic Zone, New Zealand. *Journal of Volcanology and Geothermal Research*, 288, 76-93. doi:dx.doi.org/10.1016/j.jvolgeores.2014.10.008
- Zheng, Y.-M., Cao, P., Fu, B., Hughes, J. M., & He, J.-Z. (2013). Ecological Drivers of Biogeographic Patterns of Soil Archaeal Community. *PLoS One*, 8(5). doi:dx.doi.org/10.1371/journal.pone.0063375

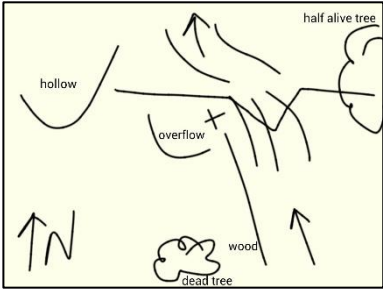
Appendices

4.1 Supplementary material for Chapter Two

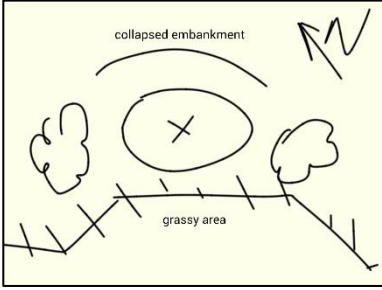
Supplementary Table 4.1: Sample number log of target pools

Feature Name	1,000 Springs Reference Number	Location	System	Month					
				Dec	Feb	April	Jun	Aug	Oct
				8 th /9 th	4 th /5 th	12 th /13 th	14 th /15 th	2 nd /3 rd	11 th /12 th
Whkr1	P1.0656	Whakareware wa Village	Rotorua		P2.0019	P2.0024	P2.0036	P2.0048	P2.0060
Whkr2	P1.0647	Whakareware wa Village	Rotorua	P2.0007	P2.0018	P2.0025	P2.0037	P2.0049	P2.0061
Whkr3	P1.0653	Whakareware wa Village	Rotorua	P2.0008	P2.0017	P2.0026	P2.0038	P2.0050	P2.0062
Whkr4	P1.0582	Whakareware wa Village	Rotorua	P2.0009	P2.0016	P2.0027	P2.0039	P2.0051	P2.0063
Whgpa	P1.0921	Atiamuri General	Atiamuri	P2.0001	P2.0010	P2.0028	P2.0040	P2.0052	P2.0064
Ohaaki	P1.0887	Ohaaki General	Ohaaki		P2.0021 (March)	P2.0022	P2.0034	P2.0046	P2.0058
TeP	P1.0583	Te Puia (Te Whakareware wa Village)	Rotorua		P2.0020	P2.0023	P2.0035	P2.0047	P2.0059
Kui1	P1.0502	Kuirau Park	Rotorua	P2.0004	P2.0013	P2.0029	P2.0041	P2.0053	P2.0065
Kui2	P1.0557	Kuirau Park	Rotorua	P2.0005	P2.0014	P2.0030	P2.0042	P2.0054	P2.0066
Kui3	P1.0379	Kuirau Park	Rotorua	P2.0006	P2.0015	P2.0031	P2.0043	P2.0055	P2.0067
Wai01	P1.0285	Waiotapu Thermal Wonderland	Waiotapu	P2.0002	P2.0012	P2.0032	P2.0044	P2.0056	P2.0068
Wai02	P1.0050	Waiotapu Thermal Wonderland	Waiotapu	P2.0003	P2.0011	P2.0033	P2.0045	P2.0057	P2.0069

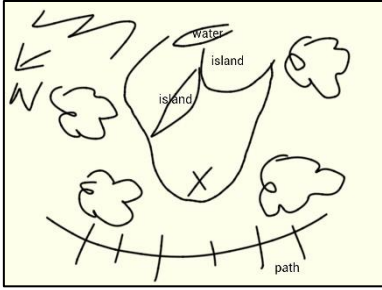
Whkr1



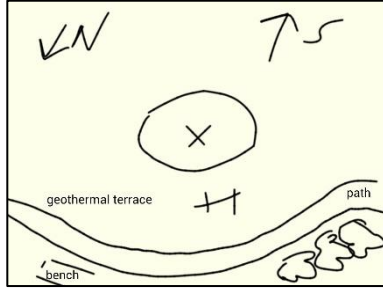
Whkr3



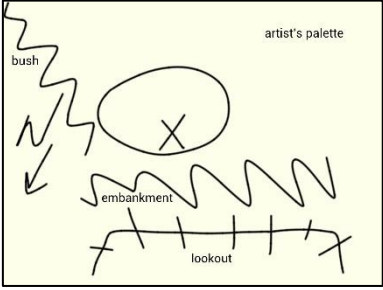
TeP



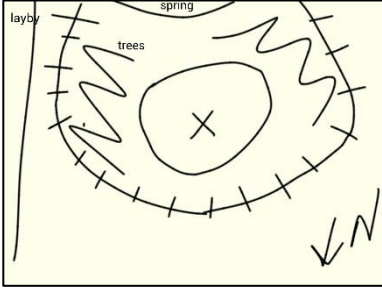
Wai01



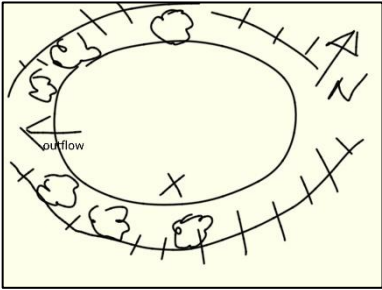
Wai02



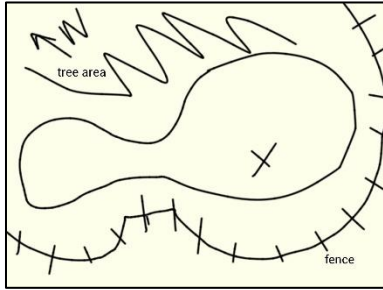
Kui3



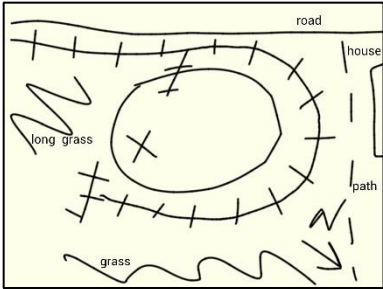
Whgpa



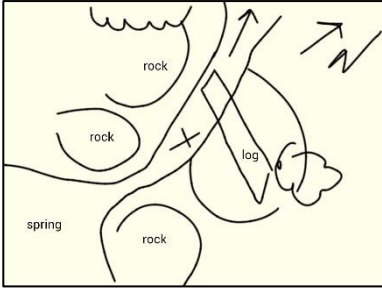
Kui1



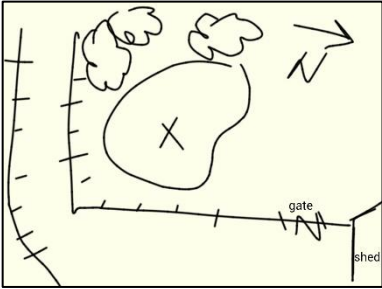
Kui2



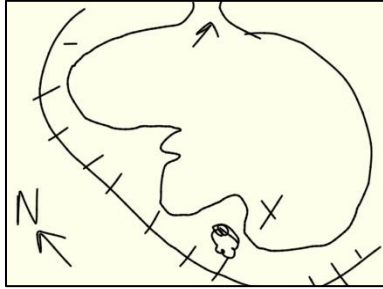
Whkr2



Whkr4



Ohaaki



Supplementary Figures 4.1: Target hotspring sketches and sample location



Whkr1 (pH 3 Group)



Whkr3 (pH 3 Group)



TeP (pH 3 Group)



Waio1 (pH 5 Group)



Waio2 (pH 5 Group)



Kui3 (pH 5 Group)



Whgpa (pH 7 Group)



Kui1 (pH 7 Group)



Kui2 (pH 7 Group)



Whkr2 (pH 9 Group)



Whkr4 (pH 9 Group)



Ohaaki (pH 9 Group)

Supplementary Figures 4.2: Target hotspring photographs

Supplementary Table 4.2: Hotspring temperature and pH measurements

Temperature (°C)						
Site	Dec	Feb	April	June	August	October
Whkr1		60.1	59.1	57.2	50.8	53
Whkr3	71	70.3	67.1	66.3	60	60.6
TeP		71.6	67.4	66.1	61.8	64
Wai01	64.9	67.5	67.2	67	65.6	68
Wai02	59.4	67.9	66.5	64.7	66.9	71.9
Kui3	59.2	61	56.6	51.7	45.8	51.3
Whgpa	63.3	65.3	63.8	61	60.8	62.7
Kui1	62.2	63.8	61.4	57.5	62	58.5
Kui2	70.6	72.4	71.4	68.7	67.9	68.3
Whkr2	69.5	69.6	66.2	64.7	64.5	65.5
Whkr4	63.4	61.5	61.1	70.3	78.1	80.6
Ohaaki		70	70.3	66.5	65	67.9
pH						
Site	Dec	Feb	April	June	August	October
Whkr1		2.95	3.06	3.12	3.03	2.91
Whkr3	3.37	3.31	3.64	3.98	4.55	4.77
TeP		2.5	2.44	2.48	2.58	2.54
Wai01	4.56	4.57	5	4.88	4.72	4.66
Wai02	5.07	4.78	4.92	4.8	4.68	4.77
Kui3	5.18	5.21	5.27	5.02	4.85	4.47
Whgpa	7.55	7.3	7.08	7.13	7.09	7.55
Kui1	6.57	6.62	6.94	7.06	6.6	6.75
Kui2	7.06	7.29	7.06	7.26	7.04	7.22
Whkr2	8.93	8.96	8.97	8.7	8.71	8.78
Whkr4	8.3	8.38	8.39	7.98	7.76	8.41
Ohaaki		8.84	9.04	8.87	8.41	9

Supplementary Table 4.3: Whkr3 community composition percentages of sequences grouping to genera

<i>Taxonomy</i>	<i>Dec</i>	<i>Feb</i>	<i>April</i>	<i>June</i>	<i>Aug</i>	<i>Oct</i>
<i>k_Archaea;p_Crenarchaeota;c_Thermoprotei;o_Sulfolobales;f_Sulfolobaceae;g_unknown</i>	33.1%	34.7%	18.4%	9.8%	6.2%	0.9%
<i>k_Archaea;p_Euryarchaeota;c_Thermoplasmata;o_Thermoplasmatales;f_unknown;g_unknown</i>	6.2%	6.2%	9.6%	7.3%	10.8%	12.0%
<i>k_Bacteria;p_Aquificae;c_Aquificae;o_Aquificales;f_Aquificaceae;g_Aquifex</i>	0.8%	0.0%	0.0%	0.0%	0.0%	0.0%
<i>k_Bacteria;p_Aquificae;c_Aquificae;o_Aquificales;f_Aquificaceae;g_Hydrogenobacter</i>	5.4%	0.0%	0.0%	0.0%	0.0%	0.0%
<i>k_Bacteria;p_Aquificae;c_Aquificae;o_Aquificales;f_Aquificaceae;g_Hydrogenobaculum</i>	50.8%	56.9%	69.7%	81.0%	2.8%	0.0%
<i>k_Bacteria;p_Aquificae;c_Aquificae;o_Aquificales;f_Hydrogenothermaceae;g_Venenivibrio</i>	3.1%	1.1%	0.1%	0.1%	74.3%	84.1%
<i>k_Bacteria;p_Aquificae;c_Aquificae;o_Aquificales;f_Hydrogenothermaceae;g_unknown</i>	0.0%	0.0%	0.0%	0.0%	0.5%	0.5%

Supplementary Table 4.4: Waio1 community composition percentages of sequences grouping to genera

<i>Taxonomy</i>	<i>Dec</i>	<i>Feb</i>	<i>April</i>	<i>June</i>	<i>Aug</i>	<i>Oct</i>
<i>k_Archaea;p_Crenarchaeota;c_Thermoprotei;o_Fervidicoccales;f_Fervidicoccaceae;g_Fervidicoccus</i>	0.0%	0.0%	0.2%	0.0%	0.0%	0.1%
<i>k_Archaea;p_Crenarchaeota;c_Thermoprotei;o_Sulfolobales;f_Sulfolobaceae;g_unknown</i>	0.1%	0.1%	0.2%	0.4%	0.2%	0.5%
<i>k_Archaea;p_Euryarchaeota;c_Thermoplasmata;o_Thermoplasmatales;f_unknown;g_unknown</i>	0.0%	0.0%	0.5%	0.1%	0.1%	0.4%
<i>k_Bacteria;p_Aquificae;c_Aquificae;o_Aquificales;f_Hydrogenothermaceae;g_Venenivibrio</i>	99.6%	99.6%	98.8%	99.2%	99.3%	98.6%
<i>k_Bacteria;p_Aquificae;c_Aquificae;o_Aquificales;f_Hydrogenothermaceae;g_unknown</i>	0.2%	0.2%	0.2%	0.3%	0.2%	0.2%
<i>k_Bacteria;p_Caldiserica;c_Caldisericia;o_Caldisericales;f_Caldiseriaceae;g_Caldisericum</i>	0.0%	0.0%	0.0%	0.0%	0.0%	0.1%
<i>k_Bacteria;p_Proteobacteria;c_Deltaproteobacteria;o_Desulfurellales;f_Desulfurellaceae;g_Desulfurella</i>	0.0%	0.0%	0.0%	0.0%	0.1%	0.1%

Supplementary Table 4.5: Waio2 community composition percentages of sequences grouping to genera

<i>Taxonomy</i>	<i>Dec</i>	<i>Feb</i>	<i>April</i>	<i>June</i>	<i>Aug</i>	<i>Oct</i>
<i>k_Archaea;p_Crenarchaeota;c_Thermoprotei;o_Sulfolobales;f_Sulfolobaceae;g_unknown</i>	0.0%	0.0%	0.1%	0.7%	1.1%	0.7%
<i>k_Archaea;p_Euryarchaeota;c_Thermoplasmata;o_Thermoplasmatales;f_unknown;g_unknown</i>	0.1%	0.2%	0.0%	0.2%	0.3%	0.2%
<i>k_Bacteria;p_Aquificae;c_Aquificae;o_Aquificales;f_Hydrogenothermaceae;g_Venenivibrio</i>	94.2%	99.1%	98.5%	95.9%	97.3%	98.5%
<i>k_Bacteria;p_Aquificae;c_Aquificae;o_Aquificales;f_Hydrogenothermaceae;g_unknown</i>	0.2%	0.3%	0.2%	0.2%	0.2%	0.2%
<i>k_Bacteria;p_Proteobacteria;c_Betaproteobacteria;o_Burkholderiales;f_Burkholderiales_incertae_sedis;g_Thiomonas</i>	0.3%	0.0%	0.3%	0.4%	0.2%	0.1%
<i>k_Bacteria;p_Proteobacteria;c_Deltaproteobacteria;o_Desulfurellales;f_Desulfurellaceae;g_Desulfurella</i>	0.3%	0.1%	0.2%	0.2%	0.2%	0.0%
<i>k_Bacteria;p_Proteobacteria;c_Gammaproteobacteria;o_Acidithiobacillales;f_Acidithiobacillaceae;g_Acidithiobacillus</i>	0.2%	0.0%	0.1%	0.4%	0.1%	0.0%
<i>k_Bacteria;p_Proteobacteria;c_Gammaproteobacteria;o_Chromatiales;f_Halothiobacillaceae;g_Halothiobacillus</i>	2.0%	0.1%	0.0%	0.5%	0.1%	0.0%
<i>k_Bacteria;p_Proteobacteria;c_Gammaproteobacteria;o_Chromatiales;f_Halothiobacillaceae;g_Thiovirga</i>	0.3%	0.0%	0.0%	0.1%	0.0%	0.0%
<i>k_Bacteria;p_Thermodesulfobacteria;c_Thermodesulfobacteria;o_Thermodesulfobacteriales;f_Thermodesulfobacteriaceae;g_Caldimicrobium</i>	0.4%	0.0%	0.0%	0.1%	0.1%	0.0%
<i>k_Bacteria;p_Thermotogae;c_Thermotogae;o_Thermotogales;f_Thermotogaceae;g_Mesoaciditoga</i>	0.1%	0.0%	0.1%	0.1%	0.0%	0.0%
<i>k_Bacteria;p_unknown;c_unknown;o_unknown;f_unknown;g_unknown</i>	0.7%	0.0%	0.1%	0.5%	0.1%	0.0%

Supplementary Table 4.6: Kui3 community composition percentages of sequences grouping to genera

<i>Taxonomy</i>	<i>Dec</i>	<i>Feb</i>	<i>April</i>	<i>June</i>	<i>Aug</i>	<i>Oct</i>
<i>k_Archaea;p_Euryarchaeota;c_Thermoplasmata;o_Thermoplasmatales;f_unknown;g_unknown</i>	0.0%	0.0%	0.2%	0.1%	0.1%	0.1%
<i>k_Bacteria;p_Aquificae;c_Aquificae;o_Aquificales;f_Aquificaceae;g_Hydrogenobaculum</i>	0.7%	5.3%	0.0%	0.1%	0.0%	0.1%
<i>k_Bacteria;p_Aquificae;c_Aquificae;o_Aquificales;f_Hydrogenothermaceae;g_Venenivibrio</i>	44.4%	79.3%	81.5%	79.3%	4.1%	94.4%
<i>k_Bacteria;p_Aquificae;c_Aquificae;o_Aquificales;f_Hydrogenothermaceae;g_unknown</i>	0.3%	0.5%	0.5%	0.7%	0.1%	0.5%
<i>k_Bacteria;p_Caldiserica;c_Caldiserica;o_Caldisericales;f_Caldiseriaceae;g_Caldisericum</i>	0.1%	0.7%	0.3%	1.0%	0.4%	0.8%
<i>k_Bacteria;p_Chlorobi;c_Chlorobacteria;o_Chlorobiales;f_Chlorobiaceae;g_Chlorobaculum</i>	0.0%	0.0%	0.0%	0.0%	0.6%	0.0%
<i>k_Bacteria;p_Dictyoglomi;c_Dictyoglomia;o_Dictyoglomales;f_Dictyoglomaceae;g_Dictyoglomus</i>	0.0%	0.1%	0.2%	0.5%	0.1%	0.0%
<i>k_Bacteria;p_Firmicutes;c_Negativicutes;o_Selenomonadales;f_Veillonellaceae;g_unknown</i>	0.0%	0.0%	0.0%	0.1%	0.3%	0.0%
<i>k_Bacteria;p_Proteobacteria;c_Betaproteobacteria;o_Burkholderiales;f_Burkholderiales_incertae_sedis;g_Thiomonas</i>	43.3%	12.3%	1.9%	3.4%	2.3%	0.7%
<i>k_Bacteria;p_Proteobacteria;c_Betaproteobacteria;o_unknown;f_unknown;g_unknown</i>	0.0%	0.0%	0.1%	0.4%	0.2%	0.1%
<i>k_Bacteria;p_Proteobacteria;c_Deltaproteobacteria;o_Desulfurellales;f_Desulfurellaceae;g_Desulfurella</i>	0.0%	0.0%	0.1%	0.3%	0.2%	0.4%
<i>k_Bacteria;p_Proteobacteria;c_Epsilonproteobacteria;o_Nautiliales;f_Nautiliaceae;g_Nitratiruptor</i>	10.3%	0.0%	0.0%	6.4%	68.3%	0.0%
<i>k_Bacteria;p_Proteobacteria;c_Gammaproteobacteria;o_Chromatiales;f_Halothiobacillaceae;g_Thiovirga</i>	0.1%	0.0%	13.3%	0.6%	18.7%	0.0%
<i>k_Bacteria;p_Proteobacteria;c_Gammaproteobacteria;o_Xanthomonadales;f_Sinobacteraceae;g_Nevskia</i>	0.0%	0.0%	0.4%	0.0%	0.0%	0.0%
<i>k_Bacteria;p_Proteobacteria;c_unknown;o_unknown;f_unknown;g_unknown</i>	0.0%	0.0%	0.1%	2.9%	1.2%	0.0%
<i>k_Bacteria;p_Thermodesulfobacteria;c_Thermodesulfobacteria;o_Thermodesulfobacteriales;f_Thermodesulfobacteriaceae;g_Caldimicrobium</i>	0.1%	0.7%	0.1%	0.2%	0.0%	0.0%

<i>k_Bacteria;p_Thermotogae;c_Thermotogae;o_Thermotogales;f_Thermotogaceae;g_Mesoaciditoga</i>	0.2%	0.2%	0.1%	0.3%	0.2%	0.9%
<i>k_Bacteria;p_Verrucomicrobia;c_Subdivision3;o_Subdivision3_genera_incertae_sedis;f_unknown;g_unknown</i>	0.0%	0.0%	0.1%	0.2%	0.1%	0.1%
<i>k_Bacteria;p_unknown;c_unknown;o_unknown;f_unknown;g_unknown</i>	0.3%	0.5%	0.5%	2.5%	2.4%	1.3%

Supplementary Table 4.7: Whgpa community composition percentages of sequences grouping to genera

<i>Taxonomy</i>	<i>Dec</i>	<i>Feb</i>	<i>April</i>	<i>June</i>	<i>Aug</i>	<i>Oct</i>
<i>k_Bacteria;p_Aquificae;c_Aquificae;o_Aquificales;f_Aquificaceae;g_Aquifex</i>	0.1%	0.2%	0.2%	0.2%	0.4%	0.6%
<i>k_Bacteria;p_Aquificae;c_Aquificae;o_Aquificales;f_Aquificaceae;g_Hydrogenovirga</i>	2.2%	1.3%	0.9%	1.0%	0.8%	0.6%
<i>k_Bacteria;p_Aquificae;c_Aquificae;o_Aquificales;f_Aquificaceae;g_Hydrogenobacter</i>	1.7%	1.1%	2.2%	1.6%	4.2%	2.5%
<i>k_Bacteria;p_Aquificae;c_Aquificae;o_Aquificales;f_Hydrogenothermaceae;g_Venenivibrio</i>	0.2%	0.4%	0.7%	0.7%	0.7%	0.2%
<i>k_Bacteria;p_Armatimonadetes;c_Armatimonadetes_gp6;o_unknown;f_unknown;g_unknown</i>	0.1%	0.1%	0.1%	0.1%	0.4%	0.2%
<i>k_Bacteria;p_Armatimonadetes;c_Armatimonadetes_gp7;o_unknown;f_unknown;g_unknown</i>	38.9%	30.8%	24.4%	15.6%	20.5%	45.4%
<i>k_Bacteria;p_BRC1;c_BRC1_genera_incertae_sedis;o_unknown;f_unknown;g_unknown</i>	0.1%	0.0%	0.0%	0.2%	0.4%	0.2%
<i>k_Bacteria;p_Bacteroidetes;c_Cytophagia;o_Cytophagales;f_Flammeovirgaceae;g_Thermonema</i>	1.8%	1.0%	0.9%	0.5%	0.2%	0.2%
<i>k_Bacteria;p_Bacteroidetes;c_Sphingobacteriia;o_Sphingobacteriales;f_Rhodothermaceae;g_Rhodothermus</i>	0.4%	0.6%	0.0%	0.0%	0.0%	0.0%
<i>k_Bacteria;p_Bacteroidetes;c_unknown;o_unknown;f_unknown;g_unknown</i>	0.7%	0.0%	0.2%	2.9%	1.7%	2.4%
<i>k_Bacteria;p_Candidatus_Calescamantes;c_Candidatus_Calescibacterium;o_unknown;f_unknown;g_unknown</i>	0.0%	0.0%	0.0%	0.1%	0.1%	0.3%
<i>k_Bacteria;p_Chloroflexi;c_Anaerolineae;o_Anaerolineales;f_Anaerolineaceae;g_unknown</i>	0.1%	0.0%	0.0%	0.1%	0.6%	0.0%
<i>k_Bacteria;p_Chloroflexi;c_Caldilineae;o_Caldilineales;f_Caldilineaceae;g_Caldilinea</i>	0.1%	0.0%	0.0%	0.1%	0.3%	0.2%
<i>k_Bacteria;p_Deinococcus-Thermus;c_Deinococci;o_Thermales;f_Thermaceae;g_Thermus</i>	39.9%	56.7%	63.6%	45.1%	30.6%	21.6%
<i>k_Bacteria;p_Firmicutes;c_Bacilli;o_Bacillales;f_Bacillaceae;g_Anoxybacillus</i>	0.2%	0.1%	0.0%	0.0%	0.0%	0.1%
<i>k_Bacteria;p_Proteobacteria;c_Beta_proteobacteria;o_Burkholderiales;f_Burkholderiales_incertae_sedis;g_Tepidimonas</i>	0.2%	0.1%	0.0%	0.0%	0.2%	0.0%

<i>k_Bacteria;p_Proteobacteria;c_Beta proteobacteria;o_Hydrogenophilales ;f_Hydrogenophilaceae;g_Hydrogenophilus</i>	0.2%	0.1%	0.1%	0.1%	0.1%	0.2%
<i>k_Bacteria;p_Proteobacteria;c_Gammaproteobacteria;o_unknown;f_unknown;g_unknown</i>	1.6%	0.4%	0.2%	1.0%	3.2%	5.9%
<i>k_Bacteria;p_Thermodesulfobacteria;c_Thermodesulfobacteria;o_Thermodesulfobacteriales;f_Thermodesulfobacteriaceae;g_Caldimicrobium</i>	0.1%	0.1%	0.0%	0.1%	0.1%	0.1%
<i>k_Bacteria;p_Thermotogae;c_Thermotogae;o_Thermotogales;f_Fervidobacteriaceae;g_Fervidobacterium</i>	0.0%	0.1%	0.1%	0.0%	0.0%	0.1%
<i>k_Bacteria;p_Verrucomicrobia;c_Subdivision3;o_Limisphaera;f_unknown;g_unknown</i>	0.9%	0.7%	0.2%	1.2%	0.3%	0.3%
<i>k_Bacteria;p_unknown;c_unknown;o_unknown;f_unknown;g_unknown</i>	9.4%	5.3%	5.5%	27.6%	32.6%	16.8%
<i>k_unknown;p_unknown;c_unknown;o_unknown;f_unknown;g_unknown</i>	0.1%	0.2%	0.5%	1.1%	0.2%	0.2%

Supplementary Table 4.8: Kuy1 community composition percentages of sequences grouping to genera

Taxonomy	Dec	Feb	April	June	Aug	Oct
<i>k_Archaea;p_Pacearchaeota;c_Pacearchaeota Incertae Sedis ARI3;o_unknown;f_unknown;g_unknown</i>	0.1%	0.2%	0.0%	0.5%	0.1%	0.2%
<i>k_Bacteria;p_Aminicenantes;c_Aminicenantes_g enera_incertae_sedis;o_unknown;f_unknown;g_u nknown</i>	0.0%	0.1%	0.0%	0.2%	0.1%	0.1%
<i>k_Bacteria;p_Aquificae;c_Aquificae;o_Aquifical es;f_Hydrogenothermaceae;g_Venenivibrio</i>	78.1%	74.6%	91.6%	67.4%	78.5%	75.8%
<i>k_Bacteria;p_Bacteroidetes;c_Cytophagia;o_Cyt ophagales;f_Flammeovirgaceae;g_Thermonema</i>	0.1%	0.4%	0.0%	0.0%	0.0%	0.0%
<i>k_Bacteria;p_Bacteroidetes;c_unknown;o_unkno wn;f_unknown;g_unknown</i>	2.0%	5.2%	0.3%	1.5%	1.7%	0.9%
<i>k_Bacteria;p_Caldiserica;c_Caldisericia;o_Cald isericales;f_Caldiseriaceae;g_Caldisericum</i>	0.1%	0.2%	0.0%	0.1%	0.7%	0.0%
<i>k_Bacteria;p_Chloroflexi;c_Anaerolineae;o_Ana erolineales;f_Anaerolineaceae;g_unknown</i>	0.9%	0.1%	0.1%	0.3%	0.1%	0.4%
<i>k_Bacteria;p_Chloroflexi;c_unknown;o_unknow n;f_unknown;g_unknown</i>	0.2%	0.3%	0.0%	0.4%	0.4%	0.5%
<i>k_Bacteria;p_Deferribacteres;c_Deferribacteres; o_Deferribacterales;f_Deferribacteraceae;g_Cal diterrivibrio</i>	0.3%	0.1%	0.2%	0.1%	0.1%	0.0%
<i>k_Bacteria;p_Deinococcus-Thermus; c_Deinococci;o_Thermales;f_Thermaceae;g_Mei othermus</i>	0.1%	0.3%	0.0%	0.0%	0.0%	0.0%
<i>k_Bacteria;p_Deinococcus-Thermus; c_Deinococci;o_Thermales;f_Thermaceae;g_The rmus</i>	1.9%	3.4%	1.1%	0.1%	0.6%	0.3%
<i>k_Bacteria;p_Dictyoglomi;c_Dictyoglomia;o_Di ctyoglomales;f_Dictyoglomaceae;g_Dictyoglomu s</i>	1.5%	0.8%	0.8%	1.1%	1.0%	0.5%
<i>k_Bacteria;p_Firmicutes;c_Bacilli;o_Bacillales; f_Bacillaceae 1;g_Anoxybacillus</i>	0.0%	0.3%	0.0%	0.1%	0.1%	0.2%
<i>k_Bacteria;p_Firmicutes;c_Clostridia;o_Clostri diales;f_Clostridiales_Incertae_Sedis III;g_Thermoanaerobacterium</i>	0.5%	0.0%	0.2%	0.0%	0.0%	0.0%
<i>k_Bacteria;p_Nitrospirae;c_Nitrospira;o_Nitros pirales;f_Nitrospiraceae;g_Thermodesulfovibrio</i>	0.3%	0.2%	0.1%	1.1%	0.3%	0.3%
<i>k_Bacteria;p_Nitrospirae;c_Nitrospira;o_Nitros pirales;f_Nitrospiraceae;g_unknown</i>	0.1%	0.1%	0.1%	0.2%	0.3%	0.3%
<i>k_Bacteria;p_Proteobacteria;c_Betaproteobacter ia;o_Burkholderiales;f_Burkholderiales_incertae _sedis;g_Tepidimonas</i>	2.6%	3.0%	0.2%	1.5%	0.6%	2.4%

<i>k_Bacteria;p_Proteobacteria;c_Betaproteobacteria;o_Burkholderiales;f_Burkholderiales_incertae_sedis;g_Thiobacter</i>	0.3%	0.0%	0.1%	0.0%	0.0%	0.1%
<i>k_Bacteria;p_Proteobacteria;c_Betaproteobacteria;o_Hydrogenophilales;f_Hydrogenophilaceae;g_Hydrogenophilus</i>	1.2%	1.5%	0.2%	0.6%	0.2%	0.4%
<i>k_Bacteria;p_Proteobacteria;c_Deltaproteobacteria;o_unknown;f_unknown;g_unknown</i>	0.1%	0.1%	0.1%	0.5%	0.2%	0.4%
<i>k_Bacteria;p_Proteobacteria;c_Gammaproteobacteria;o_Chromatiales;f_Halothiobacillaceae;g_Thiovirga</i>	0.1%	0.1%	0.0%	0.1%	0.1%	0.3%
<i>k_Bacteria;p_Proteobacteria;c_unknown;o_unknown;f_unknown;g_unknown</i>	0.1%	0.2%	0.1%	0.9%	0.4%	0.6%
<i>k_Bacteria;p_Thermodesulfobacteria;c_Thermodesulfobacteria;o_Thermodesulfobacteriales;f_Thermodesulfobacteriaceae;g_Caldimicrobium</i>	0.9%	1.6%	0.9%	4.2%	4.0%	1.8%
<i>k_Bacteria;p_Thermotogae;c_Thermotogae;o_Thermotogales;f_Fervidobacteriaceae;g_Fervidobacterium</i>	0.2%	0.2%	0.1%	0.1%	0.4%	0.1%
<i>k_Bacteria;p_Verrucomicrobia;c_Subdivision3;o_Limisphaera;f_unknown;g_unknown</i>	0.3%	0.3%	0.1%	0.0%	0.1%	0.0%
<i>k_Bacteria;p_unknown;c_unknown;o_unknown;f_unknown;g_unknown</i>	6.1%	5.7%	2.9%	16.6%	8.5%	12.8%

Supplementary Table 4.9: Whkr2 community composition percentages of sequences grouping to genera

<i>Taxonomy</i>	<i>Dec</i>	<i>Feb</i>	<i>April</i>	<i>June</i>	<i>Aug</i>	<i>Oct</i>
<i>k_Bacteria;p_Aquificae;c_Aquificae;o_Aquificales;f_Aquificaceae;g_Aquifex</i>	9.4%	19.1%	11.0%	3.2%	4.1%	1.3%
<i>k_Bacteria;p_Aquificae;c_Aquificae;o_Aquificales;f_Aquificaceae;g_Hydrogenobacter</i>	27.5%	39.6%	18.5%	25.0%	6.9%	22.5%
<i>k_Bacteria;p_Aquificae;c_Aquificae;o_Aquificales;f_Aquificaceae;g_Hydrogenobaculum</i>	0.2%	1.4%	0.0%	0.0%	0.2%	0.1%
<i>k_Bacteria;p_Aquificae;c_Aquificae;o_Aquificales;f_Hydrogenothermaceae;g_Sulfurihydrogenibium</i>	0.0%	0.1%	0.1%	0.0%	12.6%	6.4%
<i>k_Bacteria;p_Aquificae;c_Aquificae;o_Aquificales;f_Hydrogenothermaceae;g_Venenivibrio</i>	5.9%	3.5%	12.5%	8.0%	7.9%	4.3%
<i>k_Bacteria;p_Aquificae;c_Aquificae;o_Aquificales;f_Hydrogenothermaceae;g_unknown</i>	0.0%	0.1%	0.1%	0.1%	0.1%	0.1%
<i>k_Bacteria;p_Chlorobi;c_Chlorobia;o_Chlorobiales;f_Chlorobiaceae;g_Chlorobaculum</i>	0.0%	0.0%	0.3%	0.1%	0.2%	0.7%
<i>k_Bacteria;p_Chloroflexi;c_Anaerolineae;o_Anaerolineales;f_Anaerolineaceae;g_Anaerolinea</i>	0.0%	0.0%	0.1%	0.1%	0.2%	0.0%
<i>k_Bacteria;p_Chloroflexi;c_Anaerolineae;o_Anaerolineales;f_Anaerolineaceae;g_unknown</i>	0.1%	0.1%	0.0%	0.1%	0.2%	0.1%
<i>k_Bacteria;p_Chloroflexi;c_Chloroflexia;o_Chloroflexales;f_Chloroflexineae;g_Chloroflexaceae</i>	0.1%	0.0%	0.3%	0.1%	0.1%	0.4%
<i>k_Bacteria;p_Deinococcus-Thermus;c_Deinococci;o_Thermales;f_Thermaceae;g_Thermus</i>	6.6%	12.8%	11.4%	4.9%	1.9%	4.8%
<i>k_Bacteria;p_Dictyoglomi;c_Dictyoglomia;o_Dictyoglomales;f_Dictyoglomaceae;g_Dictyoglomus</i>	3.9%	1.4%	1.5%	1.0%	3.2%	1.1%
<i>k_Bacteria;p_Firmicutes;c_Clostridia;o_Clostridiales;f_Clostridiales_Incertae_Sedis_III;g_Caldicellulosiruptor</i>	0.4%	0.3%	0.5%	0.1%	0.3%	0.1%
<i>k_Bacteria;p_Proteobacteria;c_Alphaproteobacteria;o_Rhodospirillales;f_Acetobacteraceae;g_Acidiphilium</i>	0.5%	0.0%	0.0%	0.0%	0.0%	0.0%
<i>k_Bacteria;p_Proteobacteria;c_Betaproteobacteria;o_Burkholderiales;f_Burkholderiales_incertae_sedis;g_Tepidimonas</i>	0.5%	0.4%	1.1%	2.4%	0.6%	1.3%
<i>k_Bacteria;p_Proteobacteria;c_Betaproteobacteria;o_Burkholderiales;f_Burkholderiales_incertae_sedis;g_Thiomonas</i>	0.2%	0.0%	0.0%	0.1%	0.2%	0.3%
<i>k_Bacteria;p_Proteobacteria;c_Betaproteobacteria;o_Hydrogenophilales;f_Hydrogenophilaceae;g_Hydrogenophilus</i>	11.0%	6.0%	18.6%	23.1%	21.2%	27.3%

<i>k_Bacteria;p_Proteobacteria;c_Betaproteobacteria;o_unknown;f_unknown;g_unknown</i>	0.1%	0.0%	0.0%	0.5%	0.0%	0.0%
<i>k_Bacteria;p_Proteobacteria;c_Epsilonproteobacteria;o_Campylobacteriales;f_Helicobacteraceae;g_Sulfurimonas</i>	0.0%	0.0%	0.0%	0.0%	0.3%	0.0%
<i>k_Bacteria;p_Proteobacteria;c_Epsilonproteobacteria;o_Nautiliales;f_Nautiliaceae;g_Nitratiruptor</i>	0.0%	0.0%	0.1%	0.0%	3.0%	0.0%
<i>k_Bacteria;p_Proteobacteria;c_Gammaproteobacteria;o_Acidithiobacillales;f_Acidithiobacillaceae;g_Acidithiobacillus</i>	2.0%	0.1%	0.3%	0.2%	0.1%	0.2%
<i>k_Bacteria;p_Proteobacteria;c_Gammaproteobacteria;o_Chromatiales;f_Halothiobacillaceae;g_Thiofaba</i>	0.0%	0.0%	0.2%	0.2%	0.1%	0.0%
<i>k_Bacteria;p_Proteobacteria;c_Gammaproteobacteria;o_Chromatiales;f_Halothiobacillaceae;g_Thiovirga</i>	1.1%	0.1%	3.3%	6.6%	8.1%	2.4%
<i>k_Bacteria;p_Proteobacteria;c_Gammaproteobacteria;o_Xanthomonadales;f_Xanthomonadaceae;g_unknown</i>	0.1%	0.0%	0.2%	0.0%	0.0%	0.0%
<i>k_Bacteria;p_Proteobacteria;c_unknown;o_unknown;f_unknown;g_unknown</i>	0.1%	0.0%	0.2%	1.0%	0.5%	1.0%
<i>k_Bacteria;p_Thermodesulfobacteria;c_Thermodesulfobacteria;o_Thermodesulfobacteriales;f_Thermodesulfobacteriaceae;g_Caldimicrobium</i>	15.9%	8.9%	8.0%	9.5%	10.2%	13.3%
<i>k_Bacteria;p_Thermotogae;c_Thermotogae;o_Thermotogales;f_Fervidobacteriaceae;g_Fervidobacterium</i>	1.4%	1.1%	2.5%	0.8%	4.4%	1.7%
<i>k_Bacteria;p_Thermotogae;c_Thermotogae;o_Thermotogales;f_Thermotogaceae;g_Thermotoga</i>	0.1%	0.1%	0.3%	0.1%	0.2%	0.0%
<i>k_Bacteria;p_Thermotogae;c_Thermotogae;o_Thermotogales;f_Thermotogaceae;g_unknown</i>	0.1%	0.1%	0.1%	0.1%	0.1%	0.2%
<i>k_Bacteria;p_Verrucomicrobia;c_Subdivision3;o_Limisphaera;f_unknown;g_unknown</i>	0.0%	0.0%	0.5%	0.6%	0.2%	0.3%
<i>k_Bacteria;p_Verrucomicrobia;c_Subdivision3;o_Subdivision3_genera_incertae_sedis;f_unknown;g_unknown</i>	0.0%	0.0%	0.2%	0.0%	0.3%	0.1%
<i>k_Bacteria;p_unknown;c_unknown;o_unknown;f_unknown;g_unknown</i>	8.7%	3.6%	6.0%	9.8%	9.4%	6.6%

Supplementary Table 4.10: Whkr4 community composition percentages of sequences grouping to genera

<i>Taxonomy</i>	<i>Dec</i>	<i>Feb</i>	<i>April</i>	<i>June</i>	<i>Aug</i>	<i>Oct</i>
<i>k_Bacteria;p_Aquificae;c_Aquificae;o_Aquificales;f_Aquificaceae;g_Aquifex</i>	1.0%	1.8%	2.7%	2.0%	8.0%	7.5%
<i>k_Bacteria;p_Aquificae;c_Aquificae;o_Aquificales;f_Aquificaceae;g_Hydrogenobacter</i>	17.8%	11.6%	10.0%	12.1%	53.3%	59.0%
<i>k_Bacteria;p_Aquificae;c_Aquificae;o_Aquificales;f_Hydrogenothermaceae;g_Venenivibrio</i>	1.8%	1.8%	4.4%	6.4%	12.3%	4.9%
<i>k_Bacteria;p_Aquificae;c_Aquificae;o_Aquificales;f_Hydrogenothermaceae;g_unknown</i>	0.0%	0.0%	0.0%	0.1%	0.2%	0.1%
<i>k_Bacteria;p_Deinococcus-Thermus;c_Deinococci;o_Thermales;f_Thermaceae;g_Thermus</i>	64.9%	63.9%	46.7%	55.5%	3.5%	3.9%
<i>k_Bacteria;p_Bacteroidetes;c_Cytophagia;o_Cytophagales;f_Flammeovirgaceae;g_Thermonema</i>	0.8%	0.3%	0.1%	0.1%	0.0%	0.0%
<i>k_Bacteria;p_Bacteroidetes;c_Flavobacteriia;o_Flavobacteriales;f_Cryomorphaceae;g_Fluviicola</i>	0.0%	0.0%	0.0%	0.0%	0.0%	0.4%
<i>k_Bacteria;p_Bacteroidetes;c_Flavobacteriia;o_Flavobacteriales;f_Schleiferiaceae;g_Schleiferia</i>	0.3%	0.6%	1.7%	0.0%	0.0%	0.0%
<i>k_Bacteria;p_Bacteroidetes;c_unknown;o_unknown;f_unknown;g_unknown</i>	0.3%	7.1%	5.7%	0.0%	0.0%	0.4%
<i>k_Bacteria;p_Dictyoglomi;c_Dictyoglomia;o_Dictyoglomales;f_Dictyoglomaceae;g_Dictyoglomus</i>	0.4%	0.3%	1.1%	1.9%	5.9%	2.5%
<i>k_Bacteria;p_Proteobacteria;c_Betaproteobacteria;o_Burkholderiales;f_Burkholderiales_incertae_sedis;g_Tepidimonas</i>	0.6%	1.8%	1.4%	0.1%	0.1%	0.0%
<i>k_Bacteria;p_Proteobacteria;c_Betaproteobacteria;o_Hydrogenophilales;f_Hydrogenophilaceae;g_Hydrogenophilus</i>	4.3%	2.7%	4.5%	0.6%	1.4%	0.2%
<i>k_Bacteria;p_Thermodesulfobacteria;c_Thermodesulfobacteria;o_Thermodesulfobacteriales;f_Thermodesulfobacteriaceae;g_Caldimicrobium</i>	3.0%	1.7%	6.0%	10.8%	10.5%	14.8%
<i>k_Bacteria;p_Thermotogae;c_Thermotogae;o_Thermotogales;f_Fervidobacteriaceae;g_Fervidobacterium</i>	0.8%	0.5%	1.2%	1.6%	1.5%	1.6%
<i>k_Bacteria;p_Verrucomicrobia;c_Subdivision3;o_Limisphaera;f_unknown;g_unknown</i>	0.3%	0.5%	0.3%	0.1%	0.0%	0.0%

<i>k_Bacteria;p_unknown;c_unknown;o_</i> <i>unknown;f_unknown;g_unknown</i>	2.8%	3.7%	11.6%	6.5%	1.4%	2.2%
--	------	------	-------	------	------	------

Supplementary Table 4.11: Ohaaki community composition percentages of sequences grouping to genera

<i>Taxonomy</i>	<i>March</i>	<i>April</i>	<i>June</i>	<i>Aug</i>	<i>Oct</i>
<i>k_Bacteria;p_Acetothermia;c_Acetothermia_g enera_incertae_sedis;o_unknown;f_unknown;g_unknown</i>	0.0%	0.0%	0.0%	0.0%	1.3%
<i>k_Bacteria;p_Aquificae;c_Aquificae;o_Aquifi cales;f_Aquificaceae;g_Hydrogenobacter</i>	92.0%	96.1%	94.1%	93.7%	9.5%
<i>k_Bacteria;p_Aquificae;c_Aquificae;o_Aquifi cales;f_Hydrogenothermaceae;g_Venenivibrio</i>	0.0%	0.2%	0.1%	0.0%	0.0%
<i>k_Bacteria;p_Armatimonadetes;c_Armatimon adetes_gp7;o_unknown;f_unknown;g_unknow n</i>	0.2%	0.2%	1.3%	0.9%	0.9%
<i>k_Bacteria;p_Bacteroidetes;c_Cytophagia;o_ Cytophagales;f_Flammeovirgaceae;g_Thermo nema</i>	0.0%	0.0%	0.0%	0.0%	0.2%
<i>k_Bacteria;p_Bacteroidetes;c_unknown;o_unk nown;f_unknown;g_unknown</i>	0.0%	0.0%	0.2%	0.4%	0.0%
<i>k_Bacteria;p_Deinococcus-Thermus; c_Deinococci;o_Thermales;f_Thermaceae; g_Thermus</i>	7.6%	2.8%	2.2%	3.1%	73.2%
<i>k_Bacteria;p_Dictyoglomi;c_Dictyoglomia;o_ Dictyoglomales;f_Dictyoglomaceae;g_Dictyog lomus</i>	0.0%	0.1%	0.0%	0.0%	1.4%
<i>k_Bacteria;p_Proteobacteria;c_Betaproteobac teria;o_Hydrogenophilales;f_Hydrogenophila ceae;g_Hydrogenophilus</i>	0.1%	0.2%	0.9%	1.1%	2.0%
<i>k_Bacteria;p_Thermodesulfobacteria;c_Ther modesulfobacteria;o_Thermodesulfobacteriale s;f_Thermodesulfobacteriaceae;g_Caldimicro bium</i>	0.1%	0.3%	0.3%	0.2%	9.7%
<i>k_Bacteria;p_Thermotogae;c_Thermotogae;o_ Thermotogales;f_Fervidobacteriaceae;g_Fer vidobacterium</i>	0.0%	0.0%	0.0%	0.0%	0.6%
<i>k_Bacteria;p_unknown;c_unknown;o_unknow n;f_unknown;g_unknown</i>	0.1%	0.0%	0.5%	0.3%	0.2%

4.2 Supplementary: Full site physicochemical dataset

Spring Info Whkr1	Sample	P2.0019	P2.0024	P2.0036	P2.0048	P2.0060
	Site	Whkr1	Whkr1	Whkr1	Whkr1	Whkr1
	Month	Feb	April	June	Aug	Oct
Metadata	Temperature	60.1	59.1	57.2	50.8	53
	pH	2.95	3.06	3.12	3.03	2.91
Elements (ppm)	B 10	3.832	3.317	3.662	3.389	3.290
	Li 7	2.981	2.591	2.706	2.628	2.284
	Na 23	405.673	348.063	369.386	350.273	344.516
	Mg 24	0.540	0.245	0.368	0.365	0.327
	Al 27	2.092	1.492	1.446	1.792	1.768
	Si 28	128.501	110.109	110.313	118.771	126.581
	S 32	146.332	<5	62.777	<5	<5
	K 39	48.047	41.697	42.947	41.119	40.964
	Ca 43	7.908	3.954	6.187	6.381	5.640
	V 51	<0.002	<0.002	<0.002	<0.002	<0.002
	Cr 52	<0.0005	<0.0005	<0.0005	<0.0005	<0.0005
	Fe 54	<0.02	<0.02	<0.02	<0.02	<0.02
	Mn 55	0.024	0.018	0.021	0.028	0.029
	Co 59	<0.0002	<0.0002	<0.0002	<0.0002	<0.0002
	Ni 60	0.006	0.001	0.004	0.003	0.003
	Cu 63	0.005	0.003	0.006	0.004	0.005
	Zn 66	<0.001	<0.001	<0.001	0.008	0.026
	As 75	0.228	0.210	0.212	0.248	0.230
	Se 82	0.006	0.006	<0.001	<0.001	0.002
	Br 79	2.062	1.752	1.754	1.853	1.793
	Rb 85	0.355	0.311	0.333	0.343	0.327
	Sr 88	0.229	0.135	0.209	0.167	0.118
	Mo 98	<0.0005	<0.0005	<0.0005	<0.0005	<0.0005
	Ag 109	<0.0001	0.001	0.003	0.003	0.004
	Cd 111	<0.00005	<0.00005	<0.00005	<0.00005	<0.00005
	Cs 133	0.340	0.296	0.309	0.290	0.303
	Ba 137	0.113	0.045	0.061	0.082	0.069
	Tl 205	<0.00005	<0.00005	0.000	<0.00005	0.000
	Hg 202	0.002	0.002	0.001	0.001	<0.0002
	Pb 207	<0.0002	<0.0002	<0.0002	<0.0002	0.002
	U 238	<0.00002	<0.00002	<0.00002	<0.00002	<0.00002
	Cl ⁻	519	502	551	484	521
	SO ₄ ²⁻	337	305	305	303	337
S ²⁻	<0.01	<0.01	<0.01	0	<0.01	
HCO ₃ ⁻	<20	<20	<20	<20	<20	
Nutrients (ppm)	NO ₂ ⁻	0.028	0.029	0.028	0.004	0.006
	NO ₃ ⁻	0.001	0.000	0.000	0.001	0.000
	PO ₄ ³⁻	0.055	0.060	0.004	0.121	0.108
	NH ₄ ⁺	0.476	0.600	0.074	0.336	0.026
Iron (ppm)	Fe ²⁺	<3	<3	<3	<3	<3
Gases (µm)	H ₂	0.410	0.087	0.196	0.047	0.147
	CO	0.088	0.037	0.037	0.050	0.075
	CH ₄	0.155	0.282	0.226	0.215	0.277

Spring Info Whkr3	Sample	P2.0008	P2.0017	P2.0026	P2.0038	P2.0050	P2.0062
	Site	Whkr3	Whkr3	Whkr3	Whkr3	Whkr3	Whkr3
	Month	Dec	Feb	April	June	Aug	Oct
Metadata	Temperature	71	70.3	67.1	66.3	60	60.6
	pH	3.37	3.31	3.64	3.98	4.55	4.77
Elements (ppm)	B 10	3.899	4.094	4.103	3.767	3.907	4.067
	Li 7	1.780	1.966	1.901	1.801	1.703	1.772
	Na 23	327.751	349.968	354.784	329.598	340.003	350.097
	Mg 24	0.764	0.793	0.502	0.369	0.441	0.336
	Al 27	1.862	2.291	1.751	1.237	0.915	0.590
	Si 28	93.959	104.004	102.651	97.809	111.281	112.120
	S 32	<5	77.397	127.255	<5	<5	<5
	K 39	15.891	17.185	15.907	14.792	14.335	14.572
	Ca 43	6.796	8.406	6.406	4.524	6.629	5.341
	V 51	<0.002	<0.002	<0.002	<0.002	<0.002	<0.002
	Cr 52	<0.0005	0.001	0.001	<0.0005	0.001	<0.0005
	Fe 54	<0.02	<0.02	<0.02	<0.02	<0.02	<0.02
	Mn 55	0.039	0.044	0.041	0.031	0.035	0.026
	Co 59	<0.0002	<0.0002	<0.0002	<0.0002	<0.0002	<0.0002
	Ni 60	0.011	0.010	0.006	0.002	0.005	0.003
	Cu 63	0.006	0.011	0.030	0.004	0.025	0.003
	Zn 66	0.011	0.012	0.032	<0.001	0.008	0.009
	As 75	0.004	0.010	0.006	0.009	0.016	0.019
	Se 82	0.005	0.005	<0.001	<0.001	0.001	0.005
	Br 79	1.681	1.709	1.784	1.575	1.772	1.741
	Rb 85	0.123	0.136	0.133	0.117	0.116	0.115
	Sr 88	0.231	0.209	0.111	0.061	0.094	0.055
	Mo 98	<0.0005	<0.0005	<0.0005	<0.0005	<0.0005	<0.0005
	Ag 109	0.003	0.000	0.001	0.002	0.002	0.004
	Cd 111	<0.00005	<0.00005	<0.00005	<0.00005	<0.00005	<0.00005
	Cs 133	0.078	0.085	0.078	0.064	0.058	0.055
	Ba 137	0.135	0.118	0.097	0.116	0.082	0.074
	Tl 205	<0.00005	<0.00005	<0.00005	<0.00005	<0.00005	<0.00005
	Hg 202	0.000	0.001	0.000	<0.0002	0.001	0.001
	Pb 207	0.000	0.001	0.035	<0.0002	0.000	0.002
	U 238	<0.00002	<0.00002	<0.00002	<0.00002	0.000	0.000
	Cl ⁻	532	532	507	524	518	519
	SO ₄ ²⁻	208	219	202	200	185	202
S ²⁻	19	15	15	9	11	18	
HCO ₃ ⁻	97	109	126	64	111	78	
Nutrients (ppm)	NO ₂ ⁻	0.029	0.028	0.029	0.012	0.005	0.005
	NO ₃ ⁻	0.000	0.000	0.000	0.000	0.000	0.000
	PO ₄ ³⁻	0.024	0.009	0.012	0.004	0.011	0.009
	NH ₄ ⁺	2.011	1.231	1.947	0.075	1.119	1.154
Iron (ppm)	Fe ²⁺	<3	<3	<3	<3	<3	<3
Gases (µm)	H ₂	0.215	0.125	0.079	0.089	0.064	0.148
	CO	0.081	0.124	0.028	0.041	0.054	0.090
	CH ₄	6.928	<0.01	5.879	5.076	7.648	7.102

Spring Info TeP	Sample	P2.0020	P2.0023	P2.0035	P2.0047	P2.0059
	Site	TeP	TeP	TeP	TeP	TeP
	Month	Feb	April	June	Aug	Oct
Metadata	Temperature	71.6	67.4	66.1	61.8	64
	pH	2.5	2.44	2.48	2.58	2.54
Elements (ppm)	B 10	4.301	3.726	3.937	3.478	3.489
	Li 7	2.992	2.676	2.590	2.387	2.181
	Na 23	360.216	318.908	316.459	284.424	293.284
	Mg 24	0.492	0.420	0.309	0.249	0.156
	Al 27	5.671	6.296	4.825	4.921	5.146
	Si 28	154.406	132.072	125.694	110.929	125.081
	S 32	99.899	118.319	16.779	<5	<5
	K 39	40.059	35.357	35.153	31.466	31.797
	Ca 43	5.348	7.082	4.821	3.761	2.764
	V 51	<0.002	<0.002	<0.002	<0.002	<0.002
	Cr 52	<0.0005	0.073	<0.0005	<0.0005	<0.0005
	Fe 54	0.057	0.842	<0.02	<0.02	<0.02
	Mn 55	0.013	0.027	0.012	0.011	0.010
	Co 59	<0.0002	<0.0002	<0.0002	<0.0002	<0.0002
	Ni 60	0.009	0.002	0.003	0.002	0.002
	Cu 63	0.006	0.026	0.025	0.005	0.005
	Zn 66	0.010	0.035	0.009	<0.001	<0.001
	As 75	0.332	0.256	0.288	0.235	0.245
	Se 82	0.002	0.006	<0.001	<0.001	<0.001
	Br 79	1.982	1.595	1.655	1.518	1.527
	Rb 85	0.346	0.310	0.315	0.284	0.296
	Sr 88	0.203	0.103	0.146	0.099	0.046
	Mo 98	<0.0005	<0.0005	<0.0005	<0.0005	<0.0005
	Ag 109	0.001	0.000	0.002	0.002	0.001
	Cd 111	0.000	<0.00005	<0.00005	<0.00005	<0.00005
	Cs 133	0.330	0.309	0.301	0.278	0.283
	Ba 137	0.118	0.567	0.125	0.101	0.089
	Tl 205	<0.00005	<0.00005	0.000	<0.00005	0.000
	Hg 202	0.003	0.003	0.001	0.001	0.000
	Pb 207	0.002	0.636	0.000	0.000	0.002
U 238	0.000	<0.00002	<0.00002	0.000	<0.00002	
Cl ⁻	469	426	502	422	465	
SO ₄ ²⁻	387	388	389	370	396	
S ²⁻	<0.01	<0.01	<0.01	<0.01	<0.01	
HCO ₃ ⁻	27	37	<20	33	<20	
Nutrients (ppm)	NO ₂ ⁻	0.028	0.028	0.028	0.006	0.006
	NO ₃ ⁻	0.001	0.001	0.000	0.001	0.000
	PO ₄ ³⁻	0.041	0.050	0.003	0.075	0.079
	NH ₄ ⁺	1.112	1.185	0.073	0.671	0.201
Iron (ppm)	Fe ²⁺	<3	<3	<3	<3	<3
Gases (µm)	H ₂	0.153	0.028	0.034	0.017	0.072
	CO	0.102	0.056	0.037	0.012	0.059
	CH ₄	2.158	2.313	1.952	0.410	2.269

Spring Info Waiol	Sample	P2.0002	P2.0012	P2.0032	P2.0044	P2.0056	P2.0068
	Site	Waiol	Waiol	Waiol	Waiol	Waiol	Waiol
	Month	Dec	Feb	April	June	Aug	Oct
Metadata	Temperature	64.9	67.5	67.2	67	65.6	68
	pH	4.56	4.57	5	4.88	4.72	4.66
Elements (ppm)	B 10	6.74	6.68	6.60	5.99	6.00	6.09
	Li 7	1.56	1.59	1.57	1.46	1.37	1.42
	Na 23	375.10	367.07	362.67	322.43	337.91	335.08
	Mg 24	0.45	0.54	0.30	0.32	0.24	0.10
	Al 27	0.41	0.37	0.29	0.50	0.38	0.22
	Si 28	188.24	196.07	183.67	171.04	181.14	187.33
	S 32	77.43	<5	67.14	<5	<5	<5
	K 39	63.92	62.40	60.07	56.14	57.80	57.81
	Ca 43	10.10	11.33	10.43	9.78	8.99	8.04
	V 51	<0.002	<0.002	<0.002	<0.002	<0.002	<0.002
	Cr 52	<0.0005	<0.0005	<0.0005	<0.0005	<0.0005	<0.0005
	Fe 54	<0.02	<0.02	<0.02	<0.02	<0.02	<0.02
	Mn 55	0.01	0.01	0.01	0.02	0.02	0.01
	Co 59	<0.0002	<0.0002	<0.0002	<0.0002	<0.0002	<0.0002
	Ni 60	0.01	0.01	0.00	0.00	0.00	<0.001
	Cu 63	0.01	0.01	0.01	0.01	0.00	0.00
	Zn 66	0.01	0.00	0.01	0.02	0.01	<0.001
	As 75	0.45	0.44	0.46	0.43	0.44	0.42
	Se 82	0.01	0.00	0.00	<0.001	<0.001	0.00
	Br 79	2.35	2.43	2.37	2.22	2.14	2.26
	Rb 85	0.19	0.18	0.19	0.18	0.18	0.18
	Sr 88	0.19	0.29	0.18	0.14	0.08	0.06
	Mo 98	<0.0005	<0.0005	<0.0005	<0.0005	<0.0005	<0.0005
	Ag 109	0.00	0.00	0.00	0.00	0.00	0.00
	Cd 111	<0.00005	<0.00005	<0.00005	<0.00005	<0.00005	<0.00005
	Cs 133	0.05	0.04	0.04	0.04	0.04	0.04
	Ba 137	0.18	0.16	0.14	0.18	0.22	0.12
	Tl 205	<0.00005	<0.00005	<0.00005	<0.00005	<0.00005	<0.00005
	Hg 202	0.00	0.00	<0.0002	<0.0002	<0.0002	<0.0002
	Pb 207	<0.0002	0.00	<0.0002	0.00	0.00	0.00
	U 238	<0.00002	<0.00002	<0.00002	<0.00002	<0.00002	<0.00002
	Cl ⁻	715	667	670	705	665	682
SO ₄ ²⁻	87	95	89	87	91	95	
S ²⁻	0.04	0.04	0.03	0.05	0.03	0.02	
HCO ₃ ⁻	90	76	83	73	55	49	
Nutrients (ppm)	NO ₂ ⁻	0.031	0.028	0.028	0.005	0.004	0.005
	NO ₃ ⁻	0.001	0.000	0.000	0.000	0.001	0.000
	PO ₄ ³⁻	0.005	0.007	0.008	0.003	0.048	0.007
	NH ₄ ⁺	17.530	29.210	26.590	33.100	0.034	32.620
Iron (ppm)	Fe ²⁺	<3	<3	<3	<3	6.6667	<3
Gases (µm)	H ₂	0.465	0.316	0.326	0.119	0.430	0.535
	CO	0.057	0.098	0.049	0.024	0.033	0.031
	CH ₄	2.168	2.594	3.522	3.155	3.311	3.477

Spring Info Waio2	Sample	P2.0003	P2.0011	P2.0033	P2.0045	P2.0057	P2.0069
	Site	Waio2	Waio2	Waio2	Waio2	Waio2	Waio2
	Month	Dec	Feb	April	June	Aug	Oct
Metadata	Temperature	59.4	67.9	66.5	64.7	66.9	71.9
	pH	5.07	4.78	4.92	4.8	4.68	4.77
Elements (ppm)	B 10	20.716	19.415	19.471	17.999	15.347	15.945
	Li 7	7.307	6.983	7.019	6.857	5.266	5.552
	Na 23	1017.501	943.083	928.065	910.773	780.631	805.153
	Mg 24	0.361	0.477	0.282	0.280	0.352	0.127
	Al 27	0.246	0.253	0.256	0.390	0.685	0.320
	Si 28	145.926	150.966	146.797	158.594	138.048	134.310
	S 32	<5	13.779	<5	<5	<5	<5
	K 39	142.113	132.508	130.557	124.056	108.079	115.464
	Ca 43	38.368	37.011	36.782	36.118	35.030	30.636
	V 51	<0.002	<0.002	<0.002	<0.002	<0.002	<0.002
	Cr 52	<0.0005	<0.0005	<0.0005	<0.0005	0.001	<0.0005
	Fe 54	<0.02	<0.02	<0.02	<0.02	<0.02	<0.02
	Mn 55	0.064	0.062	0.065	0.064	0.066	0.056
	Co 59	<0.0002	<0.0002	<0.0002	<0.0002	<0.0002	<0.0002
	Ni 60	0.011	0.007	0.006	0.002	0.005	<0.001
	Cu 63	0.006	0.021	0.004	0.003	0.051	0.006
	Zn 66	0.025	<0.001	<0.001	0.002	0.108	0.010
	As 75	2.193	1.320	2.908	1.074	1.153	0.944
	Se 82	0.018	0.015	0.008	0.014	0.012	0.004
	Br 79	7.096	6.723	6.450	6.873	5.416	5.892
	Rb 85	1.259	1.204	1.263	1.261	1.016	1.059
	Sr 88	0.416	0.459	0.356	0.349	0.239	0.213
	Mo 98	<0.0005	<0.0005	<0.0005	<0.0005	<0.0005	<0.0005
	Ag 109	0.002	0.001	0.003	0.003	0.004	0.004
	Cd 111	<0.00005	<0.00005	<0.00005	<0.00005	<0.00005	<0.00005
	Cs 133	1.056	0.984	0.952	0.928	0.838	0.855
	Ba 137	0.100	0.058	0.036	0.075	0.083	0.032
	Tl 205	<0.00005	<0.00005	<0.00005	<0.00005	<0.00005	<0.00005
	Hg 202	0.003	0.002	0.000	<0.0002	<0.0002	<0.0002
	Pb 207	<0.0002	<0.0002	<0.0002	<0.0002	0.016	0.003
U 238	<0.00002	<0.00002	<0.00002	<0.00002	<0.00002	<0.00002	
Cl ⁻	2021	1991	1820	1864	1656	1683	
SO ₄ ²⁻	137	183	153	161	154	155	
S ²⁻	22	22	22	20	18	23	
HCO ₃ ⁻	271	160	172	175	164	111	
Nutrients (ppm)	NO ₂ ⁻	0.033	0.028	0.027	0.004	0.004	0.004
	NO ₃ ⁻	0.001	0.000	0.000	0.001	0.001	0.001
	PO ₄ ³⁻	0.026	0.013	0.016	0.006	0.061	0.011
	NH ₄ ⁺	52.650	31.250	52.940	71.640	0.038	18.500
Iron (ppm)	Fe ²⁺	<3	<3	<3	<3	<3	<3
Gases (µm)	H ₂	9.748	0.192	3.012	4.914	1.749	1.184
	CO	0.050	<0.01	0.052	0.038	0.056	0.048
	CH ₄	8.206	0.019	7.463	7.740	4.168	5.476

Spring Info Kui3	Sample	P2.0006	P2.0015	P2.0031	P2.0043	P2.0055	P2.0067
	Site	Kui3	Kui3	Kui3	Kui3	Kui3	Kui3
	Month	Dec	Feb	April	June	Aug	Oct
Metadata	Temperature	59.2	61	56.6	51.7	45.8	51.3
	pH	5.18	5.21	5.27	5.02	4.85	4.47
Elements (ppm)	B 10	0.896	1.102	1.104	0.929	0.541	0.601
	Li 7	0.344	0.410	0.417	0.377	0.227	0.236
	Na 23	58.641	66.332	67.006	60.492	42.735	43.067
	Mg 24	1.451	1.715	1.536	1.441	1.074	0.943
	Al 27	0.096	0.450	0.286	0.392	0.404	0.346
	Si 28	78.672	79.918	74.535	70.640	68.988	81.745
	S 32	<5	38.586	<5	<5	<5	<5
	K 39	13.354	14.461	14.123	12.946	9.787	10.756
	Ca 43	9.699	13.563	12.241	13.885	10.309	7.530
	V 51	<0.002	<0.002	<0.002	<0.002	<0.002	<0.002
	Cr 52	<0.0005	<0.0005	<0.0005	<0.0005	<0.0005	<0.0005
	Fe 54	<0.02	<0.02	<0.02	<0.02	0.049	<0.02
	Mn 55	0.168	0.208	0.217	0.213	0.154	0.147
	Co 59	<0.0002	<0.0002	<0.0002	<0.0002	<0.0002	<0.0002
	Ni 60	0.006	0.006	0.004	0.003	0.004	<0.001
	Cu 63	0.006	0.005	0.004	0.028	0.007	0.001
	Zn 66	<0.001	0.032	0.004	0.074	0.015	0.007
	As 75	<0.001	<0.001	0.008	0.008	0.015	0.008
	Se 82	<0.001	<0.001	<0.001	<0.001	<0.001	<0.001
	Br 79	0.219	0.229	0.274	0.253	0.126	0.085
	Rb 85	0.085	0.091	0.096	0.092	0.071	0.076
	Sr 88	0.265	0.232	0.200	0.146	0.078	0.054
	Mo 98	<0.0005	<0.0005	<0.0005	<0.0005	<0.0005	<0.0005
	Ag 109	0.001	<0.0001	0.002	0.003	0.004	0.004
	Cd 111	<0.00005	<0.00005	<0.00005	<0.00005	<0.00005	<0.00005
	Cs 133	0.071	0.078	0.074	0.068	0.053	0.065
	Ba 137	0.134	0.189	0.150	0.166	0.123	0.107
	Tl 205	<0.00005	<0.00005	<0.00005	<0.00005	<0.00005	<0.00005
	Hg 202	<0.0002	<0.0002	<0.0002	<0.0002	<0.0002	<0.0002
	Pb 207	<0.0002	0.001	0.001	0.010	0.003	0.001
	U 238	<0.00002	<0.00002	<0.00002	<0.00002	<0.00002	<0.00002
	Cl ⁻	54	70	115	63	31	27
SO ₄ ²⁻	71	83	89	89	70	92	
S ²⁻	2	2	1	2	1	2	
HCO ₃ ⁻	56	77	41	79	140	110	
Nutrients (ppm)	NO ₂ ⁻	0.029	0.029	0.028	0.006	0.006	0.006
	NO ₃ ⁻	0.001	0.001	0.001	0.020	0.000	0.003
	PO ₄ ³⁻	0.055	0.049	0.064	0.043	0.027	0.094
	NH ₄ ⁺	1.022	1.484	1.383	1.470	0.071	0.964
Iron (ppm)	Fe ²⁺	<3	3.333	<3	<3	<3	<3
Gases (µm)	H ₂	0.064	0.524	0.027	0.078	0.030	0.040
	CO	0.053	0.095	<0.01	0.045	0.038	<0.01
	CH ₄	29.806	28.473	3.403	11.175	7.017	0.763

Spring Info Whgpa	Sample	P2.0001	P2.0010	P2.0028	P2.0040	P2.0052	P2.0064
	Site	Whgpa	Whgpa	Whgpa	Whgpa	Whgpa	Whgpa
	Month	Dec	Feb	April	June	Aug	Oct
Metadata	Temperature	63.3	65.3	63.8	61	60.8	62.7
	pH	7.55	7.3	7.08	7.13	7.09	7.55
Elements (ppm)	B 10	8.680	8.685	8.823	8.446	8.198	8.136
	Li 7	3.045	3.260	3.252	3.142	2.894	2.866
	Na 23	366.524	364.932	360.432	339.408	349.498	348.775
	Mg 24	0.492	0.827	0.288	0.097	0.168	0.146
	Al 27	0.674	0.777	0.626	0.251	0.479	0.468
	Si 28	77.405	65.606	74.308	76.366	83.435	112.079
	S 32	<5	<5	<5	<5	<5	<5
	K 39	18.384	18.516	17.464	16.925	16.892	17.053
	Ca 43	4.710	8.352	4.449	1.591	3.244	3.379
	V 51	0.006	0.005	0.003	<0.002	<0.002	<0.002
	Cr 52	0.001	0.003	<0.0005	<0.0005	<0.0005	<0.0005
	Fe 54	<0.02	<0.02	<0.02	<0.02	<0.02	<0.02
	Mn 55	0.003	0.011	0.003	0.002	0.004	0.004
	Co 59	<0.0002	<0.0002	<0.0002	<0.0002	<0.0002	<0.0002
	Ni 60	0.011	0.008	0.003	0.001	0.002	0.003
	Cu 63	0.061	0.076	0.008	0.007	0.004	0.004
	Zn 66	0.010	0.223	0.014	<0.001	0.009	0.006
	As 75	0.651	0.610	0.651	0.598	0.615	0.625
	Se 82	0.005	<0.001	0.004	<0.001	<0.001	<0.001
	Br 79	1.012	0.936	0.970	0.789	0.877	0.935
	Rb 85	0.140	0.135	0.136	0.127	0.133	0.130
	Sr 88	0.142	0.196	0.131	0.055	0.037	0.045
	Mo 98	0.003	<0.0005	<0.0005	<0.0005	<0.0005	<0.0005
	Ag 109	<0.0001	0.000	0.002	0.003	0.003	0.002
	Cd 111	0.000	<0.00005	0.000	<0.00005	<0.00005	<0.00005
	Cs 133	0.828	0.801	0.804	0.733	0.769	0.750
	Ba 137	0.056	0.164	0.168	0.024	0.082	0.056
	Tl 205	<0.00005	<0.00005	<0.00005	<0.00005	<0.00005	<0.00005
	Hg 202	0.004	0.003	0.001	0.001	0.001	0.001
	Pb 207	0.001	0.027	0.001	<0.0002	0.001	0.001
	U 238	<0.00002	<0.00002	<0.00002	<0.00002	<0.00002	<0.00002
	Cl ⁻	371	324	325	330	317	345
	SO ₄ ²⁻	28	31	36	38	36	29
S ²⁻	<0.01	<0.01	<0.01	<0.01	<0.01	<0.01	
HCO ₃ ⁻	521	539	519	530	525	507	
Nutrients (ppm)	NO ₂ ⁻	0.229	0.058	0.042	0.035	0.042	0.175
	NO ₃ ⁻	0.025	0.008	0.003	0.032	0.047	0.105
	PO ₄ ³⁻	0.233	0.190	0.305	0.199	0.186	0.198
	NH ₄ ⁺	0.688	0.977	1.645	1.283	0.636	0.768
Iron (ppm)	Fe ³⁺	<3	<3	<3	<3	<3	<3
Gases (µm)	H ₂	0.057	0.100	0.052	0.034	0.016	0.055
	CO	0.038	0.089	0.028	0.034	<0.01	0.063
	CH ₄	7.707	14.224	18.210	6.891	0.609	4.182

Spring Info Kui1	Sample	P2.0004	P2.0013	P2.0029	P2.0041	P2.0053	P2.0065
	Site	Kui1	Kui1	Kui1	Kui1	Kui1	Kui1
	Month	Dec	Feb	April	June	Aug	Oct
Metadata	Temperature	62.2	63.8	61.4	57.5	62	58.5
	pH	6.57	6.62	6.94	7.06	6.6	6.75
Elements (ppm)	B 10	5.919	6.252	6.226	6.076	5.360	5.240
	Li 7	2.177	2.387	2.407	2.500	2.096	2.024
	Na 23	336.338	353.069	356.384	355.865	331.087	320.821
	Mg 24	0.675	0.506	0.300	0.305	0.178	0.259
	Al 27	0.683	0.397	0.342	0.377	0.339	0.380
	Si 28	59.697	68.491	75.601	91.237	96.673	93.773
	S 32	<5	<5	<5	<5	<5	<5
	K 39	23.828	23.984	23.455	22.772	21.723	21.008
	Ca 43	8.163	5.676	4.952	5.607	3.683	4.385
	V 51	<0.002	<0.002	<0.002	<0.002	<0.002	<0.002
	Cr 52	0.002	<0.0005	<0.0005	<0.0005	0.002	<0.0005
	Fe 54	0.650	<0.02	<0.02	<0.02	<0.02	<0.02
	Mn 55	0.024	0.017	0.019	0.021	0.021	0.019
	Co 59	<0.0002	<0.0002	<0.0002	<0.0002	<0.0002	<0.0002
	Ni 60	0.011	0.007	0.004	0.002	0.001	0.004
	Cu 63	0.026	0.005	0.004	0.011	0.004	0.002
	Zn 66	0.067	<0.001	0.003	0.031	<0.001	0.007
	As 75	0.110	0.094	0.087	0.091	0.089	0.063
	Se 82	0.004	0.004	0.004	<0.001	<0.001	<0.001
	Br 79	1.268	1.406	1.260	1.281	1.230	1.058
	Rb 85	0.229	0.244	0.239	0.242	0.234	0.205
	Sr 88	0.198	0.248	0.144	0.090	0.039	0.060
	Mo 98	<0.0005	<0.0005	<0.0005	<0.0005	<0.0005	<0.0005
	Ag 109	0.001	<0.0001	0.004	0.003	0.003	0.003
	Cd 111	0.000	0.000	0.000	<0.00005	<0.00005	<0.00005
	Cs 133	0.343	0.338	0.330	0.329	0.337	0.304
	Ba 137	0.072	0.070	0.021	0.033	0.054	0.074
	Tl 205	<0.00005	<0.00005	<0.00005	<0.00005	<0.00005	<0.00005
	Hg 202	0.002	0.001	<0.0002	<0.0002	<0.0002	<0.0002
	Pb 207	0.015	<0.0002	<0.0002	0.006	0.001	0.001
	U 238	<0.00002	<0.00002	<0.00002	<0.00002	<0.00002	<0.00002
	Cl ⁻	389	394	351	380	343	367
SO ₄ ²⁻	76	81	86	86	89	109	
S ²⁻	0	1	0	0	0	<0.01	
HCO ₃ ⁻	391	428	425	369	390	360	
Nutrients (ppm)	NO ₂ ⁻	0.028	0.028	0.028	0.005	0.005	0.005
	NO ₃ ⁻	0.002	0.001	0.000	0.000	0.000	0.001
	PO ₄ ³⁻	0.020	0.018	0.010	0.008	0.005	0.013
	NH ₄ ⁺	0.252	0.245	0.174	0.187	0.169	0.073
Iron (ppm)	Fe ²⁺	<3	<3	<3	<3	<3	<3
Gases (µm)	H ₂	0.362	0.092	0.031	0.020	0.025	0.035
	CO	0.038	0.086	0.025	0.019	0.029	0.056
	CH ₄	12.358	9.578	18.234	4.436	4.181	5.088

Spring Info Kui2	Sample	P2.0005	P2.0014	P2.0030	P2.0042	P2.0054	P2.0066
	Site	Kui2	Kui2	Kui2	Kui2	Kui2	Kui2
	Month	Dec	Feb	April	June	Aug	Oct
Metadata	Temperature	70.6	72.4	71.4	68.7	67.9	68.3
	pH	7.06	7.29	7.06	7.26	7.04	7.22
Elements (ppm)	B 10	5.361	5.848	5.532	5.263	5.042	5.010
	Li 7	2.322	2.507	2.466	2.441	2.125	2.204
	Na 23	317.532	326.157	324.560	313.862	302.022	304.605
	Mg 24	0.472	0.517	0.286	0.228	0.209	0.116
	Al 27	0.468	0.433	0.302	0.297	0.244	0.218
	Si 28	53.079	59.587	63.160	74.722	94.462	99.190
	S 32	<5	<5	<5	<5	<5	<5
	K 39	27.749	29.215	28.052	26.947	25.948	26.444
	Ca 43	5.535	6.610	5.148	4.410	3.791	3.285
	V 51	<0.002	<0.002	<0.002	<0.002	<0.002	<0.002
	Cr 52	<0.0005	<0.0005	<0.0005	<0.0005	<0.0005	<0.0005
	Fe 54	<0.02	<0.02	<0.02	<0.02	<0.02	<0.02
	Mn 55	0.022	0.023	0.024	0.021	0.025	0.025
	Co 59	<0.0002	<0.0002	<0.0002	<0.0002	<0.0002	<0.0002
	Ni 60	0.009	0.006	0.003	0.027	0.003	<0.001
	Cu 63	0.006	0.007	0.003	0.004	0.004	0.002
	Zn 66	0.013	0.003	0.003	<0.001	<0.001	<0.001
	As 75	0.073	0.058	0.061	0.067	0.063	0.049
	Se 82	0.003	0.003	<0.001	<0.001	0.006	<0.001
	Br 79	1.138	1.121	1.133	1.067	1.074	1.073
	Rb 85	0.246	0.251	0.259	0.258	0.249	0.237
	Sr 88	0.190	0.264	0.142	0.097	0.039	0.025
	Mo 98	<0.0005	<0.0005	<0.0005	<0.0005	<0.0005	<0.0005
	Ag 109	<0.0001	0.001	0.005	0.005	0.003	0.003
	Cd 111	<0.00005	<0.00005	<0.00005	<0.00005	<0.00005	<0.00005
	Cs 133	0.284	0.306	0.296	0.291	0.298	0.288
	Ba 137	0.073	0.017	0.007	0.037	0.128	0.009
	Tl 205	<0.00005	<0.00005	<0.00005	<0.00005	<0.00005	<0.00005
	Hg 202	0.002	0.001	<0.0002	<0.0002	<0.0002	<0.0002
	Pb 207	0.004	<0.0002	<0.0002	<0.0002	0.003	0.001
	U 238	<0.00002	<0.00002	<0.00002	<0.00002	<0.00002	<0.00002
	Cl ⁻	372	328	329	336	329	349
SO ₄ ²⁻	86	83	87	78	87	88	
S ²⁻	<0.01	<0.01	<0.01	0	<0.01	<0.01	
HCO ₃ ⁻	337	348	336	334	342	337	
Nutrients (ppm)	NO ₂ ⁻	0.031	0.029	0.030	0.005	0.005	0.006
	NO ₃ ⁻	0.003	0.001	0.001	0.011	0.000	0.003
	PO ₄ ³⁻	0.025	0.026	0.022	0.018	0.016	0.019
	NH ₄ ⁺	0.170	0.290	0.266	0.184	0.027	0.099
Iron (ppm)	Fe ²⁺	<3	<3	<3	<3	<3	<3
Gases (µm)	H ₂	0.095	1.024	0.064	0.103	0.036	0.035
	CO	0.084	0.074	0.089	<0.01	0.051	0.065
	CH ₄	4.800	2.565	4.834	2.274	3.757	2.558

Spring Info Whkr2	Sample	P2.0007	P2.0018	P2.0025	P2.0037	P2.0049	P2.0061
	Site	Whkr2	Whkr2	Whkr2	Whkr2	Whkr2	Whkr2
	Month	Dec	Feb	April	June	Aug	Oct
Metadata	Temperature	69.5	69.6	66.2	64.7	64.5	65.5
	pH	8.93	8.96	8.97	8.7	8.71	8.78
Elements (ppm)	B 10	5.226	5.233	4.886	4.940	4.710	4.659
	Li 7	2.733	2.780	2.513	2.726	2.401	2.357
	Na 23	449.453	459.518	435.123	459.937	439.953	431.582
	Mg 24	0.455	0.414	0.220	0.110	0.236	0.139
	Al 27	0.583	0.513	0.449	0.350	0.300	0.390
	Si 28	74.916	89.844	77.712	84.531	88.253	85.599
	S 32	<5	<5	<5	43.918	<5	<5
	K 39	26.964	27.260	25.337	25.897	25.909	24.886
	Ca 43	8.721	8.062	6.998	6.054	8.128	6.944
	V 51	<0.002	<0.002	<0.002	<0.002	<0.002	<0.002
	Cr 52	0.002	<0.0005	<0.0005	<0.0005	<0.0005	<0.0005
	Fe 54	<0.02	<0.02	<0.02	<0.02	<0.02	<0.02
	Mn 55	0.037	0.013	0.018	0.008	0.016	0.009
	Co 59	<0.0002	<0.0002	<0.0002	<0.0002	<0.0002	<0.0002
	Ni 60	0.004	0.007	0.002	<0.001	0.004	0.002
	Cu 63	0.006	0.006	0.005	0.007	0.005	0.001
	Zn 66	<0.001	<0.001	0.066	<0.001	0.019	<0.001
	As 75	0.133	0.081	0.096	0.096	0.091	0.138
	Se 82	0.009	0.007	<0.001	0.003	0.005	0.004
	Br 79	2.308	2.444	2.245	2.393	2.336	2.315
	Rb 85	0.244	0.246	0.250	0.258	0.256	0.248
	Sr 88	0.265	0.197	0.132	0.096	0.151	0.082
	Mo 98	<0.0005	<0.0005	<0.0005	<0.0005	<0.0005	<0.0005
	Ag 109	0.001	0.000	0.002	0.003	0.001	0.004
	Cd 111	<0.00005	<0.00005	<0.00005	<0.00005	0.000	<0.00005
	Cs 133	0.256	0.256	0.253	0.259	0.273	0.254
	Ba 137	0.029	0.069	0.088	0.035	0.038	0.047
	Tl 205	<0.00005	<0.00005	<0.00005	<0.00005	<0.00005	<0.00005
	Hg 202	0.005	0.003	0.003	0.002	0.002	0.001
	Pb 207	<0.0002	0.000	0.002	<0.0002	<0.0002	0.001
	U 238	<0.00002	<0.00002	<0.00002	<0.00002	<0.00002	<0.00002
Cl ⁻	726	675	687	716	707	635	
SO ₄ ²⁻	127	121	126	136	134	147	
S ²⁻	6	7	10	2	>1.01	4	
HCO ₃ ⁻	55	59	62	61	63	68	
Nutrients (ppm)	NO ₂ ⁻	0.029	0.028	0.029	0.028	0.005	0.004
	NO ₃ ⁻	0.001	0.000	0.000	0.000	0.000	0.001
	PO ₄ ³⁻	0.006	0.008	0.010	0.003	0.001	0.006
	NH ₄ ⁺	0.289	0.353	0.416	0.074	0.276	0.241
Iron (ppm)	Fe ²⁺	<3	<3	<3	<3	<3	<3
Gases (µm)	H ₂	0.130	0.105	0.130	0.084	0.162	0.135
	CO	0.060	0.117	0.071	0.039	<0.01	0.065
	CH ₄	1.821	0.282	0.084	0.027	0.200	0.067

Spring Info Whkr4	Sample	P2.0009	P2.0016	P2.0027	P2.0039	P2.0051	P2.0063
	Site	Whkr4	Whkr4	Whkr4	Whkr4	Whkr4	Whkr4
	Month	Dec	Feb	April	June	Aug	Oct
Metadata	Temperature	63.4	61.5	61.1	70.3	78.1	80.6
	pH	8.3	8.38	8.39	7.98	7.76	8.41
Elements (ppm)	B 10	5.384	5.558	5.133	5.054	4.815	4.605
	Li 7	3.556	3.677	3.443	3.370	3.001	2.965
	Na 23	421.211	438.480	406.451	393.611	394.620	375.951
	Mg 24	0.467	0.453	0.166	0.103	0.447	0.110
	Al 27	0.530	0.275	0.408	0.329	0.505	0.293
	Si 28	131.969	142.969	132.894	141.085	148.242	143.104
	S 32	<5	<5	<5	<5	<5	<5
	K 39	37.854	39.417	35.982	34.684	34.771	31.943
	Ca 43	5.204	4.845	3.680	3.013	7.570	3.250
	V 51	<0.002	<0.002	<0.002	<0.002	<0.002	<0.002
	Cr 52	<0.0005	<0.0005	<0.0005	<0.0005	<0.0005	<0.0005
	Fe 54	<0.02	<0.02	<0.02	<0.02	<0.02	<0.02
	Mn 55	0.001	0.001	0.001	<0.0005	0.004	0.003
	Co 59	<0.0002	<0.0002	<0.0002	<0.0002	<0.0002	<0.0002
	Ni 60	0.007	0.008	0.002	0.001	0.006	0.002
	Cu 63	0.008	0.013	0.006	0.005	0.012	0.001
	Zn 66	<0.001	0.016	0.003	0.001	0.046	<0.001
	As 75	0.400	0.410	0.397	0.341	0.409	0.277
	Se 82	0.001	0.003	<0.001	<0.001	0.001	0.002
	Br 79	2.291	2.262	2.119	2.019	2.057	1.931
	Rb 85	0.344	0.347	0.336	0.323	0.333	0.292
	Sr 88	0.282	0.205	0.100	0.063	0.163	0.045
	Mo 98	<0.0005	<0.0005	<0.0005	<0.0005	<0.0005	<0.0005
	Ag 109	0.002	0.002	0.003	0.002	0.002	0.003
	Cd 111	<0.00005	<0.00005	<0.00005	<0.00005	<0.00005	<0.00005
	Cs 133	0.416	0.413	0.384	0.394	0.412	0.340
	Ba 137	0.058	0.106	0.010	0.019	0.045	0.025
	Tl 205	0.000	<0.00005	0.001	0.000	0.001	0.000
	Hg 202	0.005	0.004	0.003	0.002	0.003	0.003
	Pb 207	<0.0002	0.002	0.001	<0.0002	0.001	0.000
	U 238	<0.00002	<0.00002	<0.00002	<0.00002	<0.00002	<0.00002
	Cl ⁻	631	583	594	619	605	622
SO ₄ ²⁻	73	67	74	68	77	69	
S ²⁻	1	0	0	3	0	6	
HCO ₃ ⁻	199	201	193	192	197	173	
Nutrients (ppm)	NO ₂ ⁻	0.028	0.028	0.029	0.005	0.005	0.005
	NO ₃ ⁻	0.000	0.000	0.000	0.001	0.000	0.000
	PO ₄ ³⁻	0.076	0.053	0.061	0.001	0.039	0.006
	NH ₄ ⁺	0.349	0.270	0.225	0.231	0.209	0.243
Iron (ppm)	Fe ²⁺	<3	<3	<3	<3	<3	<3
Gases (µm)	H ₂	0.059	0.146	0.064	0.103	0.055	0.075
	CO	0.063	0.112	0.062	0.065	0.075	0.069
	CH ₄	0.835	<0.01	0.763	0.413	0.100	0.736

Spring Info Ohaaki	Sample	P2.0021	P2.0022	P2.0034	P2.0046	P2.0058
	Site	Ohaaki	Ohaaki	Ohaaki	Ohaaki	Ohaaki
	Month	Feb	April	June	Aug	Oct
Metadata	Temperature	70	70.3	66.5	65	67.9
	pH	8.84	9.04	8.87	8.41	9
Elements (ppm)	B 10	23.399	20.734	26.799	33.412	23.726
	Li 7	8.785	8.009	7.440	10.033	6.206
	Na 23	769.419	733.096	740.695	855.194	675.073
	Mg 24	0.118	0.200	0.308	0.211	0.151
	Al 27	0.321	0.654	0.277	0.195	0.365
	Si 28	165.116	133.255	87.555	92.383	147.367
	S 32	<5	<5	<5	<5	<5
	K 39	107.543	91.560	129.219	150.463	126.395
	Ca 43	3.482	4.052	5.548	5.743	4.542
	V 51	0.004	0.005	0.004	<0.002	<0.002
	Cr 52	<0.0005	<0.0005	<0.0005	<0.0005	<0.0005
	Fe 54	<0.02	<0.02	<0.02	<0.02	<0.02
	Mn 55	<0.0005	<0.0005	0.001	<0.0005	0.001
	Co 59	<0.0002	<0.0002	<0.0002	<0.0002	<0.0002
	Ni 60	0.001	0.001	0.005	0.001	0.002
	Cu 63	0.005	0.004	0.006	0.004	0.002
	Zn 66	<0.001	0.003	0.074	0.001	0.003
	As 75	1.335	1.213	1.821	1.963	1.407
	Se 82	0.012	0.005	0.004	0.005	0.011
	Br 79	3.975	3.593	4.455	5.740	4.313
	Rb 85	0.748	0.624	0.960	1.168	0.952
	Sr 88	0.104	0.121	0.187	0.151	0.092
	Mo 98	<0.0005	<0.0005	<0.0005	<0.0005	<0.0005
	Ag 109	0.002	<0.0001	0.002	0.004	0.002
	Cd 111	<0.00005	0.000	<0.00005	<0.00005	<0.00005
	Cs 133	0.679	0.570	0.816	1.043	0.784
	Ba 137	0.040	0.140	0.088	0.017	0.116
	Tl 205	0.002	0.002	0.003	0.004	0.003
	Hg 202	0.011	0.012	0.005	0.004	0.006
	Pb 207	<0.0002	0.001	0.001	0.000	0.001
	U 238	<0.00002	<0.00002	<0.00002	<0.00002	<0.00002
	Cl ⁻	1047	907	1218	1566	1157
SO ₄ ²⁻	95	106	64	36	62	
S ²⁻	0	0	0	0	4	
HCO ₃ ⁻	425	461	247	302	187	
Nutrients (ppm)	NO ₂ ⁻	0.028	0.028	0.033	0.004	0.005
	NO ₃ ⁻	0.000	0.000	0.001	0.001	0.000
	PO ₄ ³⁻	0.978	0.551	0.778	0.257	0.064
	NH ₄ ⁺	1.081	0.589	0.717	1.098	0.034
Iron (ppm)	Fe ²⁺	<3	<3	<3	<3	<3
Gases (µm)	H ₂	0.054	0.012	0.034	0.040	0.048
	CO	0.027	<0.01	0.047	0.052	<0.01
	CH ₄	0.194	0.014	0.031	0.034	0.029